広島大学学位請求論文

Analysis of Model with Vector-like Quark through Standard Model Effective Field Theory

（標準模型有効理論による
Vector-like クォーク模型の解析）

２０２０年

広島大学大学院理学研究科
物理科学専攻

髙橋　隼也

Analysis of Model with Vector-like Quark through Standard Model Effective Field Theory

Shunya Takahashi

Department of Physics, Graduate School of Science,
Hiroshima University

February 2020

Abstract

We consider a model with one down-type $\mathrm{SU}(2)_L$ singlet vector-like quark (VLQ). The VLQ is defined as a new quark whose left- and right-handed components belong to the same representation of the gauge symmetry. In other words, both the left- and right-handed components of VLQ feel the same interactions unlike the standard model (SM) quarks. The VLQs are introduced in many new physics models, such as the universal see-saw model which explains hierarchical structure of the SM quark mass spectrum.

The recent lower limits for the VLQ mass from ATLAS and CMS experiments are about 1 TeV, ten times larger than the electroweak scale ∼100 GeV. The standard model effective field theory (SMEFT) is a powerful tool for to investigation of such a heavy particle. We investigate the model with VLQ on the basis of the SMEFT.

If we add the VLQs to the SM particle content, flavor-changing-neutral currents (FCNCs) among the SM quarks are induced at the tree level. The tree level FCNCs lead to new contributions to the observables of FCNC processes in the neutral B meson systems. In order to clarify constraints on the parameters of VLQ, we evaluate the FCNC processes with respect to $b \to s$ transition in the neutral $B_{d,s}$ meson system; B_s^0-$\overline{B_s^0}$ mixing, $\overline{B_s^0} \to \mu^+\mu$ and $\overline{B_d^0} \to X_s\gamma$. We construct SMEFT from the model with VLQ up to the one-loop level in order to analyze these processes.

We find that the constraint on the model parameters from the branching ratio of $\overline{B_s^0} \to \mu^+\mu$ is more stringent than that from the branching ratio of $\overline{B_d^0} \to X_s\gamma$. Although we focused on the FCNC processes related to the $b \to s$ transition, the SMEFT constructed in this thesis can be applied to both $b \to d$ and $s \to d$ transitions. In addition, the Wilson coefficient for the radiative transition $b \to s\gamma$ also contributes to the CP asymmetry in the radiative decays, the inclusive and the exclusive $b \to sl^+l$ processes.

Table of contents

Chapter 1
Introduction

It is known that there are six quarks and six leptons in the standard model (SM) of particle physics. The SM describes three fundamental interactions, strong, weak and electromagnetic interactions. These interactions are introduced through a gauge symmetry, $\mathrm{SU}(3)_c \times \mathrm{SU}(2)_L \times U(1)_Y$. The SM particles are representations of the gauge group $\mathrm{SU}(3)_c \times \mathrm{SU}(2)_L \times U(1)_Y$. Left-handed quarks are triplet $\mathbf{3}$ of $\mathrm{SU}(3)_c$, doublet $\mathbf{2}$ of $\mathrm{SU}(2)_L$ and have $U(1)_Y$ charge $\frac{1}{3}$. Right-handed quarks are triplet $\mathbf{3}$ of $\mathrm{SU}(3)_c$, singlet $\mathbf{1}$ of $\mathrm{SU}(2)_L$ and have $U(1)_Y$ charge $\frac{4}{3}$ for up-type quarks or $\frac{2}{3}$ for down-type quarks. The assignment of $\mathrm{SU}(2)_L$ for the SM quarks is determined so that the weak interaction acts only the left-handed quarks.

In the SM, interactions among the different flavors are controlled by two unitary matrices, Cabibbo–Kobayashi–Maskawa (CKM) matrix [1, 2, 3] for the quarks and Pontecorvo–Maki–Nakagawa–Sakata (PMNS) matrix [4, 5] for the leptons. In other words, the flavor mixing of quarks and leptons are governed by the CKM and PMNS matrices in the SM, respectively. Characteristics of the quark sector in the SM are,

Flavor-changing neutral currents (FCNCs) are suppressed by Glashow–Iliopoulos–Maiani (GIM) mechanism [6].

CP violation is induced by one Dirac CP phase in the CKM matrix.

The FCNCs mean interactions which change species of quarks but do not change the electromagnetic charge of the quarks. For example, a transition from b-quark to s-quark ($b \to s$) is the FCNC process. Such interactions do not exist in the SM, and thus FCNCs are induced at the one-loop level through the charged current in the SM. This is one of the aspects of the GIM mechanism and leads to the suppression of the FCNC processes in the SM. For example, we show a FCNC process $b \to sZ$ in the case of the SM in the left figure of Fig.1.1. The characteristics such as the GIM mechanism are verified by precise measurements in B and K meson systems and consistent with current experimental data. Especially the verification of the unitarity of the CKM matrix is one of the most successful aspects of the SM [7, 8].

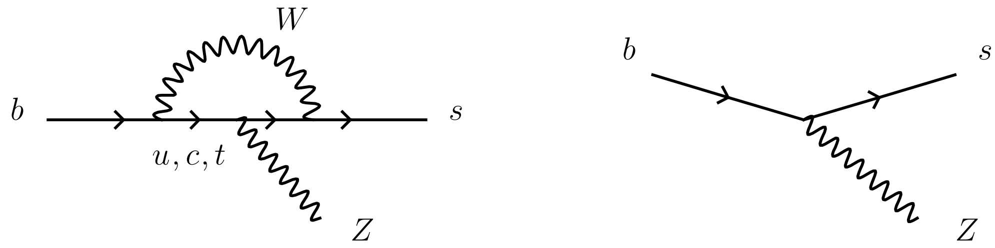

Figure 1.1. *Left figure* : Flavor changing neutral current (FCNC) induced at the one-loop level through the charged current. *Right figure* : FCNC among the SM quarks at the tree level.

Although predictions of the SM are consistent with almost all experimental results, there are several phenomena which the SM cannot explain. For example, the SM cannot predict measured angles of the flavor mixing. These angles are free parameters in the SM. The measured angles of the flavor mixing indicate a small mixing in the quark sector while a large mixing in the lepton sector [7, 8, 9]. This implies that there is some mechanism which leads to the characteristic pattern of the flavor mixing behind the SM.

There are various models beyond the SM in order to explain the problems in the SM. For instance, we proposed the models which clarify the flavor structures of the quarks and leptons by using simplified mass matrices [10], or the models with flavor symmetries which lead to the pattern of the flavor mixing [11].

Many new physics (NP) models predict existence of new particles which are not included in the SM particle content. We focus on so-called "vector-like quarks" (VLQs), as such the new particles. The VLQs are introduced in many NP models. One of the NP models with VLQs is the universal see-saw model [12, 13, 14, 15, 16, 17, 18] which explain the hierarchical structure of the SM quark mass spectrum. It is important to confirm the existence of the VLQs in order to verify the NP models.

The VLQs are defined as new quarks whose left- and right-handed components belong to the same representation of the gauge symmetry. Therefore, both the left- and right-handed components of VLQs feel the same interactions unlike the SM quarks. As we will see in Sec.2.2, this feature leads to mass terms of the VLQs without Yukawa interactions of the SM Higgs doublets and hence the masses of the VLQs are independent of the energy scale of electroweak (EW) symmetry breaking.

The direct search of the VLQs are performed by the ATLAS [19]-[34] and CMS [35]-[52] experiments at the Large Hadron Collider (LHC). Assuming VLQs are coupled with only third generation quarks, recent lower limits for a mass of down-type $SU(2)_L$ singlet VLQ are obtained as 1.22 TeV by ATLAS collaboration [34] and

1.17 TeV by CMS collaboration [49] at 95% confidence level. One finds that these limits for the VLQ mass are about one order larger than the EW scale ($\sim$100 GeV).

If we add the VLQs to the SM particle content, new features arise in the model:

- FCNCs among the SM quarks are induced at the tree level (right figure in Fig.1.1).
- The CKM matrix is not a unitary matrix.

These features mean that the GIM mechanism does not work in the model with VLQs. Since the SM contributions to the FCNC processes are suppressed by the GIM mechanism, it is expected that FCNC processes in the B and K meson systems give stringent constraints on model with VLQs. We investigate the constraints on the parameters of the VLQ from the FCNC processes in the neutral $B_{d,s}$ meson systems; B_s^0-$\overline{B_s^0}$ mixing, $\overline{B_s^0} \to \mu^+\mu^-$ and $\overline{B_d^0} \to X_s\gamma$. The $\overline{B_d^0}$ meson consists of the b-quark and anti-d-quark while $\overline{B_s^0}$ meson consists of the b-quark and anti-s-quark. Those processes correspond to the $b \to s$ transition at the quark level. One of the observables related to the B_s^0-$\overline{B_s^0}$ mixing is the mass difference of the neutral B_s meson, Δm_{B_s}. The Δm_{B_s} is used in order to determine elements of the CKM matrix. The $\overline{B_s^0} \to \mu^+\mu^-$ process is induced by the FCNC with the Z boson as shown in Fig.1.1. The branching ratio is measured by the LHCb and CMS experiments [53, 54, 55, 56] at the LHC and its recent value is $(3.0 \pm 0.6^{+0.3}_{-0.2}) \times 10^{-9}$ reported by the LHCb experiment [56]. The inclusive radiative decay $\overline{B_d^0} \to X_s\gamma$ process corresponds to the $b \to s\gamma$ transition at the quark level. The branching ratio is measured at BaBar [57, 58, 59], Belle [60, 61, 62] and CLEO [63] experiments, and the averaged value of these experimental results are $(3.32 \pm 0.15) \times 10^{-4}$ [64]. We note that these branching ratios are actually much smaller than the charged current procrss, $\mathrm{Br}[B_d^0 \to X_c e^+\nu_e] = (10.1 \pm 0.4) \times 10^{-2}$ [65].

If a new heavy particle exists, contributions from the new particle to the observables are measured as deviations from values predicted by the SM. The searches for the deviations from the SM predictions are referred to as indirect searches. Since we do not need to know kinematical information of the new heavy particle in the analysis of the indirect searches, it is useful to describe the models without dynamical degrees of freedom of the new heavy particle. This description is called standard model effective field theory (SMEFT). The SMEFT is an effective field theory (EFT) which consists of only the SM particles. There are higher-dimensional operators which are invariant under the gauge symmetry of the SM; $\mathrm{SU}(3)_c \times \mathrm{SU}(2)_L \times U(1)_Y$. Effects from the new heavy particles are embedded in the higher-

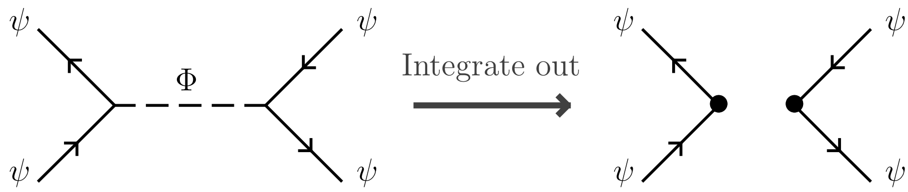

Figure 1.2. Integrating out a heavy particle Φ. The symbol ψ represents a SM particle. The set of disk marks means insertion of an effective operator.

dimensional operators. The whole Lagrangian for the SMEFT can be written as [66, 67],

$$\mathcal{L}_{\rm SMEFT} \;=\; \mathcal{L}_{\rm SM} + \sum_i \left[\frac{c_i^{(5)}}{\Lambda_{\rm NP}} \mathcal{O}_i^{(5)} + \frac{c_i^{(6)}}{\Lambda_{\rm NP}^2} \mathcal{O}_i^{(6)} + O\!\left(\frac{1}{\Lambda_{\rm NP}^3} \right) \right], \tag{1.1}$$

where $\mathcal{O}_i^{(n)}$ with $n > 4$ denotes dimension n operators and $\Lambda_{\rm NP}$ corresponds to a NP scale, such as the mass of new heavy particles. The term $\mathcal{L}_{\rm SM}$ is the SM Lagrangian including only dimension 4 operators. The coefficients $c_i^{(n)}$ are coupling constants for dimension n operators and called Wilson coefficients. The effects from the higher-dimensional operators become small as the dimension of the operators increases because of the suppression factor $\Lambda^{4\quad n}$. If we impose the lepton number conservation, the lowest dimension of the higher dimensional operators is six. A first attempt to construct a complete set of dim.6 operators was given in Ref.[66]. In the following, we use so-called "Warsaw basis" [67] which contains 59 baryon number conserving operators. The SMEFT allows us to analyze phenomena independently of NP models. For instance, some constraints on the Wilson coefficients of the SMEFT from precise measurements with respect to phenomena at the EW scale, namely electroweak precision tests (EWPT) [68, 69, 70, 71, 72, 73, 74].

Once we fix a specific NP model with new heavy particles, the Wilson coefficents can be expressed in terms of parameters of the NP model by integrating out the new heavy particles. Figure.1.2 shows the procedure "integrating out". The symbol Φ represents a heavy particle which is integrated out while the symbol ψ represents a SM particle. The set of disk marks means insertion of an effective operator. The procedure "integrating out" is performed around the mass scale of the new heavy particle. The mass scale of the new heavy particle is generally much higher than the EW scale. The difference between the NP scale $\Lambda_{\rm NP}$ and the EW scale $\Lambda_{\rm EW}$ gives rise to corrections which are proportional to $\ln(\Lambda_{\rm NP}/\Lambda_{\rm EW})$. Such corrections will be large in the case of $\Lambda_{\rm NP} \gg \Lambda_{\rm EW}$. We can take account of the logarithmic corrections by solving renormalization group (RG) equations for the Wilson coefficients with an anomalous dimension matrix of the SMEFT [75, 76, 77]. The SMEFT allows us to connect observables at different energy scales, such as observables of the B meson system and the EWPT.

In this thesis, we consider a model with one down-type $\mathrm{SU}(2)_L$ singlet VLQ as a simple model to clarify constraints on parameters of the VLQ. We expect that the VLQ is much heavier than the EW scale because of the constraints from the direct search at the LHC, and thus we investigate the model on the basis of the SMEFT. There are rich phenomenology in the model with VLQ, for instance [78, 79, 80, 81]. The analyses of the model with VLQs in terms of the SMEFT were performed in Refs.[82, 83, 84]. One of the new points of our work [84] is an analysis of the inclusive radiative B_d^0 meson decay $\overline{B_d^0} \to X_s\gamma$ on the basis of the SMEFT. We have to construct SMEFT from the model with VLQ up to the one-loop level in order to analyze the $\overline{B_d^0} \to X_s\gamma$ process. We clarify constraints on the parameters of the VLQ from the $\overline{B_d^0} \to X_s\gamma$ process in addition to the $\overline{B_s^0} \to \mu^+\mu$ process. The SMEFT constructed in this thesis can be applied to other FCNC processes, namely $b \to d$ and $s \to d$ transitions. In addition, the Wilson coefficient for the radiative transition $b \to s\gamma$ also contributes to the CP asymmetry in the radiative decays [85, 86, 87], the inclusive [88, 89] and the exclusive [90, 91, 92] $b \to s l^+ l$ processes.

This thesis is organized as follows. In Chap.2 and Chap.3, we give some reviews as introduction. We briefly summarize the SM and the model with VLQ in Chap.2. We show the features of the model with VLQ, such as the tree level FCNC and violation of the CKM matrix. In Chap.3, we give the basic idea of EFT. As a simple example, we construct an EFT by integrating out heavy SM particles, like W boson. We refer that EFT as weak EFT in this thesis.

After these chapters, we present our results based on Ref.[84]. In Chap.4, we construct the SMEFT by integrating out the down-type $\mathrm{SU}(2)_L$ singlet VLQ. Inserting a vacuum expectation value into the Higgs field in the derived effective operators of the SMEFT, we obtain the Lagrangian below the EW scale. The FCNCs and the violation of the CKM unitarity are expressed in terms of the Wilson coefficients of the SMEFT. We investigate RG effects for the Wilson coefficients obtained at the tree level.

In the analysis of the neutral B meson systems, we use the weak EFT. We present a procedure of matching the model with VLQ in terms of the SMEFT with the weak EFT in Chap.5. In order to determine Wilson coefficients which we need to compute the $\overline{B_d^0} \to X_s\gamma$ process, we calculate the amplitude of the $b \to s\gamma$ transition. We carefully investigate the cancellation of the divergence in the $b \to s\gamma$ amplitudes since the violation of the CKM unitarity leads new divergence which does not appear in the SM calculation.

We give numerical results in Chap.6. We show the dependence of the branching ratios of the $\overline{B_s^0} \to \mu^+\mu$ and the $\overline{B_d^0} \to X_s\gamma$ processes on the parameters of the VLQ. We also present parameter regions allowed by the experimental data of the branching ratios of the $\overline{B_s^0} \to \mu^+\mu$ and the $\overline{B_d^0} \to X_s\gamma$ processes. Then, the summary and discussion are given in Chap.7.

In Appendix.A, we give the derivation of formulae for the observables of the neutral B meson systems, which are used in Chap.5. Appendix.B is devoted to the computation of the amplitude for the $b \to s\gamma$ process. Here we focus on the diagrams which also exist in the SM. We do not use the CKM unitarity in contrast to the SM calculations.

Chapter 2

Standard Model and Vector-like Quark

2.1 The Standard Model

In this section, we see the standard model (SM) of the particle physics. It is known that there are four interactions acting among the elementary particles, namely strong, weak, electromagnetic interactions and the gravity. The gauge symmetry $\mathrm{SU}(3)_c \times \mathrm{SU}(2)_L \times U(1)_Y$ induces these interactions except the gravity in the SM. The particle content with the quantum numbers under the SM gauge symmetry are shown in Table 2.1. There are three generations of the fermions in the SM. All the generations have the same quantum numbers. In Table 2.1, the symbols G^a_μ, W^I_μ and B_μ with $a = 1 \sim 8$, $I = 1, 2, 3$ represent the $\mathrm{SU}(3)_c$ gauge boson (gluons), the $\mathrm{SU}(2)_L$ gauge bosons and the $U(1)_Y$ gauge boson, respectively. The symbol ϕ is the $\mathrm{SU}(2)_L$ Higgs doublet. The $U(1)_Y$ hypercharge Y is written in the fourth row of the Table 2.1 and relates to the electromagnetic charge Q as,

$$Q = I^W_3 + \frac{Y}{2} \,, \tag{2.1}$$

where I^W_3 denotes the third component of the weak isospin. The SM quark Lagrangian which is invariant under the SM gauge symmetry is given as,

$$\mathcal{L}^q_{\mathrm{SM}} = \mathcal{L}^q_{\mathrm{SM},K} + \mathcal{L}^q_{\mathrm{SM},Y} \,, \tag{2.2}$$

with

$$\mathcal{L}^q_{\mathrm{SM},K} = \bar{q}^i_L i\gamma^\mu D^q_{L\mu} q^i_L + \bar{u}^i_R i\gamma^\mu D^u_{R\mu} u^i_R + \bar{d}^i_R i\gamma^\mu D^d_{R\mu} d^i_R \,, \tag{2.3}$$

$$\mathcal{L}^q_{\mathrm{SM},Y} = [y^{ij}_d \bar{q}^i_L \phi d^j_R + y^{ij}_u \bar{q}^i_L \tilde{\phi} u^j_R + h.c.] \,. \tag{2.4}$$

Particles	Fermions					Gauge Bosons			Scalar
	$q_L^i=(u_L^i,d_L^i)$	u_R^i	d_R^i	$l_L^i=(\nu_L^i,e_L^i)$	e_R^i	G_μ^a	W_μ^I	B_μ	ϕ
SU(3)$_c$	**3**	**3**	**3**	**1**	**1**	**8**	**1**	**1**	**1**
SU(2)$_L$	**2**	**1**	**1**	**2**	**1**	**1**	**3**	**1**	**2**
$U(1)_Y$	$+1/3$	$+4/3$	$2/3$	1	2	0	0	0	1

Table 2.1. The particle content with quantum numbers in the SM. The index $i=1,2,3$ denotes generation of the fermions. The symbols G_μ^a, W_μ^I and B_μ with $a=1\sim 8$, $I=1,2,3$ represent SU(3)$_c$ gauge boson (gluons), SU(2)$_L$ gauge bosons and $U(1)_Y$ gauge boson, respectively. The symbol ϕ is SU(2)$_L$ Higgs doublet.

The gauge interactions come from the covariant derivatives D_L^q and $D_R^{u,d}$ in the kinetic terms Eq.(2.3):

$$D_{L\mu}^q = \partial_\mu + i g' \frac{Y_{qL}}{2} B_\mu + i g \frac{\tau^I}{2} W_\mu^I + i g_s \frac{\lambda^a}{2} G_\mu^a \,, \tag{2.5}$$

$$D_{R\mu}^u = \partial_\mu + i g' \frac{Y_{uR}}{2} B_\mu + i g_s \frac{\lambda^a}{2} G_\mu^a \,, \tag{2.6}$$

$$D_{R\mu}^d = \partial_\mu + i g' \frac{Y_{uR}}{2} B_\mu + i g_s \frac{\lambda^a}{2} G_\mu^a \,, \tag{2.7}$$

where Y_{qL}, Y_{uR} and Y_{dR} denote the $U(1)_Y$ hypercharge of the q_L, u_R and d_R respectively. The 2×2 matrices τ^I with $I=1,2,3$ are called Pauli matrices and the 3×3 matrices λ^a with $a=1\sim 8$ are called Gell-mann matrices. The coupling constants g_s, g and g' correspond to the gauge couplings for the SU(3)$_c$, SU(2)$_L$ and $U(1)_Y$, respectively. The field $\tilde{\phi}$ in Eq.(2.4) is defined by $\tilde{\phi}=i\tau^2\phi^*$.

The subscript i in Eqs.(2.3) and (2.4) represents the generations of the quarks; $i=1,2,3$. We can see from the Eqs.(2.3) and (2.4) that the different generations are mixed by the Yukawa interactions in Eq.(2.4) but not mixed by the gauge interactions in Eq.(2.3). This basis is referred to as interaction basis or weak basis.

In Eq.(2.4), the both Yukawa coupling matrix y_d and y_u are general complex matrix. One can take a basis where one of the Yukawa coupling matrices is real diagonal without loss of generality. Here we adopt a real diagonal basis of the up-type Yukawa coupling y_u. This can be done by introducing the following unitary transformtaions,

$$\begin{cases} q_L^i = U_{qL}^{ij} q_L^{0j} \\ u_R^i = U_{uR}^{ij} u_R^{0j} \end{cases} , \tag{2.8}$$

where the 3×3 unitary matrices U_{qL} and U_{uR} diagonalize the Yukawa coupling y_u:

$$[U_{qL}^\dagger y_u U_{uR}]^{kl} \overline{q_L^{0k}} \tilde{\phi} u_R^{0l} \;\equiv\; Y_u^k \overline{q_L^{0k}} \tilde{\phi} u_R^{0k} \,, \tag{2.9}$$

with $Y_u^k \equiv \mathrm{diag}[Y_u, Y_c, Y_t]$. The unitary transformtaions Eq.(2.8) affect the down-type Yukawa interaction $y_d^{ij}\bar{q_L^i}\phi d_R^j$, but the modification can be absorbed into the Yukawa coupling y_d as,

$$y_d^{ij}\bar{q_L^i}\phi d_R^j \;=\; [U_{qL}^\dagger y_d]^{kj}\overline{q_L^{0k}}\phi d_R^j \;\equiv\; y_d'^{kj}\overline{q_L^{0k}}\phi d_R^j\,. \tag{2.10}$$

Therefore, we can take the basis where the Yukawa coupling of the up-type quarks is real diagonal while that of the down-type quarks is general complex matrix without loss of generality. We note that the kinetic terms in Eq.(2.3) do not change under the transformations Eq.(2.8). The unitary transformation which do not change the gauge interactions, such as the transformation Eq.(2.8), is called weak basis transformation. In the following, we simply take the Yukawa coupling y_u in Eq.(2.4) as a real diagonal matrix, that is $y_u^{ij} \to y_u^i\delta^{ij}$.

2.1.1 Quark masses

We can see from the Table 2.1 that the left-handed fermions have different quantum numbers from the right-handed fermions. This assignment of the quantum numbers forbids mass terms of the SM fermions, like $m_u\bar{u}_L u_R$, because of the electroweak (EW) gauge symmetry $\mathrm{SU}(2)_L \times U(1)_Y$. In the SM, the Yukawa interactions in Eq.(2.4) lead to the mass of the SM fermions. The EW gauge symmetry $\mathrm{SU}(2)_L \times U(1)_Y$ is broken down to the electromagnetic (EM) gauge symmetry $U(1)_{\mathrm{EM}}$ by a vacuum expectation value (VEV) v of the Higgs doublet ϕ,

$$\phi \;\to\; \frac{1}{\sqrt{2}}\begin{pmatrix} 0 \\ v \end{pmatrix}. \tag{2.11}$$

The Yukawa interactions become mass terms of the SM quarks by inserting the VEV into the Higgs doublet ϕ:

$$\mathcal{L}_{\mathrm{SM},Y}^q \;\to\; [m_d^{ij}\bar{d_L^i}d_R^j + M_u^i\bar{u_L^i}u_R^i + h.c.]\,, \tag{2.12}$$

where the 3×3 mass matrices m_d and M_u are defiend as,

$$m_d^{ij} \;\equiv\; \frac{v}{\sqrt{2}}y_d^{ij}\,, \tag{2.13}$$

$$M_u^i \;\equiv\; \frac{v}{\sqrt{2}}y_u^i\,. \tag{2.14}$$

These mass matrix m_d is generally non-diagonal complex matrix. We can obtain the physical quark masses by diagonalizing m_d. We consider a bi-unitry transformation of the quark fileds with unitary matrices K_{dL} and K_{dR}:

$$\begin{cases} d_L^i = K_{dL}^{im}d_L'^m \\ d_R^i = K_{dR}^{im}d_R'^m \end{cases}. \tag{2.15}$$

The unitary matrices in Eq.(2.15) diagonalize the mass matrix m_d as,

$$K_{dL}^\dagger m_d K_{dR} \;=\; \mathrm{diag}[m_d, m_s, m_b] \;\equiv\; M_d\,, \tag{2.16}$$

where $m_{d,s,b}$ are the physical quark masses. The quark mass terms Eq.(2.12) become,

$$\mathcal{L}^q_{\mathrm{SM},Y} \;\to\; \quad \left[M_d^i \overline{d'^i_L} d'^i_R + M_u^i \overline{u^i_L} u^i_R + h.c. \right] . \tag{2.17}$$

The basis where the quark mass matrices are diagonal is called mass basis.

2.1.2 Charged current and CKM matrix

In contrast to the weak basis transformation Eq.(2.8), the unitary transformations in Eq.(2.15) change the gauge interactions in the kinetic terms Eq.(2.3). This is because the left-handed down-type quarks in the quark doublet q_L transform under the transformation in Eq.(2.15) while the left-handed up-type quarks remain as they are. Here we focus on the gauge interactions of the $\mathrm{SU}(2)_L$ gauge bosons W^1_μ and W^2_μ in the kinetic term of $\mathrm{SU}(2)_L$ doublet quarks q_L. After the transformations in Eq.(2.15), these gauge interactions become,

$$\begin{aligned} \bar{q}^i_L i\gamma^\mu D^q_{L\mu} q^i_L \;&\supset\; \frac{g}{2}\begin{pmatrix} \overline{u^i_L} & \bar{d}^i_L \end{pmatrix} \gamma^\mu \begin{pmatrix} 0 & W^1_\mu \quad iW^2_\mu \\ W^1_\mu + iW^2_\mu & 0 \end{pmatrix} \begin{pmatrix} u^i_L \\ d^i_L \end{pmatrix} \\ &= \frac{g}{\sqrt{2}} [\overline{u^i_L} \gamma^\mu K^{im}_{dL} d'^m_L W^+_\mu + \overline{d'^m_L} K^{\dagger mi}_{dL} \gamma^\mu u^i_L W_\mu \;] , \end{aligned} \tag{2.18}$$

where the charged gauge boson $W^\pm$ is defined as,

$$W^\pm_\mu \;\equiv\; \frac{1}{\sqrt{2}} (W^1_\mu \mp i W^2_\mu) . \tag{2.19}$$

In the mass basis of the quarks, the different generations of the quarks are mixed by the gauge interaction of the W boson. The mixing matrix K_{dL} in Eq.(2.18) is called Cabibbo–Kobayashi–Maskawa (CKM) matrix,

$$V_{\mathrm{CKM}} \;\equiv\; K_{dL} . \tag{2.20}$$

Since the CKM matrix is a unitary matrix, the CKM matrix satisfies the relations,

$$\sum_{i=u,c,t} V^{im*}_{\mathrm{CKM}} V^{in}_{\mathrm{CKM}} \;=\; \delta^{mn} , \tag{2.21}$$

$$\sum_{m=d,s,b} V^{im}_{\mathrm{CKM}} V^{jm*}_{\mathrm{CKM}} \;=\; \delta^{ij} . \tag{2.22}$$

The quark mass terms Eq.(2.17) is invariant under rephasing of the quark fields,

$$\begin{cases} d'^m_L \to e^{i\phi^m_{dL}} d'^m_L \\ d'^m_R \to e^{i\phi^m_{dR}} d'^m_R \end{cases} , \quad \text{and} \quad \begin{cases} u^i_L \to e^{i\phi^i_{uL}} u^i_L \\ u^i_R \to e^{i\phi^i_{uR}} u^i_R \end{cases} , \tag{2.23}$$

and hence some phases of the CKM matrix are absorbed into the quark fields. Taking account of the rephasing and the unitarity relations Eqs.(2.21) and (2.22), the number of degree of freedom in the CKM matrix is,

$$\text{Mixing angle} \;:\; \frac{n_g(n_g \quad 1)}{2} , \tag{2.24}$$

$$\text{Physical phase} \;:\; \frac{(n_g \quad 2)(n_g \quad 1)}{2} , \tag{2.25}$$

where n_g is the number of generations of quarks, that is $n_g = 3$ in the SM. Thus the CKM matrix in the SM has three mixing angles and one physical phase.

2.1.3 Neutral currents

Next we focus on the gauge interactions of the $\mathrm{SU}(2)_L$ gauge bosons W^3_μ and the $U(1)_Y$ gauge boson B_μ. Taking account of the transformations in Eq.(2.15), these gauge interactions become,

$$
\begin{aligned}
\mathcal{L}^q_{\mathrm{SM},K} \supset\ & \frac{1}{2}\begin{pmatrix} \overline{u^i_L} & \bar{d}^i_L \end{pmatrix}\gamma^\mu \begin{pmatrix} gW^3_\mu + g'Y_{qL}B_\mu & 0 \\ 0 & gW^3_\mu + g'Y_{qL}B_\mu \end{pmatrix}\begin{pmatrix} u^i_L \\ d^i_L \end{pmatrix} \\
& \frac{g'}{2}[Y_{uR}\overline{u^i_R}\gamma^\mu u^i_R + Y_{dR}\overline{d^i_R}\gamma^\mu d^i_R]B_\mu \\
=\ & \frac{g}{c_w}\left[\bar{u}^i\gamma^\mu\left(\frac{1}{2}L \quad Q_u s_w^2\right)u^i + \overline{d'^m}\gamma^\mu\left(\quad\frac{1}{2}L \quad Q_d s_w^2\right)d'^m\right]Z_\mu \\
& e[Q_u\bar{u}^i\gamma^\mu u^i + Q_d\overline{d'^m}\gamma^\mu d'^m]A_\mu\,,
\end{aligned} \tag{2.26}
$$

where $c_w = \cos\theta_w$ and $s_w = \sin\theta_w$ with the Weinberg angle θ_w. The symbol Z_μ is the Z boson while A_μ denotes the photon field, which are defined as

$$
\begin{pmatrix} W^3_\mu \\ B_\mu \end{pmatrix} \equiv \begin{pmatrix} c_w & s_w \\ s_w & c_w \end{pmatrix}\begin{pmatrix} Z_\mu \\ A_\mu \end{pmatrix}. \tag{2.27}
$$

The electromagnetic charge e is related to the gauge couplings g and g':

$$
e \equiv \frac{gg'}{\sqrt{g^2 + g'^2}} = gs_w = g'c_w\,. \tag{2.28}
$$

One of the features in the SM is that the different generations (flavors) of the quarks are not mixed by the Z and photon interactions Eq.(2.26). In other words, there is no flavor changing neutral current (FCNC) at the tree level and the FCNCs are induced by loop diagrams in the SM. This is one of the aspects of the Glashow–Iliopoulos–Maiani (GIM) mechanism [6].

2.2 Model with Vector-like Quark

We are going to investigate the model with VLQ in terms of the full theory. We consider a model which contains one $\mathrm{SU}(2)_L$ singlet down-type VLQ denoted as d^4. The representation of the VLQ under $\mathrm{SU}(3)_c \times \mathrm{SU}(2)_L \times U(1)_Y$ is,

$$
d^4_{L,R}\ :\ \left(\mathbf{3}, \mathbf{1},\ \frac{2}{3}\right). \tag{2.29}
$$

The most general Lagrangian for the VLQ is

$$
\begin{aligned}
\mathcal{L}_{\mathrm{VLQ}} =\ & \bar{d}^4_L\, i\gamma_\mu D^\mu_{dR} d^4_L + \bar{d}^4_R\, i\gamma_\mu D^\mu_{dR} d^4_R \\
& [y_d^{i4}\bar{q}^i_L\phi\, d^4_R + M^{44}_{\mathrm{VLQ}}\bar{d}^4_L d^4_R + M^{4j}_{\mathrm{VLQ}}\bar{d}^4_L d^j_R + h.c.]\,,
\end{aligned} \tag{2.30}
$$

where the covariant derivative is the same as that of the SM right-handed down-type quarks. The VLQ d^4 has the mass term without the Yukawa interaction through the $\mathrm{SU}(2)_L$ Higgs doublet since the representation of the left- and right-handed VLQ is the same. In the present section, the indices i, j and k denote the generation of SM quarks ($i, j, k = 1 \sim 3$) and indices α, β and γ represent all the quarks including VLQ ($\alpha, \beta, \gamma = 1 \sim 4$).

2.2.1 Diagonalization of Mass Matrix

We consider the steps of the diagonalization of the down-type quark mass matrix. Here we take the up-type quark mass matrix diagonal. A 4×4 mass matrix which includes both the SM down-type quarks and the VLQ d^4 is given as,

$$M_D^{(0)} = \begin{pmatrix} \frac{vy_d^{11}}{\sqrt{2}} & \frac{vy_d^{12}}{\sqrt{2}} & \frac{vy_d^{13}}{\sqrt{2}} & \frac{vy_d^{14}}{\sqrt{2}} \\ \frac{vy_d^{21}}{\sqrt{2}} & \frac{vy_d^{22}}{\sqrt{2}} & \frac{vy_d^{23}}{\sqrt{2}} & \frac{vy_d^{24}}{\sqrt{2}} \\ \frac{vy_d^{31}}{\sqrt{2}} & \frac{vy_d^{32}}{\sqrt{2}} & \frac{vy_d^{33}}{\sqrt{2}} & \frac{vy_d^{34}}{\sqrt{2}} \\ M_{\mathrm{VLQ}}^{41} & M_{\mathrm{VLQ}}^{42} & M_{\mathrm{VLQ}}^{43} & M_{\mathrm{VLQ}}^{44} \end{pmatrix}. \tag{2.31}$$

We can choose a basis where the elements $\begin{pmatrix} M_{\mathrm{VLQ}}^{41} & M_{\mathrm{VLQ}}^{42} & M_{\mathrm{VLQ}}^{43} \end{pmatrix}$ are zero by using a weak basis transformation without loss of generality:

$$M_D = \begin{pmatrix} \frac{vy_d^{11}}{\sqrt{2}} & \frac{vy_d^{12}}{\sqrt{2}} & \frac{vy_d^{13}}{\sqrt{2}} & \frac{vy_d^{14}}{\sqrt{2}} \\ \frac{vy_d^{21}}{\sqrt{2}} & \frac{vy_d^{22}}{\sqrt{2}} & \frac{vy_d^{23}}{\sqrt{2}} & \frac{vy_d^{24}}{\sqrt{2}} \\ \frac{vy_d^{31}}{\sqrt{2}} & \frac{vy_d^{32}}{\sqrt{2}} & \frac{vy_d^{33}}{\sqrt{2}} & \frac{vy_d^{34}}{\sqrt{2}} \\ 0 & 0 & 0 & M_4 \end{pmatrix} \equiv \begin{pmatrix} m_D & J_D \\ 0 & M_4 \end{pmatrix}, \tag{2.32}$$

where m_D is a 3×3 matrix corresponding to the mass matrix of SM down-type quarks and J_D is a 3×1 vector. We then diagonalize the mass matrix M_D. First we consider the diagonalization of the 3×3 matrix part m_D by using a bi-unitary transformation:

$$d_L^i = K_L^{ij} d_L^{0j}, \tag{2.33}$$

$$d_R^i = K_R^{ij} d_R^{0j}, \tag{2.34}$$

where K_L and K_R are 3×3 unitary matrices which diagonalize the matrix m_D and the mass matrix becomes,

$$\begin{aligned} M_D' &\equiv \begin{pmatrix} K_L^\dagger & 0 \\ 0 & 1 \end{pmatrix} \begin{pmatrix} m_D & J_D \\ 0 & M_4 \end{pmatrix} \begin{pmatrix} K_R & 0 \\ 0 & 1 \end{pmatrix} \\ &= \begin{pmatrix} K_L^\dagger m_D K_R & K_L^\dagger J_D \\ 0 & M_4 \end{pmatrix} = \begin{pmatrix} m_D^{\mathrm{diag}} & J_D' \\ 0 & M_4 \end{pmatrix}, \end{aligned} \tag{2.35}$$

Here we define,

$$J'_D \;=\; K_L^\dagger J_D, \tag{2.36}$$
$$Y_d^{i4} \;=\; K_L^{\dagger ij} y_d^{j4}, \tag{2.37}$$

We then define unitary matrices $U_{L,R}$ which diagonalize 4×4 mass matrix M_D,

$$U_L \;\equiv\; \begin{pmatrix} K_L & 0 \\ 0 & 1 \end{pmatrix} V_L\,, \tag{2.38}$$
$$U_R \;\equiv\; \begin{pmatrix} K_R & 0 \\ 0 & 1 \end{pmatrix} V_R\,, \tag{2.39}$$

with

$$d_L^\alpha \;=\; U_L^{\alpha\beta} {d'}_L^{\beta}, \tag{2.40}$$
$$d_R^\alpha \;=\; U_R^{\alpha\beta} {d'}_R^{\beta}, \tag{2.41}$$

where $V_{L,R}$ in Eqs.(2.38) and (2.39) are 4×4 unitary matrices. The symbol d' represents the down-type quarks in the mass basis, $d' = (\,d \;\; s \;\; b \;\; B\,)^T$ where B denotes the VLQ in the mass basis. We can diagonalize $M_D M_D^\dagger$ as follows:

$$\begin{aligned} U_L^\dagger M_D M_D^\dagger U_L &= U_L^\dagger M_D U_R U_R^\dagger M_D^\dagger U_L \\ &= V_L^\dagger \begin{pmatrix} (m_D^{\rm diag})^2 + J'_D {J'_D}^\dagger & M_4 J'_D \\ M_4 {J'_D}^\dagger & M_4^2 \end{pmatrix} V_L \\ &= \begin{pmatrix} m_d^2 & 0 & 0 & 0 \\ 0 & m_s^2 & 0 & 0 \\ 0 & 0 & m_b^2 & 0 \\ 0 & 0 & 0 & M_{\rm VLQ}^2 \end{pmatrix}. \end{aligned} \tag{2.42}$$

2.2.2 CKM unitarity and Z FCNC

The kinetic terms of the down-type VLQ d^4 and the SM quarks are given as follows:

$$\mathcal{L}_K^q \;=\; \overline{q_L^i}\, i\gamma_\mu D_L^\mu q_L^i + \overline{d_R^i}\, i\gamma_\mu D_{dR}^\mu d_R^i + \overline{u_R^i}\, i\gamma_\mu D_{uR}^\mu u_R^i + \overline{d_L^4}\, i\gamma_\mu D_{dR}^\mu d_L^4 + \overline{d_R^4}\, i\gamma_\mu D_{dR}^\mu d_R^4\,. \tag{2.43}$$

After the EW symmetry breaking and the diagonalization of the quark mass matrices, the gauge interactions for the quarks including the VLQ are derived as,

$$\mathcal{L}_K^q \;\supset\; \mathcal{L}_W + \mathcal{L}_Z + \mathcal{L}_A + \mathcal{L}_G\,, \tag{2.44}$$

with

$$\mathcal{L}_W \;=\; \frac{g}{\sqrt{2}} [\overline{u_L^i} \gamma^\mu K_L^{ij} V_L^{j\beta} d_L^\beta W_\mu^+ + h.c.], \tag{2.45}$$

$$\begin{aligned} \mathcal{L}_Z \;=\; & \frac{g}{c_w} \overline{u^i} \gamma^\mu \left[\frac{1}{2} L \quad s_w^2 Q_u \right] u^i Z_\mu \\ & \frac{g}{c_w} \overline{d^\alpha} \gamma^\mu \left[\quad \frac{1}{2} \{ \delta^{\alpha\beta} \quad V_L^{4\alpha *} V_L^{4\beta} \} L \quad s_w^2 Q_d \right] d^\beta Z_\mu\,, \end{aligned} \tag{2.46}$$

$$\mathcal{L}_A \;=\; e[Q_u \overline{u^i} \gamma^\mu u^i + Q_d \overline{d^\alpha} \gamma^\mu d^\alpha] A_\mu\,, \tag{2.47}$$

$$\mathcal{L}_G \;=\; g_s \left[\overline{u^i} \gamma^\mu \frac{\lambda^a}{2} u^i + \overline{d^\alpha} \gamma^\mu \frac{\lambda^a}{2} d^\alpha \right] G_\mu^a\,, \tag{2.48}$$

where we omit the prime on the quark fields for simplicity. We can see that the gluon and the photon interactions in Eqs.(2.47) and (2.48) are the same as that in the SM. The matrix $K_L^{ij}V_L^{j\beta}$ in Eq.(2.45) corresponds to the 3×4 CKM matrix in the model with the down-type VLQ,

$$V_{\text{CKM}} \equiv K_L V_L \,. \tag{2.49}$$

It is important that FCNCs among the down-type quarks are induced by the Z boson interaction. The existence of the FCNCs comes from the difference among the isospin charge $I_3^W$of the SM quarks and that of the VLQ (Since the VLQ is $\mathrm{SU}(2)_L$ singlet, it does not have the isospin charge). Actually, the FCNCs in Eq.(2.46) is given as follows:

$$\begin{aligned}
\mathcal{L}_Z \supset& \begin{pmatrix} \bar{d}_L^1 & \bar{d}_L^2 & \bar{d}_L^3 & \bar{d}_L^4 \end{pmatrix} \gamma^\mu I_3^W(d) \begin{pmatrix} 1 & & & \\ & 1 & & \\ & & 1 & \\ & & & 0 \end{pmatrix} \begin{pmatrix} d_L^1 \\ d_L^2 \\ d_L^3 \\ d_L^4 \end{pmatrix} Z_\mu \\
=& \quad \bar{d}_L \;\; \bar{s}_L \;\; \bar{b}_L \;\; \overline{B_L} \;) \gamma^\mu I_3^W(d) V_L^\dagger \begin{pmatrix} 1 & & & \\ & 1 & & \\ & & 1 & \\ & & & 0 \end{pmatrix} V_L \begin{pmatrix} d_L \\ s_L \\ b_L \\ B_L \end{pmatrix} Z_\mu \\
=& \; \overline{d^\alpha} \gamma^\mu I_3^W(d) V_L^{i\alpha *} V_L^{i\beta} d_L^\beta Z_\mu \\
=& \; \overline{d^\alpha} \gamma^\mu I_3^W(d) (\delta^{\alpha\beta} \quad V_L^{4\alpha *} V_L^{4\beta}) d_L^\beta Z_\mu \,,
\end{aligned} \tag{2.50}$$

where $I_3^W(d) = \;\; \frac{1}{2}$ is the isospin charge of the SM down-type quarks. We use the unitarity of V_L in the last line of Eq.(2.50). This fact is that the GIM mechanism does not work in the model with VLQ.

We define a matrix which represents the FCNC interaction as,

$$Z_{d\text{NC}}^{\alpha\beta} \equiv \delta^{\alpha\beta} \quad V_L^{4\alpha *} V_L^{4\beta} \,. \tag{2.51}$$

The 3×4 CKM matrix is not a unitary matrix in the model with the VLQ:

$$\sum_{i=1}^{3} V_{\text{CKM}}^{i\alpha *} V_{\text{CKM}}^{i\beta} = \sum_{i=1}^{3} V_L^{\dagger \alpha i} V_L^{i\beta} = \delta^{\alpha\beta} \quad V_L^{4\alpha *} V_L^{4\beta} = Z_{d\text{NC}}^{\alpha\beta} \,, \tag{2.52}$$

since $\sum_{\gamma=1}^{4} V_L^{\dagger \alpha\gamma} V_L^{\gamma\beta} = \delta^{\alpha\beta}$. The relation in Eq.(2.52) shows that the unitarity of the 3×4 CKM matrix does not hold due to the factor $V_L^{4\alpha *} V_L^{4\beta}$ which is related to the matrix $Z_{d\text{NC}}$ in the FCNC interactions. In contrast to the Eq.(2.52), the CKM unitarity with respect to the up-type sector holds in the full theory description:

$$\sum_{\alpha=1}^{4} V_{\text{CKM}}^{i\alpha} V_{\text{CKM}}^{j\alpha *} = \delta^{ij} \,. \tag{2.53}$$

Chapter 3
Effective Field Theory

An effective field theory (EFT) is a useful tool to investigate a physical system. In order to describe a physical system at an energy scale μ, we do not need to know dynamics at a higher energy scale $\mu_0 \gg \mu$. An EFT at the scale μ is built by removing some dynamical degree of freedom related to the higher energy scale μ_0. The EFT allows us to simplify computations of the physical system at the energy scale μ since we can focus on the relevant degree of freedom at the energy scale μ.

In the present chapter, we derive an EFT by removing the heavy particles in the SM. In other words, we integrate out the heavy particles in the SM, such as top quark, $W^{\pm}$, Z and Higgs boson. Here we refer to the EFT as weak EFT. The weak EFT is used to describe physical systems below the EW scale, such as B meson system. The typical energy scale of the B meson system is the bottom quark mass scale, $\mu_b \sim m_b \sim 5$ GeV while the EW scale is around $W^{\pm}$ boson mass scale, $\mu_{\rm EW} \sim M_W \sim 80$ GeV. Since the SM particles whose masses are around the EW scale are heavy degrees of freedom in the B meson system, the weak EFT is suitable to describe it. In this chapter, we give the basic idea of EFTs through simple examples of the weak EFT.

3.1 Example of weak EFT: β decay

First we consider the weak EFT for the β decay as a simple example. The β decay $n \to p + e \ \ + \bar{\nu}_e$ corresponds to $d \to u + e \ \ + \bar{\nu}_e$ process at the quark level. This process is induced by the weak interaction of $W^{\pm}$ boson. The diagrams of the β decay in the SM and the weak EFT are shown in Fig.3.1. The left-hand side figure of Fig.3.1 is the diagram in the SM while the right-hand side figure of Fig.3.1 is the diagram in the weak EFT. In the right-hand side figure of Fig.3.1, the $W^{\pm}$ boson is integrated out. The amplitude of the β decay in the SM is obtained as,

$$
\begin{aligned}
i\mathcal{A}_{\rm SM} &= \left[\overline{u_u}\left(\ \ i\frac{g}{\sqrt{2}}V_{ud}\gamma^{\mu}L\right)u_d\right]\frac{i g_{\mu\nu}}{p^2 \ \ M_W^2}\left[\bar{u_e}\left(\ \ i\frac{g}{\sqrt{2}}\gamma^{\nu}L\right)u_{\nu_e}\right] \\
&= i\frac{g^2}{2}V_{ud}\frac{1}{p^2 \ \ M_W^2}[\overline{u_u}\gamma^{\mu}L u_d][\bar{u_e}\gamma_{\mu}L u_{\nu_e}]\,, \qquad (3.1)
\end{aligned}
$$

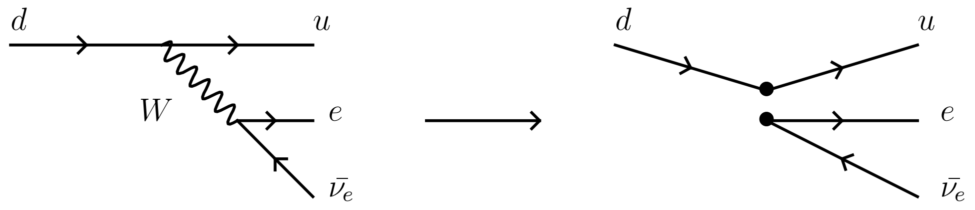

Figure 3.1. The β decay in the quark level. The left-hand side figure is the diagram in the SM while the right-hand side figure is the diagram in the weak EFT.

where u_i with $i = u, d, e, \nu_e$ denote Dirac spinors and V_{ud} is the element of the CKM matrix, $V_{ij} \equiv V_{\rm CKM}^{ij}$. The symbol p is the momentum of the internal $W^\pm$ boson. Since the typical scale of the momentum p is a mass scale of the initial state, that is mass of the neutron; $p^2 \sim m_N^2 \sim 1\,\mathrm{GeV}^2$. It allows us to expand the denominator of the $W^\pm$ boson propagator:

$$\mathcal{A}_{\rm SM} \simeq \frac{g^2}{2M_W^2} V_{ud} [\overline{u_u} \gamma^\mu L u_d][\bar{u}_e \gamma_\mu L u_{\nu_e}] + \mathcal{O}\left(\frac{p^2}{M_W^2}\right). \tag{3.2}$$

On the other hand, the amplutide in the weak EFT can be computed by introducing an effective operator $O^{(\beta)}(\mu)$,

$$\mathcal{H}_{eff}(d \to u + e \quad + \bar{\nu}_e) = C^{(\beta)}(\mu) O^{(\beta)} \equiv C^{(\beta)}(\mu) [\bar{u}\gamma^\mu L d][\bar{e}\gamma_\mu L \nu_e], \tag{3.3}$$

where $C^{(\beta)}(\mu)$ is a coupling constant of the operator $O^{(\beta)}$ at energy scale μ. The coupling constant $C^{(\beta)}(\mu)$ is called Wilson coefficient. The effective operator $O^{(\beta)}$ has mass dimension 6, and thus it is called higher dimensional operator. Since $O^{(\beta)}$ has dim.6 and the mass dimension of Hamiltonian is four, the mass dimension of the Wilson coefficient $C^{(\beta)}(\mu)$ is 2. Using the Hamiltonian Eq.(3.3), we can calculate the amplitude of β decay:

$$\mathcal{A}_{\rm EFT} = C^{(\beta)}(\mu) [\overline{u_u} \gamma^\mu L u_d][\bar{u}_e \gamma_\mu L u_{\nu_e}]. \tag{3.4}$$

The Wilson coefficient $C^{(\beta)}$ in Eq.(3.3) is determined so that the amplitude in the weak EFT Eq.(3.4) is equal to that in the SM Eq.(3.2). The Wilson coefficient $C^{(\beta)}$ is given as,

$$C^{(\beta)}(\mu_{\rm EW}) = \frac{g^2}{2M_W^2} V_{ud} = \frac{4G_F}{\sqrt{2}} V_{ud}, \tag{3.5}$$

where $G_F = \frac{g^2}{4\sqrt{2}M_W^2} = \frac{1}{\sqrt{2}v^2}$ is Fermi constant. The matching condition $\mathcal{A}_{\rm SM} = \mathcal{A}_{\rm EFT}$ holds at the scale of integrating out $W^\pm$ boson field, $\mu_{\rm EW} \simeq M_W$. Therefore, the Wilson coefficient in Eq.(3.5) is defined at the scale $\mu_{\rm EW} \simeq M_W$. In the following, we call the scale of integrating out heavy particles as the matching scale. The Wilson coefficient at an arbitrary scale μ can be obtained by solving renormalization group (RG) equations as we will see in section 3.2. Here we neglect RG effects for simplicity.

We can see from Eq.(3.3) that the Hamiltonian contains only the light degrees of freedom which appear in the initial and final state of β decay. The Hamiltonian does not contain the $W^\pm$ boson as a dynamical degree of freedom but contains the information of the $W^\pm$ boson, the mass M_W and coupling g, in the Wilson coefficient. Measurements of the β decay give constraints on the Wilson coefficient. Taking account of the relation in Eq.(3.5), we can determine a value of $V_{ud}G_F$ from the constraints on the Wilson coefficient.

3.2 Renormalization Group Effect

3.2.1 One-loop level matching

As we see in the previous section, we can determine concrete expression of Wilson coefficients at the matching scale. However, the energy scale of a physical system is generally different from that of the EW scale. In the present section, we see how to compute the scale dependence of Wilson coefficients. In order to clarify the scale dependence on the Wilson coefficients, we need RG equations of the Wilson coefficients. Here we investigate the different example from the previous section to derive the RG equation. We follow Ref.[93]. We consider the following Hamiltonian:

$$\mathcal{H}_{eff} = \frac{4G_F}{\sqrt{2}} V_{cb}^* V_{cs} [C_1(\mu) O_1 + C_2(\mu) O_2] \,, \tag{3.6}$$

where the effective operators are defiend as,

$$O_1 = [\bar{b}_\alpha \gamma^\mu L c_\beta][\bar{c}_\beta \gamma^\mu L s_\alpha] \,, \tag{3.7}$$

$$O_2 = [\bar{b}_\beta \gamma^\mu L c_\beta][\bar{c}_\beta \gamma^\mu L s_\beta] \,. \tag{3.8}$$

The subscripts α, β in O_1 and O_2 denote color indices, $\alpha, \beta = r, g, b$. For example, we can compute the $\bar{b} \to \bar{s}\, c\, \bar{c}$ process by using the effective operators O_1 and O_2. In order to clarify the scale dependence of the Wilson coefficients, we are going to calculate amplitudes of the $\bar{b} \to \bar{s}\, c\, \bar{c}$ process up to the one-loop level.

The Wilson coefficient C_2 can be determined by a similar diagram to the left-hand side of Fig.3.1 at the tree level. The tree level amplitude of the $\bar{b} \to \bar{s}\, c\, \bar{c}$ process is,

$$\mathcal{A}_{\rm SM}^{(0)} \simeq \frac{g^2}{2M_W^2} V_{cb}^* V_{cs} [\overline{v_b^\alpha} \gamma^\mu L v_c^\alpha][\overline{u_c^\beta} \gamma^\mu L v_s^\beta] \,, \tag{3.9}$$

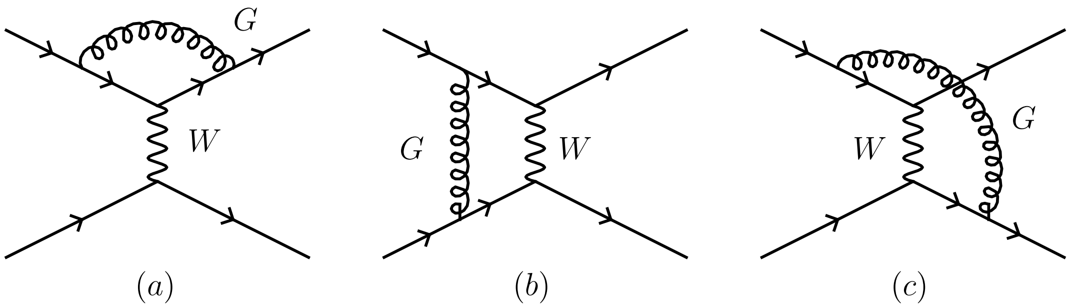

Figure 3.2. Diagrams in the SM which contribute to C_1 and C_2 [93].

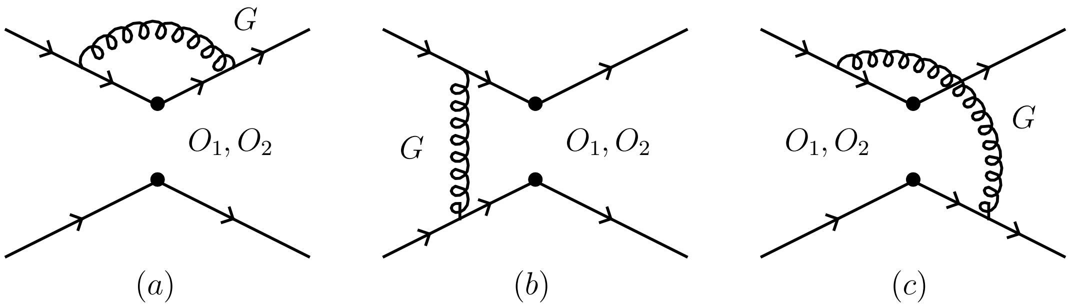

Figure 3.3. Diagrams in the weak EFT which contain to C_1 and C_2 [93]. The set of disc marks represent the effective operators O_1 or O_2.

which leads to the Wilson coefficient,

$$C_2(\mu_{\rm EW}) \;=\; +1\,. \tag{3.10}$$

The Wilson coefficient C_1 at the matching scale $\mu_{\rm EW}$ is zero at the tree level since the weak interaction do not change the color indices.

Next we consider matching at the one-loop level. Diagrams are induced by quantum chromodynamics (QCD) corrections. The relevant diagrams are shown in Figs.3.2 and 3.3. The diagrams shown in Fig.3.2 are one-loop diagrams in the SM while diagrams in Fig.3.3 are one-loop diagrams in the weak EFT. These diagrams corresponds to one-loop QCD corrections to the tree level diagram which is used to determine the Wilson coefficient C_2 at the tree level Eq.(3.10). The set of disk marks in Fig.3.3 represents insertions of the effective operators O_1 or O_2.

We show amplitudes of the $\bar{b}\to\bar{s}\,c\,\bar{c}$ process with the diagrams (a)-(c) in Fig.3.2:

$$\mathcal{A}_{\rm SM}^{(a)} \;=\; \frac{4G_F}{\sqrt{2}}V_{cb}^*V_{cs}C_F\frac{\alpha_s}{4\pi}\left[C_{\rm UV}+\ln\frac{\mu^2}{\lambda^2}\quad\frac{1}{2}\right][\overline{v_b^\alpha}\gamma^\mu L\,v_c^\alpha][\overline{u_c^\beta}\gamma^\mu L\,v_s^\beta]\,, \tag{3.11}$$

$$\mathcal{A}_{\rm SM}^{(b)} \;=\; \frac{4G_F}{\sqrt{2}}V_{cb}^*V_{cs}\frac{\alpha_s}{4\pi}\ln\left[\frac{M_W^2}{\lambda^2}\right][\overline{v_b^\alpha}\gamma^\mu T^a_{\alpha\beta}L\,v_c^\beta][\overline{u_c^\gamma}\gamma^\mu T^a_{\gamma\delta}L\,v_s^\delta]\,, \tag{3.12}$$

$$\mathcal{A}_{\rm SM}^{(c)} \;=\; \frac{16G_F}{\sqrt{2}}V_{cb}^*V_{cs}\frac{\alpha_s}{4\pi}\ln\left[\frac{M_W^2}{\lambda^2}\right][\overline{v_b^\alpha}\gamma^\mu T^a_{\alpha\beta}L\,v_c^\beta][\overline{u_c^\gamma}\gamma^\mu T^a_{\gamma\delta}L\,v_s^\delta]\,, \tag{3.13}$$

where $\alpha_s \equiv g_s^2/(4\pi)$ and $T^a \equiv \lambda^a/2$. The subscripts α, β, γ and δ denote the color indices. The symbol $C_F = 4/3$ defined by,

$$(T^a T^a)_{a\beta} \;=\; C_F \delta_{\alpha\beta} \,. \tag{3.14}$$

The symbol μ in Eq.(3.11) is the matching scale while λ is IR cut-off scale which have to be set to zero at the end of computations. The term $C_{\rm UV}$ in Eq.(3.11) is divergent term in the $\overline{\rm MS}$ scheme,

$$C_{\rm UV} \;=\; \frac{2}{\eta} \quad \gamma + \ln 4\pi \,, \tag{3.15}$$

where γ is the Euler's constant. The parameter η is introduced in dimensional regularization and defiend as $\eta = 4 \quad d$ with $d \to 4$.

The total amplitude of $\bar{b} \to \bar{s}\, c\, \bar{c}$ process from the one-loop diagrams is given by,

$$\mathcal{A}^{(1)}_{\rm SM} \;=\; 2 \times \sum_{i=a,b,c} \mathcal{A}^{(i)}_{\rm SM} \,, \tag{3.16}$$

where the factor 2 comes from the diagrams obtained by exchanging the external quarks in Fig.3.2. Adding the amplitude at the tree level $\mathcal{A}^{(0)}_{\rm SM}$ to the amplitude $\mathcal{A}^{(1)}_{\rm SM}$, we obtain the whole amplitude in the SM:

$$\begin{aligned} \mathcal{A}_{\rm SM} \;&=\; \mathcal{A}^{(0)}_{\rm SM} + \mathcal{A}^{(1)}_{\rm SM} \\ &=\; \frac{4G_F}{\sqrt{2}} V^*_{cb} V_{cs} \left[1 + 2C_F \frac{\alpha_s}{4\pi} \left(C_{\rm UV} + \ln \frac{\mu^2}{\lambda^2} \quad \frac{1}{2} \right) + \frac{3}{N} \frac{\alpha_s}{4\pi} \ln \frac{M_W^2}{\lambda^2} \right] Q_2 \\ &\quad\; \frac{4G_F}{\sqrt{2}} V^*_{cb} V_{cs} \left[\quad 3 \frac{\alpha_s}{4\pi} \ln \frac{M_W^2}{\lambda^2} \right] Q_1 \,, \end{aligned} \tag{3.17}$$

where

$$Q_1 \;\equiv\; [\overline{v_b^\alpha} \gamma^\mu L v_c^\beta][\overline{u_c^\beta} \gamma^\mu L v_s^\alpha] \,, \tag{3.18}$$

$$Q_2 \;\equiv\; [\overline{v_b^\alpha} \gamma^\mu L v_c^\alpha][\overline{u_c^\beta} \gamma^\mu L v_s^\beta] \,, \tag{3.19}$$

and we used the Fierz identity,

$$(T^a)_{\alpha\beta} (T^a)_{\gamma\delta} \;=\; \quad \frac{1}{2N} \delta_{\alpha\beta} \delta_{\gamma\delta} + \frac{1}{2} \delta_{\alpha\delta} \delta_{\delta\beta} \,, \tag{3.20}$$

with $N = 3$. We have to renormalize the amplitude $\mathcal{A}_{\rm SM}$ in Eq.(3.17) since there is divergence $C_{\rm UV}$. This can be achieved by taking account of the wave function renormalization for the external quark fields,

$$q \;\to\; q^{(0)} = \sqrt{Z_q}\, q \,, \tag{3.21}$$

where $q^{(0)}$ is bare quark fields and the renormalization constant $\sqrt{Z_q}$ can be determined by a self-energy diagram in the QCD:

$$Z_q \;=\; 1 \quad C_F \frac{\alpha_s}{4\pi} C_{\rm UV} \,. \tag{3.22}$$

Then a renormalized amplitude $\mathcal{A}^r_{\mathrm{SM}}$ in the SM is given as,

$$
\begin{aligned}
\mathcal{A}^r_{\mathrm{SM}} &= \frac{4G_F}{\sqrt{2}}V^*_{cb}V_{cs}\left[1+2C_F\frac{\alpha_s}{4\pi}\left(\ln\frac{\mu^2}{\lambda^2} \quad \frac{1}{2}\right)+\frac{3}{N}\frac{\alpha_s}{4\pi}\ln\frac{M_W^2}{\lambda^2}\right]Q_2 \\
& \quad \frac{4G_F}{\sqrt{2}}V^*_{cb}V_{cs}\left[\quad 3\frac{\alpha_s}{4\pi}\ln\frac{M_W^2}{\lambda^2}\right]Q_1\,. \qquad (3.23)
\end{aligned}
$$

Next we show amplitudes of $\bar{b}\to\bar{s}\,c\,\bar{c}$ process with the diagrams (a)-(c) in Fig.3.3 in addition to the tree level amplitude $\mathcal{A}^{(1,0)}_{\mathrm{EFT}}$, and $\mathcal{A}^{(2,0)}_{\mathrm{EFT}}$. In the case of the insertion of O_1,

$$
\begin{aligned}
\mathcal{A}^{(1,0)}_{\mathrm{EFT}} &= C_1(\mu)\frac{4G_F}{\sqrt{2}}V^*_{cb}V_{cs}Q_1\,, & (3.24)\\
\mathcal{A}^{(1a)}_{\mathrm{EFT}} &= C_1(\mu)\frac{4G_F}{\sqrt{2}}V^*_{cb}V_{cs}\frac{\alpha_s}{4\pi}\left(C_{\mathrm{UV}}+\ln\frac{\mu^2}{\lambda^2} \quad \frac{1}{2}\right)\left[\quad \frac{1}{2N}Q_1+\frac{1}{2}Q_2\right], & (3.25)\\
\mathcal{A}^{(1b)}_{\mathrm{EFT}} &= C_1(\mu)\frac{4G_F}{\sqrt{2}}V^*_{cb}V_{cs}C_F\frac{\alpha_s}{4\pi}\left(C_{\mathrm{UV}}+\ln\frac{\mu^2}{\lambda^2} \quad \frac{1}{2}\right)Q_1\,, & (3.26)\\
\mathcal{A}^{(1c)}_{\mathrm{EFT}} &= C_1(\mu)\frac{4G_F}{\sqrt{2}}V^*_{cb}V_{cs}\frac{\alpha_s}{4\pi}\left(4C_{\mathrm{UV}}+4\ln\frac{\mu^2}{\lambda^2}+5\right)\left[\quad \frac{1}{2N}Q_1+\frac{1}{2}Q_2\right]. & (3.27)
\end{aligned}
$$

For the insertion of O_2,

$$
\begin{aligned}
\mathcal{A}^{(2,0)}_{\mathrm{EFT}} &= C_2(\mu)\frac{4G_F}{\sqrt{2}}V^*_{cb}V_{cs}Q_2\,, & (3.28)\\
\mathcal{A}^{(2a)}_{\mathrm{EFT}} &= C_2(\mu)\frac{4G_F}{\sqrt{2}}V^*_{cb}V_{cs}C_F\frac{\alpha_s}{4\pi}\left(C_{\mathrm{UV}}+\ln\frac{\mu^2}{\lambda^2} \quad \frac{1}{2}\right)Q_2\,, & (3.29)\\
\mathcal{A}^{(2b)}_{\mathrm{EFT}} &= C_2(\mu)\frac{4G_F}{\sqrt{2}}V^*_{cb}V_{cs}\frac{\alpha_s}{4\pi}\left(C_{\mathrm{UV}}+\ln\frac{\mu^2}{\lambda^2} \quad \frac{1}{2}\right)\left[\frac{1}{2}Q_1 \quad \frac{1}{2N}Q_2\right], & (3.30)\\
\mathcal{A}^{(2c)}_{\mathrm{EFT}} &= C_2(\mu)\frac{4G_F}{\sqrt{2}}V^*_{cb}V_{cs}\frac{\alpha_s}{4\pi}\left(4C_{\mathrm{UV}}+4\ln\frac{\mu^2}{\lambda^2}+5\right)\left[\frac{1}{2}Q_1 \quad \frac{1}{2N}Q_2\right]. & (3.31)
\end{aligned}
$$

The whole amplitudes are,

$$
\begin{aligned}
\mathcal{A}^{(C1)}_{\mathrm{EFT}} &= \mathcal{A}^{(1,0)}_{\mathrm{EFT}}+2\times\sum_{i=a,b,c}\mathcal{A}^{(1i)}_{\mathrm{EFT}} \\
&= C_1(\mu)\frac{4G_F}{\sqrt{2}}V^*_{cb}V_{cs}\left[1+2C_F\frac{\alpha_s}{4\pi}\left(C_{\mathrm{UV}}+\ln\frac{\mu^2}{\lambda^2} \quad \frac{1}{2}\right)+\frac{\alpha_s}{4\pi}\frac{3}{N}\left(C_{\mathrm{UV}}+\ln\frac{\mu^2}{\lambda^2}+\frac{11}{6}\right)\right]Q_1 \\
& \quad C_1(\mu)\frac{4G_F}{\sqrt{2}}V^*_{cb}V_{cs}\left[\quad 3\frac{\alpha_s}{4\pi}\left(C_{\mathrm{UV}}+\ln\frac{\mu^2}{\lambda^2}+\frac{11}{6}\right)\right]Q_2\,, \qquad (3.32)
\end{aligned}
$$

$$
\begin{aligned}
\mathcal{A}^{(C2)}_{\mathrm{EFT}} &= \mathcal{A}^{(2,0)}_{\mathrm{EFT}}+2\times\sum_{i=a,b,c}\mathcal{A}^{(2i)}_{\mathrm{EFT}} \\
&= C_2(\mu)\frac{4G_F}{\sqrt{2}}V^*_{cb}V_{cs}\left[1+2C_F\frac{\alpha_s}{4\pi}\left(C_{\mathrm{UV}}+\ln\frac{\mu^2}{\lambda^2} \quad \frac{1}{2}\right)+\frac{\alpha_s}{4\pi}\frac{3}{N}\left(C_{\mathrm{UV}}+\ln\frac{\mu^2}{\lambda^2}+\frac{11}{6}\right)\right]Q_2 \\
& \quad C_2(\mu)\frac{4G_F}{\sqrt{2}}V^*_{cb}V_{cs}\left[\quad 3\frac{\alpha_s}{4\pi}\left(C_{\mathrm{UV}}+\ln\frac{\mu^2}{\lambda^2}+\frac{11}{6}\right)\right]Q_1\,. \qquad (3.33)
\end{aligned}
$$

There are the divergent terms $C_{\rm UV}$ in $\mathcal{A}_{\rm EFT}^{(C1)}$ and $\mathcal{A}_{\rm EFT}^{(C2)}$. We regard the Wilson coefficient and the quark fields in the effective operators in Eq.(3.6) as bare quantities,

$$\begin{aligned}
\mathcal{H}_{eff} &\to \frac{4G_F}{\sqrt{2}} V_{cb}^* V_{cs} [C_1^{(0)} O_1(q^{(0)}) + C_2^{(0)} O_2(q^{(0)})] \\
&= \frac{4G_F}{\sqrt{2}} V_{cb}^* V_{cs} [C_1(\mu) O_1 + C_2(\mu) O_2] \\
&\quad + \frac{4G_F}{\sqrt{2}} V_{cb}^* V_{cs} \sum_{i,j=1,2} [\ \ Z_q^2 Z_{ij}^{(C)} \quad \delta_{ij}) C_j(\mu) O_i] \,,
\end{aligned} \tag{3.34}$$

where $C_{1,2}^{(0)}(\mu)$ denote bare Wilson coefficients and $O_{1,2}(q^{(0)})$ are effective operators written by the bare quark fields. The symbol $Z_{ij}^{(C)}$ represents renormalization constant of the Wilson coefficients defined as $C_i^{(0)} = Z_{ij}^{(C)} C_j$. The Hamiltonian Eq.(3.34) leads to counterterms,

$$\mathcal{A}_{\rm EFT}^{(C1),c} = C_1(\mu) \frac{4G_F}{\sqrt{2}} V_{cb}^* V_{cs} \ \ Z_q^2 Z_{i1}^{(C)} \quad \delta_{i1}) Q_i \,, \tag{3.35}$$

$$\mathcal{A}_{\rm EFT}^{(C2),c} = C_2(\mu) \frac{4G_F}{\sqrt{2}} V_{cb}^* V_{cs} \ \ Z_q^2 Z_{i2}^{(C)} \quad \delta_{i2}) Q_i \,. \tag{3.36}$$

The renormalization constant Z_q is given in Eq.(3.22) while the renormalization constant $Z_{ij}^{(C)}$ is determined so that the counterterms remove these divergence:

$$Z^{(C)} = 1 \quad \frac{\alpha_s}{4\pi} C_{\rm UV} \begin{pmatrix} \frac{3}{N} & 3 \\ 3 & \frac{3}{N} \end{pmatrix} . \tag{3.37}$$

Then we obtain renormalized amplitudes in the weak EFT as,

$$\begin{aligned}
\mathcal{A}_{\rm EFT}^{(C1),r} &\equiv \mathcal{A}_{\rm EFT}^{(C1)} + \mathcal{A}_{\rm EFT}^{(C1),c} \\
&= C_1(\mu) \frac{4G_F}{\sqrt{2}} V_{cb}^* V_{cs} \left[1 + 2C_F \frac{\alpha_s}{4\pi} \left(\ln \frac{\mu^2}{\lambda^2} \quad \frac{1}{2} \right) + \frac{\alpha_s}{4\pi} \frac{3}{N} \left(\ln \frac{\mu^2}{\lambda^2} + \frac{11}{6} \right) \right] Q_1 \\
&\quad C_1(\mu) \frac{4G_F}{\sqrt{2}} V_{cb}^* V_{cs} \left[\quad 3 \frac{\alpha_s}{4\pi} \left(\ln \frac{\mu^2}{\lambda^2} + \frac{11}{6} \right) \right] Q_2 \,,
\end{aligned} \tag{3.38}$$

$$\begin{aligned}
\mathcal{A}_{\rm EFT}^{(C2),r} &\equiv \mathcal{A}_{\rm EFT}^{(C2)} + \mathcal{A}_{\rm EFT}^{(C2),c} \\
&= C_2(\mu) \frac{4G_F}{\sqrt{2}} V_{cb}^* V_{cs} \left[1 + 2C_F \frac{\alpha_s}{4\pi} \left(\ln \frac{\mu^2}{\lambda^2} \quad \frac{1}{2} \right) + \frac{\alpha_s}{4\pi} \frac{3}{N} \left(\ln \frac{\mu^2}{\lambda^2} + \frac{11}{6} \right) \right] Q_2 \\
&\quad C_2(\mu) \frac{4G_F}{\sqrt{2}} V_{cb}^* V_{cs} \left[\quad 3 \frac{\alpha_s}{4\pi} \left(\ln \frac{\mu^2}{\lambda^2} + \frac{11}{6} \right) \right] Q_1 \,.
\end{aligned} \tag{3.39}$$

The Wilson coefficients C_1 and C_2 can be determined by matching the renormalized amplitude in the SM Eq.(3.23) with that in the weak EFT, Eqs.(3.38) and (3.39):

$$C_1(\mu_{\rm EW}) = \quad 3 \frac{\alpha_s}{4\pi} \left[\ln \frac{M_W^2}{\mu_{\rm EW}^2} \quad \frac{11}{6} \right] + \mathcal{O}(\alpha_s^2) \,, \tag{3.40}$$

$$C_2(\mu_{\rm EW}) = 1 + \frac{\alpha_s}{4\pi} \frac{3}{N} \left[\ln \frac{M_W^2}{\mu_{\rm EW}^2} \quad \frac{11}{6} \right] + \mathcal{O}(\alpha_s^2) \,. \tag{3.41}$$

and the effective Hamiltonian becomes,

$$\mathcal{H}_{eff} \;=\; \frac{4G_F}{\sqrt{2}} V_{cb}^{*} V_{cs} [C_1(\mu) O_1^{\mathrm{ren}} + C_2(\mu) O_2^{\mathrm{ren}}]\,, \tag{3.42}$$

with the effective operators in terms of the renormalized quark fields:

$$O_1^{\mathrm{ren}} \;=\; [\bar{b}_\alpha \gamma^\mu L c_\beta][\bar{c}_\beta \gamma^\mu L s_\alpha]\,, \tag{3.43}$$

$$O_2^{\mathrm{ren}} \;=\; [\bar{b}_\beta \gamma^\mu L c_\beta][\bar{c}_\beta \gamma^\mu L s_\beta]\,. \tag{3.44}$$

We can see that the Wilson coefficients in Eqs.(3.40) and (3.41) do not depend on the IR cut off λ.

3.2.2 RG equations and anomalous dimension matrix

The combination $C_i^{(0)} O_i = C_i O_i^{\mathrm{ren}}$ is independent of the energy scale μ. Since $C_i^{(0)} = Z_{ij}^{(C)} C_j$, the effective operator can be written as $O_i = Z_{ji}^{(C)\;\;1} O_j^{\mathrm{ren}}$. This leads to [93],

$$\begin{aligned} 0 \;&=\; \mu\frac{\partial}{\partial\mu}\{C_i^{(0)} O_i\} \\ &=\; \left(\mu\frac{\partial}{\partial\mu}C_i\right) O_i^{\mathrm{ren}} + C_i \left(Z_{kj}^{(C)\;\;1} \mu\frac{\partial}{\partial\mu} Z_{ji}^{(C)}\right) O_k^{\mathrm{ren}} \\ &=\; \left(\mu\frac{\partial}{\partial\mu}C_i\right) O_i^{\mathrm{ren}} \quad C_i (Z^{\;\;1})_{ij} \left(\mu\frac{\partial}{\partial\mu} Z_{jk}\right) O_k^{\mathrm{ren}}\,, \end{aligned} \tag{3.45}$$

where we define $Z_{kj}^{(C)\;\;1} = Z_{jk}$. The matrix $(Z^{\;\;1})_{ij}\left(\mu\frac{\partial}{\partial\mu}Z_{jk}\right)$ is called an anomalous dimension matrix denoted as γ,

$$\gamma_{ik} \;\equiv\; (Z^{\;\;1})_{ij}\left(\mu\frac{\partial}{\partial\mu} Z_{jk}\right). \tag{3.46}$$

An explicit form of the anomalous dimension matrix can be obtained by Eq.(3.37):

$$\gamma \;=\; \frac{\alpha_s}{4\pi}\begin{pmatrix} \frac{6}{N} & 6 \\ 6 & \frac{6}{N} \end{pmatrix} \;\equiv\; \frac{\alpha_s}{4\pi}\gamma^{(0)}\,. \tag{3.47}$$

We obtain a differential equation with respect to the energy scale μ from Eq.(3.45):

$$\mu\frac{\partial}{\partial\mu} C_k(\mu) \;=\; C_i(\mu)\gamma_{ik} \;=\; \gamma_{ki}^T C_i(\mu)\,. \tag{3.48}$$

We refer to this differential equation as RG equation. A solution of the RG equation with an initial condition $\mu = \mu_{\mathrm{EW}}$ is given as,

$$C_i(\mu) \;=\; U_{ij}(\mu, \mu_{\mathrm{EW}}) C_j(\mu_{\mathrm{EW}})\,, \tag{3.49}$$

with an evolution matrix U,

$$U(\mu, \mu_{\mathrm{EW}}) \;=\; \exp\left[\int_{g_s(\mu_{\mathrm{EW}})}^{g_s(\mu)} dg_s' \frac{\gamma^T(g_s')}{\beta(g_s')}\right], \tag{3.50}$$

where the function $\beta(g_s)$ is defined by,

$$\beta(g_s) \;\equiv\; \mu\frac{\partial g_s}{\partial \mu} \;=\; \quad \beta_0\frac{g_s^3}{16\pi^2}+\mathcal{O}(g_s^5)\,, \tag{3.51}$$

with $\beta_0 = 11 \quad 2f/3$ and f is number of flavors. The evolution matrix at leading order is obtained from Eq.(3.50),

$$U^{(0)}(\mu,\mu_{\rm EW}) \;=\; V\,\mathrm{diag}\left(\left[\frac{\alpha_s(\mu_{\rm EW})}{\alpha_s(\mu)}\right]^{\frac{\vec{\gamma}^{(0)}}{2\beta_0}}\right)V^{\;\;1}\,, \tag{3.52}$$

where the matrix V diagonalizes the matrix $\gamma^{(0)}$,

$$\gamma_D^{(0)} \;=\; V^{\;\;1}\gamma^{(0)T}V\,, \tag{3.53}$$

with a diagonal matrix $\gamma_D^{(0)}$. The vector $\vec{\gamma}^{(0)}$ is defined as,

$$\vec{\gamma}^{(0)} \;=\; \begin{pmatrix} \quad (\gamma_D^{(0)})_{11} & \quad (\gamma_D^{(0)})_{22} \end{pmatrix}. \tag{3.54}$$

Inserting Eq.(3.52) into Eq.(3.49), we obtain the Wilson coefficients at an arbitrary scale μ. We can see from Eq.(3.49) that the Wilson coefficient C_1 are mixed with C_2 when we take account of the RG effect and vice versa.

Chapter 4
Matching with the SMEFT

4.1 Full Theory Lagrangian

In the following chapters, we present our results based on the Ref.[84]. We consider the model with one $\mathrm{SU}(2)_L$ singlet down-type VLQ whose representation is shown in Eq.(2.29). In the present chapter, we match the model with the SMEFT by integrating out VLQ field up to the one-loop level. The full theory Lagrangian for the quarks $\mathcal{L}^q_{\mathrm{Full}}$ which is invariant under the SM gauge symmetry $\mathrm{SU}(3)_c \times \mathrm{SU}(2)_L \times U(1)_Y$ is,

$$
\begin{aligned}
\mathcal{L}^q_{\mathrm{Full}} &= \mathcal{L}^q_{\mathrm{SM}} + \bar{d}^4_L i\gamma^\mu D^d_{R\mu} d^4_L + \overline{d^4_R} i\gamma^\mu D^d_{R\mu} d^4_R \quad [y^{i4}_d \bar{q}^i_L \phi\, d^4_R + M_4 \bar{d}^4_L d^4_R + h.c.]\,, &(4.1)\\
\mathcal{L}^q_{\mathrm{SM}} &= \bar{q}^i_L i\gamma^\mu D^q_{L\mu} q^i_L + \overline{u^i_R} i\gamma^\mu D^u_{R\mu} u^i_R + \overline{d^i_R} i\gamma^\mu D^d_{R\mu} d^i_R \quad [y^{ij}_d \bar{q}^i_L \phi\, d^j_R + y^i_u \bar{q}^i_L \tilde{\phi}\, u^i_R + h.c.]\,, &(4.2)
\end{aligned}
$$

where d^4_L and d^4_R denote the left- and right-handed VLQ, respectively. The fields with subscript $i, j = 1, 2, 3$ are the SM quarks. The symbol ϕ is the Higgs doublet in the SM and $\tilde{\phi} = i\tau^2\phi^*$ where τ^2 is the Pauli matrix. The 3×3 Yukawa coupling for the up-type quarks y_u is taken to be real diagonal. The 3×4 matrix y_d denotes the Yukawa couplings among the down-type quarks including couplings among the SM quark and the VLQ . A mixing term $M^{4j} \bar{d}^4_L d^j_R$ is also allowed by the SM gauge symmetry. However, we can remove the mixing term by rotating the down-type quark fields as mentioned in Sec.2.2. The covariant derivatives in Eq.(4.1) are shown in Eqs(2.5)-(2.7). In Eq.(4.1), both the kinetic terms of the left- and right-handed VLQ contain $D^d_{R\mu}$ since the left- and right-handed components belong the same representation in the case of the VLQ.

4.2 Integrating out VLQ field at Tree Level

We integrate the VLQ field in the full theory Lagrangian Eq.(4.1) to obtain the operators in the form of the SMEFT. We can also determine their Wilson coefficients by matching the amplitudes computed in the full theory with those in the SMEFT. We perform this procedure at the tree level. First we compute tree level amplitudes which contain the VLQ field as an internal line. The computed amplitudes are expanded up to $O({M_4}^2)$ while assuming that M_4 is much larger than momenta of the external fields. Then, we introduce higher-dimensional operators and Wilson

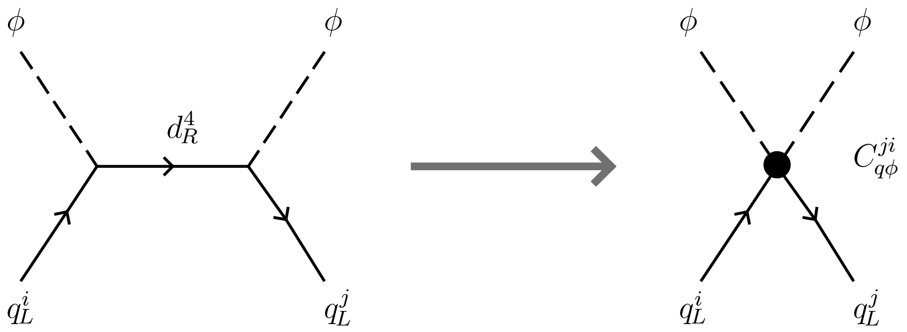

Figure 4.1. The figure in left-hand side is tree level diagram of $q^i\phi \to q^j\phi$ process induced by the VLQ field [84]. The figure in right-hand side is corresponding diagram after integrating out the VLQ field. The $C_{q\phi}^{ji}$ denotes Wilson coefficient.

coefficients, which can reproduce the amplitudes. For the present model, the tree level amplitude corresponds to the diagram in the left-hand side of Fig.4.1. The diagram corresponds to $q^i\phi \to q^j\phi$ process induced by the VLQ field. The amplitude of $q^i\phi \to q^j\phi$ process is obtained as,

$$\begin{aligned} \mathcal{A} &= \frac{1}{i}(\ iy_d^{j4})(\ iy_d^{i4*})\bar{u}_q^j\left[R\frac{i(\not{p}+M_4)}{p^2 \quad M_4^2}L\right]u_q^i \\ &\simeq \frac{y_d^{j4}y_d^{i4*}}{M_4^2}\bar{u}_q^j(\not{p}L)u_q^i + O(M_4^{\ 4}), \end{aligned} \tag{4.3}$$

where u_q^i denotes spinor of the external quark field q^i and p is momentum of the internal VLQ field. We assume $p^2 \ll M_4^2$ in the last line of Eq.(4.3). We can introduce an effective operator which reproduce the amplitude Eq.(4.3) up to $O(M_4^{\ 4})$ accuracy. Taking account of the invariance under the SM gauge symmetry, the effective operator is given as [82, 83, 84, 94, 95, 96],

$$\mathcal{L}_{eff}^{(\mathrm{tree})} = iC_{q\phi}^{ji}(\bar{q}_L^j\phi)\gamma^\mu D_{R\mu}^d(\phi^\dagger q_L^i), \tag{4.4}$$

where the Wilson coefficient $C_{q\phi}^{ji}$ is,

$$C_{q\phi}^{ji} = \frac{y_d^{j4}y_d^{i4*}}{M_4^2}. \tag{4.5}$$

The diagram in the right-hand side of Fig.4.1 corresponds to the effective operator in Eq.(4.4). We can rewrite the effective operator in Eq.(4.4) by using equations of motion derived by SM Lagrangian:

$$\mathcal{L}_{eff}^{(\mathrm{tree})} = \frac{C_{q\phi}^{ji}}{4}\left[\mathcal{O}_{\phi q}^{(1)ji} + \mathcal{O}_{\phi q}^{(3)ji}\right] + \left[\frac{C_{q\phi}^{jk}}{2}y_d^{ki}\mathcal{O}_{d\phi}^{ji} + h.c.\right], \tag{4.6}$$

where the effective operators are defined in the SMEFT operator basis [67] as,

$$\mathcal{O}_{\phi q}^{(1)ji} = [\bar{q}_L^j\gamma^\mu q_L^i][i\phi^\dagger(D_\mu\phi) \quad i(D_\mu\phi)^\dagger\phi], \tag{4.7}$$

$$\mathcal{O}_{\phi q}^{(3)ji} = [\bar{q}_L^j\gamma^\mu\tau^I q_L^i][i\phi^\dagger\tau^I(D_\mu\phi) \quad i(D_\mu\phi)^\dagger\tau^I\phi], \tag{4.8}$$

$$\mathcal{O}_{d\phi}^{ji} = (\phi^\dagger\phi)(\bar{q}_L^j\phi d_R^i)\,. \tag{4.9}$$

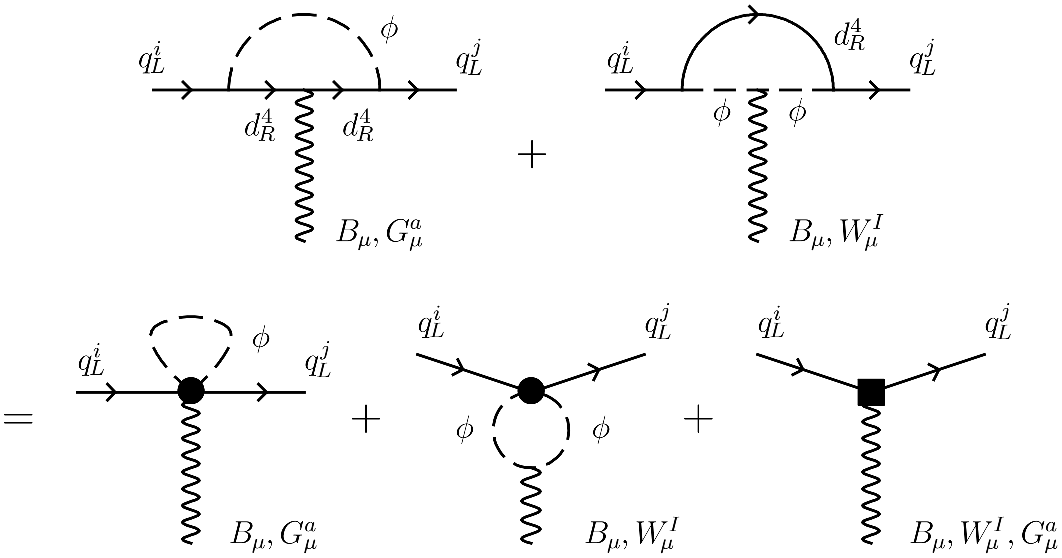

Figure 4.2. The one-loop diagrams for the decays $q_L^i \to q_L^j B_\mu$, $q_L^i \to q_L^j W_\mu^I$ and $q_L^i \to q_L^j G_\mu^a$ [84]. The top figures are diagrams in the full theory while bottom-left and bottom-right figures are diagrams in the effective field theory. The circular marks denotes the tree level effective operators in Eq.(4.4). The square mark denotes new effective operators.

Wilson coefficients for the effective operators $\mathcal{O}_{\phi q}^{(1)ji}$, $\mathcal{O}_{\phi q}^{(3)ji}$ and $\mathcal{O}_{d\phi}^{ji}$ are denoted as $\mathcal{C}_{\phi q}^{(1)ji}$, $\mathcal{C}_{\phi q}^{(3)ji}$ and $\mathcal{C}_{d\phi}^{ji}$, respectively. They can be obtained from Eq.(4.6) as follows [83]:

$$\mathcal{C}_{\phi q}^{(1)ji}(\mu_{\rm VLQ}) \;=\; \mathcal{C}_{\phi q}^{(3)ji}(\mu_{\rm VLQ}) \;=\; \frac{C_{q\phi}^{ji}}{4} \;=\; \frac{y_d^{j4} y_d^{i4*}}{4M_4^2}, \tag{4.10}$$

$$\mathcal{C}_{d\phi}^{ji}(\mu_{\rm VLQ}) \;=\; \frac{C_{q\phi}^{jk}}{2} y_d^{ki} \;=\; \frac{y_d^{j4} y_d^{k4*}}{2M_4^2} y_d^{ki}. \tag{4.11}$$

Since the expressions of the Wilson coefficients in Eqs(4.10) and (4.11) are defined at a matching scale $\mu_{\rm VLQ} \sim M_4$, we show the scale of the Wilson coefficients explicitly. Finally, we obtain the effective Lagrangian $\mathcal{L}_{eff}^{(\rm tree)}$ in terms of the SMEFT operator basis as,

$$\mathcal{L}_{eff}^{(\rm tree)} \;=\; \mathcal{C}_{\phi q}^{(1)ji} \mathcal{O}_{\phi q}^{(1)ji} + \mathcal{C}_{\phi q}^{(3)ji} \mathcal{O}_{\phi q}^{(3)ji} + [\mathcal{C}_{d\phi}^{ji} \mathcal{O}_{d\phi}^{ji} + h.c.]\,. \tag{4.12}$$

4.3 Integrating out VLQ field at One-loop Level

The interactions among the SM quarks and the VLQ lead to the one-loop level contributions to radiative decays of the SM quarks, such as $b \to s\gamma$ process. Therefore, we have to match the model with the SMEFT at the one-loop level. The procedure is ,

i. We compute the amplitudes of the one-loop diagrams for the decays $q_L^i \to q_L^j B_\mu$, $q_L^i \to q_L^j W_\mu^I$ and $q_L^i \to q_L^j G_\mu^a$ in terms of the full theory (see the top figures in Fig.(4.2)). These diagrams contain the VLQ in internal lines. In order to remove divergence in the amplitudes, we renormalize the amplitudes with the $\overline{\text{MS}}$ scheme.

ii. We calculate the amplitudes for the same decays as the step (i) by using the effective operator Eq.(4.4) in addition to the SM Lagrangian (see the bottom-left and bottom-center figures in Fig.(4.2)). We also renormalize the computed amplitudes with the $\overline{\text{MS}}$ scheme.

iii. We introduce new effective operators. Wilson coefficients of the new operators are determined so that the renormalized amplitudes computed in the step (ii) are equal to the renormalized amplitudes computed in the step (i).

4.3.1 Step (i): Renormalized amplitudes in the full theory

In the step (i), we derive renormalized amplitudes by using the full theory Lagrangian Eq.(4.1) in addition to the SM Lagrangian. We define momenta of the external fields q_L^i, q_L^j and the gauge bosons as p, p' and q, respectively. In the computation of the step (i), we treat the SM particles as massless particles. The amplitude for the diagram in the top-left figure of Fig.(4.2) is given as,

$$\begin{aligned} {}^{B,(1)ji}_{\mu} \;=\; & g'\frac{Y_{dR}}{2}\cdot\frac{y_d^{j4}y_d^{i4*}}{16\pi^2}\Bigg[\quad\frac{\gamma_\mu}{2}\left(C_{\text{UV}}+\ln\frac{\mu_{\text{VLQ}}^2}{M_4^2}\right)\quad\frac{3\gamma_\mu}{4}\quad\frac{5q^2\gamma_\mu}{36M_4^2}\quad\frac{(p^2+p'^2)\gamma_\mu}{3M_4^2} \\ & \frac{1}{M_4^2}\left\{\frac{1}{3}\not{p}'\gamma_\mu\not{p}+\frac{1}{12}(\not{p}'\gamma_\mu\not{q}\quad\not{q}\gamma_\mu\not{p})\quad\frac{1}{18}\not{q}\gamma_\mu\not{q}\right\}\Bigg]L\,, \end{aligned} \tag{4.13}$$

for the case where external gauge boson is the $U(1)_Y$ gauge boson B_μ. Here we do not write spinors of the external quarks explicitly. The symbol C_{UV} contain divergence:

$$C_{\text{UV}} \;=\; \frac{2}{\eta}\quad\gamma+\ln 4\pi, \tag{4.14}$$

where $\eta = 4 \quad d$ with $d\to 4$ comes from the dimensional regularization and γ is Euler's constant. We can obtain the amplutide for the case where the external gauge boson is the gluon G_μ^a by replacing $g'\frac{Y_{dR}}{2}$ with $g_s\frac{\lambda^a}{2}$ in Eq.(4.13).

The amplitude for the diagram in the top-right figure of Fig.(4.2) is given as,

$$\begin{aligned} {}^{B,(2)ji}_{\mu} \;=\; & g'\frac{Y_{\phi}}{2}\cdot\frac{y_d^{j4}y_d^{i4*}}{16\pi^2}\Bigg[\quad\frac{\gamma_\mu}{2}\left(C_{\text{UV}}+\ln\frac{\mu_{\text{VLQ}}^2}{M_4^2}\right)\quad\frac{3\gamma_\mu}{4}\quad\frac{(p^2+p'^2)\gamma_\mu}{6M_4^2} \\ & +\frac{\gamma^\nu}{6M_4^2}(g_{\mu\nu}q^2\quad q_\mu q_\nu)\left(\ln\frac{q^2}{M_4^2}\quad\frac{5}{6}\right)\quad\frac{\not{p}'p_\mu+\not{p}p'_\mu}{3M_4^2}\quad\frac{\not{q}q_\mu}{6M_4^2}\Bigg]L\,, \end{aligned} \tag{4.15}$$

for the case where external gauge boson is the $U(1)_Y$ gauge boson B_μ. We can obtain the amplitude for the case where the external gauge boson is the $\mathrm{SU}(2)_L$ gauge boson W^I_μ by replacing $g'\frac{Y_\phi}{2}$ with $g\frac{\tau^I}{2}$ in Eq.(4.15).

In order to remove the divergence in Eqs.(4.13) and (4.15), we perform a wave function renormalization. A renormalization constant can be determined by a self-energy diagram of the SM quark doublet q^i_L, which include the VLQ as an internal line. The relevant diagram is shown in Fig.(4.3). The amplitude is given as,

$$\Sigma^{ji}(p) \;=\; \frac{y_d^{j4}y_d^{i4*}}{16\pi^2}\left[\frac{1}{2}\left(C_{\rm UV}+\ln\frac{\mu^2_{\rm VLQ}}{M_4^2}\right)+\frac{3}{4}+\frac{p^2}{3M_4^2}\right]\not{p}L\,. \tag{4.16}$$

The Lagrangian including counterterms for the SM quark doublet is,

$$\mathcal{L} \;=\; \bar{q^i_L}\, i\gamma^\mu D^q_{L\mu} q^i_L + \mathcal{L}_c\,, \tag{4.17}$$

$$\begin{aligned}\mathcal{L}_c \;&=\; \{\;\sqrt{Z_L}^{\dagger}\sqrt{Z_L})^{ji} \quad \delta^{ji}\}\,\bar{q^j_L}\, i\gamma^\mu\partial_\mu q^i_L \\ &\quad \{\;\sqrt{Z_L}^{\dagger}\sqrt{Z_L})^{ji} \quad \delta^{ji}\}\,\bar{q^j_L}\gamma^\mu\left[g_s\frac{\lambda^a}{2}G^a_\mu + g\frac{\tau^I}{2}W^I_\mu + g'\frac{Y_{qL}}{2}B_\mu\right]q^i_L\,,\end{aligned} \tag{4.18}$$

where $\sqrt{Z_L}$ is the renormalization constant defined by,

$$(q^0_L)^j \;=\; \sqrt{Z_L}^{ji} q^i_L\,, \tag{4.19}$$

with the bare SM quark doublet field $(q^0_L)^i$. The renormalization constant is determined so that the counterterms in Eq.(4.18) removes the divergence in Eq.(4.16):

$$\sqrt{Z_L}^{\dagger}\sqrt{Z_L})^{ji} \;=\; \delta^{ji} \quad \frac{y_d^{j4}y_d^{i4*}}{32\pi^2}C_{\rm UV}\,, \tag{4.20}$$

and then we can obtain counterterms for $q^i_L q^j_L B_\mu$, $q^i_L q^j_L W^I_\mu$ and $q^i_L q^j_L G^a_\mu$ vertices. Adding the counterterms shown in Eq.(4.18) with Eq.(4.20) to the total amplitudes for the $q^i_L \to q^j_L B_\mu$ process $\;^{B,(1)}_{\mu} + \;^{B,(2)}_{\mu}$, we obtain the renormalized amplitude:

$$\begin{aligned}{}^{B,ji}_{r\mu} \;&=\; g'\frac{Y_{qL}}{2}\cdot\frac{y_d^{j4}y_d^{i4*}}{16\pi^2}\left[\quad\frac{\gamma_\mu}{2}\left\{\ln\frac{\mu^2_{\rm VLQ}}{M_4^2}+\frac{3}{2}+\frac{p^2+p'^2}{3M_4^2}\right\}\right]L \\ &\quad g'\frac{Y_{dR}}{2}\cdot\frac{y_d^{j4}y_d^{i4*}}{16\pi^2 M_4^2}\left[\gamma_\mu\frac{p^2+p'^2}{6}+\frac{\not{p}'\gamma_\mu\not{p}}{3}+\frac{7\gamma^\nu}{36}(g_{\mu\nu}q^2 \quad q_\mu q_\nu)+\frac{\not{p}'[\gamma_\mu,\not{q}] \quad [\not{q},\gamma_\mu]\not{p}}{24}\right]L \\ &\quad +g'\frac{Y_\phi}{2}\cdot\frac{y_d^{j4}y_d^{i4*}}{16\pi^2 M_4^2}\left[\frac{\gamma^\nu}{6}(g_{\mu\nu}q^2 \quad q_\mu q_\nu)\left(\ln\frac{q^2}{M_4^2} \quad \frac{5}{6}\right) \quad \frac{\not{p}'p_\mu+\not{p}p'_\mu}{3M_4^2} \quad \frac{\not{q}q_\mu}{6M_4^2}\right]L\,,\end{aligned} \tag{4.21}$$

where we used $\frac{Y_{dR}}{2}+\frac{Y_\phi}{2}=\frac{Y_{qL}}{2}$. In the same way as to the case of the $q^i_L \to q^j_L B_\mu$ process, we can derive the renormalized amplitudes for the $q^i_L \to q^j_L W^I_\mu$ and $q^i_L \to q^j_L G^a_\mu$.

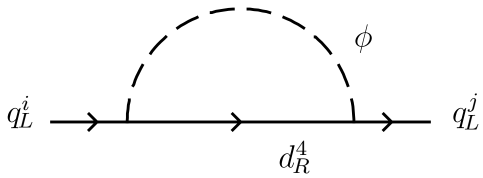

Figure 4.3. Self-energy diagram of SM quark doublet q_L^i with internal VLQ field d_R^4 [84].

4.3.2 Step (ii): Renormalized amplitudes in the effective field theory

Next we derive renormalized amplitudes by using the effective operator Eq.(4.4) in addition to the SM Lagrangian. Here we also treat the SM particles as massless particles. We can see that the amplitude of the bottom-left figure in Fig.(4.2) vanishes as long as the mass of ϕ is set to zero. The amplitude of the bottom-center figure in Fig.(4.2) is obtained as,

$$ {}^{B,(E)ji}_{\mu} \quad = \quad g'\frac{Y_\phi}{2}\cdot\frac{y_d^{j4}y_d^{i4*}}{16\pi^2 M_4^2}\gamma^\nu(g_{\mu\nu}q^2 \quad q_\mu q_\nu)\left[\frac{1}{6}C_{\rm UV} \quad \ln\frac{q^2}{\mu_{\rm VLQ}^2}+\frac{4}{9}\right]L, \tag{4.22} $$

for the case where the external gauge boson is the $U(1)_Y$ gauge boson B_μ. We can obtain the amplitude for the $\mathrm{SU}(2)_L$ gauge boson W_μ^I by replacing $g'\frac{Y_\phi}{2}$ with $g\frac{\tau^I}{2}$ in Eq.(4.22). A self-energy diagram of the quark doublet q_L^i induced by the effective operator Eq.(4.4) vanishes as long as the mass of ϕ is set to zero. Therefore, there is no wave function renormalization of q_L^i originating from the effective operator Eq.(4.4). In order to remove the divergence in Eq.(4.22), we introduce a counterterm by hand:

$$ \begin{aligned} \mathcal{L}_c^{\rm EFT} \quad &= \quad (Z_{\rm EFT}^{B,ji} \quad \delta^{ji})\bar{q}_L^j\gamma^\nu q_L^i(g_{\mu\nu}\Box \quad \partial_\mu\partial_\nu)B^\mu \\ &\quad +(Z_{\rm EFT}^{W,ji} \quad \delta^{ji})\bar{q}_L^j\gamma^\nu\tau^I q_L^i(g_{\mu\nu}\Box \quad \partial_\mu\partial_\nu)W^{I\mu}\,. \end{aligned} \tag{4.23} $$

Adding the counterterms shown in Eq.(4.23) to the amplitude Eq.(4.22), we obtain the renormalized amplitude as,

$$ {}^{B,(E)ji}_{r\mu} \quad = \quad g'\frac{Y_\phi}{2}\cdot\frac{y_d^{j4}y_d^{i4*}}{16\pi^2 M_4^2}\gamma^\nu(g_{\mu\nu}q^2 \quad q_\mu q_\nu)\left[\quad \ln\frac{q^2}{\mu_{\rm VLQ}^2}+\frac{4}{9}\right]L, \tag{4.24} $$

with the renormalization constaint:

$$ Z_{\rm EFT}^{B,ji} \quad = \quad \delta^{ji} \quad g'\frac{Y_\phi}{2}\cdot\frac{y_d^{j4}y_d^{i4*}}{16M_4^2}\cdot\frac{C_{\rm UV}}{6}\,. \tag{4.25} $$

In the same way as to the case of the $q_L^i \to q_L^j B_\mu$ process, we can derive the renormalized amplitudes for the $q_L^i \to q_L^j W_\mu^I$ and $q_L^i \to q_L^j G_\mu^a$ processes.

4.3.3 Step (iii): Introducing effective operators

The renormalized amplitudes in the effective field theory Eq.(4.24) are not equal to that in the full theory Eq.(4.21). We introduce new effective operators with Wilson coefficients so as to match the amplitudes in the effective field theory with that in the full theory. The difference between the renormalized amplitude of $q_L^i \to q_L^j B_\mu$ process Eq.(4.21) and Eq.(4.24) is,

$$
\begin{aligned}
\Delta\ {}^{B,ji}_{r\mu} &\equiv\ {}^{B,ji}_{r\mu} \quad {}^{B,(E)ji}_{r\mu} \\
&= g'\frac{Y_{qL}}{2}\cdot\frac{y_d^{j4}y_d^{i4*}}{16\pi^2}\left[\quad\frac{\gamma_\mu}{2}\left\{\ln\frac{\mu_{\mathrm{VLQ}}^2}{M_4^2}+\frac{3}{2}+\frac{p^2+p'^2}{3M_4^2}\right\}\quad\frac{\not{p}'p_\mu+\not{p}p'_\mu}{3M_4^2}\quad\frac{\not{q}q_\mu}{6M_4^2}\right]L \\
&\quad g'\frac{Y_{dR}}{2}\cdot\frac{y_d^{j4}y_d^{i4*}}{16\pi^2M_4^2}\left[\frac{7\gamma^\nu}{36}(g_{\mu\nu}q^2\quad q_\mu q_\nu)+\frac{\not{p}'[\gamma_\mu,\not{q}]\quad[\not{q},\gamma_\mu]\not{p}}{8}\right]L \\
&\quad +g'\frac{Y_\phi}{2}\cdot\frac{y_d^{j4}y_d^{i4*}}{16\pi^2M_4^2}\left[\frac{\gamma^\nu}{6}(g_{\mu\nu}q^2\quad q_\mu q_\nu)\left(\ln\frac{\mu_{\mathrm{VLQ}}^2}{M_4^2}+\frac{11}{6}\right)\right]L\,.
\end{aligned}
\tag{4.26}
$$

In the same way as to the $q_L^i \to q_L^j B_\mu$ process, we can compute difference between the amplitudes in the full theory and that in the effective field theory with respect to the $q_L^i \to q_L^j W_\mu^I$ and $q_L^i \to q_L^j G_\mu^a$ processes. Then we can introduce new effective operators which correct the difference among the full theory and the effective theory. Taking account of the finite part in the self-energy diagram Eq.(4.16), the new effective operators with Wilson coefficients are given as follows:

$$
\mathcal{L}_{eff}^{(1)} = \mathcal{L}_{eff}^K + \mathcal{L}_{eff}^B + \mathcal{L}_{eff}^W + \mathcal{L}_{eff}^G\,, \tag{4.27}
$$

where

$$
\begin{aligned}
\mathcal{L}_{eff}^K &= \frac{y_d^{j4}y_d^{i4*}}{16\pi^2}\left(\frac{1}{2}\ln\frac{\mu_{\mathrm{VLQ}}^2}{M_4^2}+\frac{3}{4}\right)\bar{q}_L^j i\gamma^\mu D_{L\mu}^q q_L^i \\
&\quad +\frac{y_d^{j4}y_d^{i4*}}{48\pi^2M_4^2}(y_d^{jl*}\overline{d_R^l}\phi^\dagger+y_u^{jl*}\overline{u_R^l}\tilde{\phi}^\dagger)i\gamma^\mu D_{L\mu}^q(y_d^{ik}\phi d_R^k+y_u^{ik}\tilde{\phi}u_R^k)\,,
\end{aligned}
\tag{4.28}
$$

$$
\begin{aligned}
\mathcal{L}_{eff}^B &= g'^2\frac{y_d^{j4}y_d^{i4*}}{16\pi^2M_4^2}\left\{\frac{Y_{dR}}{2}\cdot\frac{7}{36}\quad\frac{Y_\phi}{2}\left(\frac{1}{6}\ln\frac{\mu_{\mathrm{VLQ}}^2}{M_4^2}+\frac{11}{36}\right)\right\} \\
&\quad\times\left[\frac{Y_{lL}}{2}\mathcal{O}_{lq}^{(1)kkji}+\frac{Y_{eR}}{2}\mathcal{O}_{qe}^{jikk}+\frac{Y_{qL}}{2}\mathcal{O}_{qq}^{(1)jikk}+\frac{Y_{uR}}{2}\mathcal{O}_{qu}^{(1)jikk}+\frac{Y_{dR}}{2}\mathcal{O}_{qd}^{(1)jikk}+\frac{Y_\phi}{2}\mathcal{O}_{\phi q}^{(1)ji}\right] \\
&\quad +\frac{g'}{16\pi^2M_4^2}\left(\frac{Y_{qL}}{2}\cdot\frac{1}{12}\quad\frac{Y_{dR}}{2}\cdot\frac{1}{8}\right)[y_d^{j4}y_d^{i4*}\{y_d^{il}\mathcal{O}_{dB}^{jl}+y_u^{i}\mathcal{O}_{uB}^{ji}\}+h.c.]\,,
\end{aligned}
\tag{4.29}
$$

Effective Operators		Wilson Coefficients	
$\mathcal{O}_{uG}^{ji}$	$\overline{q_L^j}\sigma^{\mu\nu}\frac{\lambda^a}{2}u_R^i)\tilde{\phi}G_{\mu\nu}^a$	$\mathcal{C}_{uG}^{ji}(\mu_{\mathrm{VLQ}})$	$\frac{1}{24}\cdot\frac{g_s}{16\pi^2 M_4^2}y_d^{j4}y_d^{i4*}y_u^i$
$\mathcal{O}_{uW}^{ji}$	$(\overline{q_L^j}\sigma^{\mu\nu}\tau^I u_R^i)\tilde{\phi}W_{\mu\nu}^I$	$\mathcal{C}_{uW}^{ji}(\mu_{\mathrm{VLQ}})$	$\frac{1}{24}\cdot\frac{g}{16\pi^2 M_4^2}y_d^{j4}y_d^{i4*}y_u^i$
$\mathcal{O}_{uB}^{ji}$	$(\overline{q_L^j}\sigma^{\mu\nu}u_R^i)\tilde{\phi}B_{\mu\nu}$	$\mathcal{C}_{uB}^{ji}(\mu_{\mathrm{VLQ}})$	$\frac{g'}{16\pi^2 M_4^2}\left(\frac{Y_{qL}}{2}\cdot\frac{1}{12}\quad\frac{Y_{dR}}{2}\cdot\frac{1}{8}\right)y_d^{j4}y_d^{i4*}y_u^i$
$\mathcal{O}_{dG}^{ji}$	$\overline{q_L^j}\sigma^{\mu\nu}\frac{\lambda^a}{2}d_R^i)\phi G_{\mu\nu}^a$	$\mathcal{C}_{dG}^{ji}(\mu_{\mathrm{VLQ}})$	$\frac{1}{24}\cdot\frac{g_s}{16\pi^2 M_4^2}y_d^{j4}y_d^{l4*}y_d^{li}$
$\mathcal{O}_{dW}^{ji}$	$(\overline{q_L^j}\sigma^{\mu\nu}\tau^I d_R^i)\phi W_{\mu\nu}^I$	$\mathcal{C}_{dW}^{ji}(\mu_{\mathrm{VLQ}})$	$\frac{1}{24}\cdot\frac{g}{16\pi^2 M_4^2}y_d^{j4}y_d^{l4*}y_d^{li}$
$\mathcal{O}_{dB}^{ji}$	$(\overline{q_L^j}\sigma^{\mu\nu}d_R^i)\phi B_{\mu\nu}$	$\mathcal{C}_{dB}^{ji}(\mu_{\mathrm{VLQ}})$	$\frac{g'}{16\pi^2 M_4^2}\left(\frac{Y_{qL}}{2}\cdot\frac{1}{12}\quad\frac{Y_{dR}}{2}\cdot\frac{1}{8}\right)y_d^{j4}y_d^{l4*}y_d^{li}$

Table 4.1. The left-hand side table shows dipole type operators in the SMEFT [67]. The symbols $G_{\mu\nu}^a$, $W_{\mu\nu}^I$ and $B_{\mu\nu}$ denote the field strength of the $\mathrm{SU}(3)_c$, $\mathrm{SU}(2)_L$ and $U(1)_Y$ gauge bosons, respectively. The right-hand side table shows the corresponding Wilson coefficients at the matching scale μ_{VLQ} [84].

$\mathcal{O}_{lq}^{(1)klji}$	$(\overline{l_L^k}\gamma_\mu l_L^l)(\overline{q_L^j}\gamma^\mu q_L^i)$	$\mathcal{O}_{qe}^{jikl}$	$(\overline{q_L^j}\gamma_\mu q_L^i)(\overline{e_R^k}\gamma^\mu e_R^l)$
$\mathcal{O}_{lq}^{(3)klji}$	$(\overline{l_L^k}\gamma_\mu\tau^I l_L^l)(\overline{q_L^j}\gamma^\mu\tau^I q_L^i)$	$\mathcal{O}_{qu}^{(1)jikl}$	$(\overline{q_L^j}\gamma_\mu q_L^i)(\overline{u_R^k}\gamma^\mu u_R^l)$
$\mathcal{O}_{qq}^{(1)jikl}$	$(\overline{q_L^j}\gamma_\mu q_L^i)(\overline{q_L^k}\gamma^\mu q_L^l)$	$\mathcal{O}_{qu}^{(8)jikl}$	$\overline{q_L^j}\gamma_\mu\frac{\lambda^a}{2}q_L^i)\ \overline{u_R^k}\gamma^\mu\frac{\lambda^a}{2}u_R^l)$
$\mathcal{O}_{qq}^{(3)jikl}$	$(\overline{q_L^j}\gamma_\mu\tau^I q_L^i)(\overline{q_L^k}\gamma^\mu\tau^I q_L^l)$	$\mathcal{O}_{qd}^{(1)jikl}$	$(\overline{q_L^j}\gamma_\mu q_L^i)(\overline{d_R^k}\gamma^\mu d_R^l)$
$\mathcal{O}_{qq}^{(8)jikl}$	$\overline{q_L^j}\gamma_\mu\frac{\lambda^a}{2}q_L^i)\ \overline{q_L^k}\gamma^\mu\frac{\lambda^a}{2}q_L^l)$	$\mathcal{O}_{qd}^{(8)jikl}$	$\overline{q_L^j}\gamma_\mu\frac{\lambda^a}{2}q_L^i)\ \overline{d_R^k}\gamma^\mu\frac{\lambda^a}{2}d_R^l)$

Table 4.2. The 4-Fermi type effective operators in the SMEFT [67]. We note that the operator $\mathcal{O}_{qq}^{(8)jikl}$ can be written in terms of the other effective operators [67].

$$\begin{aligned}\mathcal{L}_{eff}^{W} &= \frac{g^2}{4}\cdot\frac{y_d^{j4}y_d^{i4*}}{16\pi^2 M_4^2}\left(\frac{1}{6}\ln\frac{\mu_{\mathrm{VLQ}}^2}{M_4^2}+\frac{11}{36}\right)\left[\mathcal{O}_{lq}^{(3)kkji}+\mathcal{O}_{qq}^{(3)jikk}+\mathcal{O}_{\phi q}^{(3)ji}\right]\\ &\quad+\frac{g}{16\pi^2 M_4^2}\cdot\frac{1}{24}\left[y_d^{j4}y_d^{i4*}\{y_d^{il}\mathcal{O}_{dW}^{jl}+y_u^{i}\mathcal{O}_{uW}^{ji}\}+h.c.\right],\end{aligned}\tag{4.30}$$

$$\begin{aligned}\mathcal{L}_{eff}^{G} &= g_s^2\frac{y_d^{j4}y_d^{i4*}}{16\pi^2 M_4^2}\cdot\frac{7}{36}\left[\mathcal{O}_{qq}^{(8)jikk}+\mathcal{O}_{qu}^{(8)jikk}+\mathcal{O}_{qd}^{(8)jikk}\right]\\ &\quad+\frac{g_s}{16\pi^2 M_4^2}\left(\quad\frac{1}{24}\right)\left[y_d^{j4}y_d^{i4*}\{y_d^{il}\mathcal{O}_{dG}^{jl}+y_u^{i}\mathcal{O}_{uG}^{ji}\}+h.c.\right].\end{aligned}\tag{4.31}$$

The effective operators $\mathcal{O}$ in Eqs.(4.29)-(4.31) are listed in the Tables 4.1 and 4.2. The right-hand side of the Table 4.1 shows the Wilson coefficients of the dipole operators in Eqs.(4.29)-(4.31). The symbols $G_{\mu\nu}^a$, $W_{\mu\nu}^I$ and $B_{\mu\nu}$ denote the field strength of the $\mathrm{SU}(3)_c$, $\mathrm{SU}(2)_L$ and $U(1)_Y$ gauge bosons, respectively. Note that the effective operator $\mathcal{O}_{qq}^{(8)jikk}$ can be written in terms of the other effective operators in the SMEFT by using the Fierz transformations [67],

$$\mathcal{O}_{qq}^{(8)jikl} = \frac{1}{4}\mathcal{O}_{qq}^{(1)jlki}+\frac{1}{4}\mathcal{O}_{qq}^{(3)jlki}\quad\frac{1}{6}\mathcal{O}_{qq}^{(1)jikl}.\tag{4.32}$$

4.3.4 Redefinition of the Yukawa couplings

We can see that the kinetic term of the $\mathrm{SU}(2)_L$ doublet quark field q_L^i is not a canonical form because of the first term in Eq.(4.28):

$$\mathcal{L}_K^{(q)} = \bar{q}_L^j\{\delta^{ji} + Z^{ji}(\mu_{\mathrm{VLQ}})\}i\gamma^\mu D_{L\mu}^q q_L^i \,, \tag{4.33}$$

$$Z^{ji}(\mu_{\mathrm{VLQ}}) \equiv \frac{y_d^{j4}y_d^{i4*}}{16\pi^2}\left(\frac{1}{2}\ln\frac{\mu_{\mathrm{VLQ}}^2}{M_4^2} + \frac{3}{4}\right). \tag{4.34}$$

The coefficient $Z^{ji}(\mu)$ is not suppressed by the VLQ mass M_4 but suppressed by the loop factor $\sim 1/(16\pi^2)$. We perform a rescaling of the field q_L^i to rewrite the kinetic term Eq.(4.33) into a canonical form. We define a rescaled field $q_L^{\prime k}$ as,

$$q_L^{\prime k} \equiv \left\{\delta^{ki} + \frac{1}{2}Z^{ki}(\mu_{\mathrm{VLQ}})\right\}q_L^i \,. \tag{4.35}$$

The kinetic term of the doublet quark field becomes,

$$\mathcal{L}_K^{(q)} = \overline{q_L^{\prime k}} i\gamma^\mu D_{L\mu}^q q_L^{\prime k} \,. \tag{4.36}$$

The rescaling Eq.(4.35) modifies the Yukawa interactions among the SM quarks. The modification can be absorbed into the Yukawa coupling as follows:

$$y_d^{ji}\bar{q}_L^j\phi d_R^i = \left\{\delta^{kj} \quad \frac{1}{2}Z^{kj}(\mu_{\mathrm{VLQ}})\right\}y_d^{ji}\overline{q_L^{\prime k}}\phi d_R^i \equiv Y_d^{ki}\overline{q_L^{\prime k}}\phi d_R^i \,, \tag{4.37}$$

$$y_u^i\bar{q}_L^i\tilde{\phi}u_R^i = \left\{\delta^{ki} \quad \frac{1}{2}Z^{ki}(\mu_{\mathrm{VLQ}})\right\}y_u^i\overline{q_L^{\prime k}}\tilde{\phi}u_R^i \equiv Y_u^{ki}\overline{q_L^{\prime k}}\tilde{\phi}u_R^i \,, \tag{4.38}$$

where we redefine the Yukawa coupling as,

$$Y_d^{ki} \equiv \left\{\delta^{kj} \quad \frac{1}{2}Z^{kj}(\mu_{\mathrm{VLQ}})\right\}y_d^{ji} \,, \tag{4.39}$$

$$Y_u^{ki} \equiv \left\{\delta^{ki} \quad \frac{1}{2}Z^{ki}(\mu_{\mathrm{VLQ}})\right\}y_u^i \,. \tag{4.40}$$

The tree level effective operator in Eq.(4.4) (or equivalently Eq.(4.12)) is also changed by the rescaling Eq.(4.35). The modification can be absorbed into the Yukawa coupling y_d^{i4} as,

$$\begin{aligned}
\mathcal{L}_{eff}^{(\mathrm{tree})} &= i\frac{y_d^{j4}y_d^{i4*}}{M_4^2}(\bar{q}_L^j\phi)\gamma^\mu D_{R\mu}^d(\phi^\dagger q_L^i) \\
&= i\left\{\delta^{kj} \quad \frac{1}{2}Z^{kj}(\mu_{\mathrm{VLQ}})\right\}\frac{y_d^{j4}y_d^{i4*}}{M_4^2}\left\{\delta^{il} \quad \frac{1}{2}Z^{il}(\mu_{\mathrm{VLQ}})\right\} \; \overline{q_L^{\prime k}}\phi)\gamma^\mu D_{R\mu}^d(\phi^\dagger q_L^{\prime l}) \\
&\equiv i\frac{Y_d^{k4}Y_d^{l4*}}{M_4^2} \; \overline{q_L^{\prime k}}\phi)\gamma^\mu D_{R\mu}^d(\phi^\dagger q_L^{\prime l}) \,,
\end{aligned} \tag{4.41}$$

where we define,

$$Y_d^{k4} \equiv \left\{\delta^{kj} \quad \frac{1}{2}Z^{kj}(\mu_{\mathrm{VLQ}})\right\}y_d^{j4} \,. \tag{4.42}$$

In the same way as to the tree level effective operator, the rescaling Eq.(4.35) affects the one-loop level effective operators in Eqs.(4.28)-(4.31) and leads to two-loop level corrections. We can simply take $q_L \simeq q'_L$ and $y_{u,d} \simeq Y_{u,d}$ in the one-loop level effective operators since we do not consider two-loop level contributions.

The up-type Yukawa coupling Y_u in Eq.(4.40) is not diagonal matrix because of the non-diagonal matrix $Z^{ji}(\mu_{\mathrm{VLQ}})$. We can diagonalize Y_u by unitary transformations of the SM quark fields without loss of generality. Therefore, we take the basis where the up-type Yukawa coupling is diagonal. In this basis, we write the Yukawa couplings as small letters $y_{u,d}$ and omit the prime symbol on the quark field for simplicity. We summarize the Lagrangian at matching scale μ_{VLQ}:

$$\mathcal{L}_{\mathrm{EFT}} = \mathcal{L}^q_{\mathrm{SM}} + \mathcal{L}^{(\mathrm{tree})}_{eff} + \mathcal{L}^{(1)}_{eff} , \tag{4.43}$$

where

$$\mathcal{L}^q_{\mathrm{SM}} = \bar{q}^i_L i\gamma^\mu D^q_{L\mu} q^i_L + \bar{u}^i_R i\gamma^\mu D^u_{R\mu} u^i_R + \bar{d}^i_R i\gamma^\mu D^d_{R\mu} d^i_R \quad [y^{ij}_d \bar{q}^i_L \phi\, d^j_R + y^i_u \bar{q}^i_L \tilde{\phi}\, u^i_R + h.c.] , \tag{4.44}$$

$$\mathcal{L}^{(\mathrm{tree})}_{eff} = i\,\frac{y^{j4}_d y^{i4*}_d}{M_4^2} (\bar{q}^j_L \phi)\gamma^\mu D^d_{R\mu}(\phi^\dagger q^i_L) = \mathcal{C}^{(1)ji}_{\phi q}\mathcal{O}^{(1)ji}_{\phi q} + \mathcal{C}^{(3)ji}_{\phi q}\mathcal{O}^{(3)ji}_{\phi q} + [\mathcal{C}^{ji}_{d\phi}\mathcal{O}^{ji}_{d\phi} + h.c.] , \tag{4.45}$$

and $\mathcal{L}^{(1)}_{eff}$ is given in Eq.(4.27) with Eqs.(4.29)-(4.31).

4.4 Electroweak Symmetry Breaking

We rewrite the Lagrangian Eq.(4.43) in terms of the SM fields in the broken phase of the SM gauge symmetry. We define the Higgs doublet ϕ as,

$$\phi = \begin{pmatrix} \chi^+ \\ (v + h + i\chi_0)/\sqrt{2} \end{pmatrix}, \tag{4.46}$$

where v is the VEV. The symbols h, χ^+ and χ_0 denote the physical Higgs boson, the charged and neutral Nambu–Goldstone (NG) bosons, respectively.

4.4.1 SM + tree level effective operators

First we consider substituting Eq.(4.46) to the Higgs doublet ϕ in the SM quark Lagrangian $\mathcal{L}^q_{\mathrm{SM}}$ and the tree level effective operators $\mathcal{L}^{(\mathrm{tree})}_{eff}$. We can divide $\mathcal{L}^q_{\mathrm{SM}} + \mathcal{L}^{(\mathrm{tree})}_{eff}$ into three parts after the substitution:

$$\mathcal{L}^q_{\mathrm{SM}} + \mathcal{L}^{(\mathrm{tree})}_{eff} = \mathcal{L}^{(0)}_{\mathrm{dim.4}} + \mathcal{L}^{(0)}_{\mathrm{dim.5}} + \mathcal{L}^{(0)}_{\mathrm{dim.6}} . \tag{4.47}$$

The term $\mathcal{L}^{(0)}_{\text{dim.4}}$ is constituted by the mass terms of the SM quarks and dim.4 operators including the usual SM interactions. The explicit form of $\mathcal{L}^{(0)}_{\text{dim.4}}$ is given as,

$$
\begin{aligned}
\mathcal{L}^{(0)}_{\text{dim.4}} \;=\;& \bar{u}^i i\gamma^\mu\partial_\mu u^i + \bar{d}^i i\gamma^\mu\partial_\mu d^i \quad \frac{v}{\sqrt{2}}\Big[\Big(y_d^{jk} \quad \frac{v^2}{2}\mathcal{C}^{jk}_{d\phi}\Big)\overline{d^j_L}d^k_R + y^i_u\overline{u^i_L}u^i_R + h.c.\Big] \\
& e[Q_u\overline{u^i}\gamma^\mu u^i + Q_d\overline{d^i}\gamma^\mu d^i]A_\mu \quad \frac{g}{\sqrt{2}}\big[\{\delta^{ji} + v^2\,\mathcal{C}^{(3)ji}_{\phi q}\}\overline{u^j_L}\gamma^\mu d^i_L W^+_\mu + h.c.\big] \\
& \frac{g}{2c_w}\big[\delta^{ji} \quad v^2\{\mathcal{C}^{(1)ji}_{\phi q} \quad \mathcal{C}^{(3)ji}_{\phi q}\}\big]\overline{u^j_L}\gamma^\mu u^i_L Z_\mu + \frac{g}{c_w}Q_u s_w^2\,\overline{u^i}\gamma^\mu u^i Z_\mu \\
& + \frac{g}{2c_w}\big[\delta^{ji} + v^2\{\mathcal{C}^{(1)ji}_{\phi q} + \mathcal{C}^{(3)ji}_{\phi q}\}\big]\overline{d^j_L}\gamma^\mu d^i_L Z_\mu + \frac{g}{c_w}Q_d s_w^2\,\overline{d^i}\gamma^\mu d^i Z_\mu \\
& \Big[\Big(y_d^{jk} \quad \frac{v^2}{2}\{\mathcal{C}^{jk}_{d\phi} \quad 2\mathcal{C}^{(3)ji}_{\phi q}y_d^{ik}\}\Big)\overline{u^j_L}d^k_R\chi^+ + h.c.\Big] \\
& + \big[\{\delta^{ji} + v^2\mathcal{C}^{(3)ji}_{\phi q}\}y^i_u\,\overline{d^j_L}u^i_R\chi \quad + h.c.\big] \quad \frac{1}{\sqrt{2}}\Big[\Big\{y_d^{jk} \quad \frac{3v^2}{2}\mathcal{C}^{jk}_{d\phi}\Big\}\overline{d^j_L}d^k_R h + h.c.\Big] \\
& \Big[\frac{i}{\sqrt{2}}\Big(y_d^{jk} \quad \frac{v^2}{2}\{\mathcal{C}^{jk}_{d\phi} \quad 2\;\ \mathcal{C}^{(1)ji}_{\phi q} + \mathcal{C}^{(3)ji}_{\phi q})y_d^{ik}\}\Big)\overline{d^j_L}d^k_R\chi_0 + h.c.\Big] \\
& \frac{y^i_u}{\sqrt{2}}\overline{u^i_L}u^i_R h + \Big[\frac{i}{\sqrt{2}} \quad \delta^{ji} \quad v^2\{\mathcal{C}^{(1)ji}_{\phi q} \quad \mathcal{C}^{(3)ji}_{\phi q}\})y^i_u\,\overline{u^j_L}u^i_R\chi_0 + h.c.\Big].
\end{aligned}
\tag{4.48}
$$

The combination $\mathcal{C}^{(1)ji}_{\phi q} \quad \mathcal{C}^{(3)ji}_{\phi q}$ vanishes if the relation Eq.(4.10) is taken into account. However, the relations Eqs.(4.10) and (4.11) hold only the matching scale μ_{VLQ} because of the RG effects. Therefore, we leave the terms which are proportional to the combination $\mathcal{C}^{(1)ji}_{\phi q} \quad \mathcal{C}^{(3)ji}_{\phi q}$ in Eq.(4.48). The terms $\mathcal{L}^{(0)}_{\text{dim.5}}$ and $\mathcal{L}^{(0)}_{\text{dim.6}}$ contain dim.5 and dim.6 operators which do not exist in the SM. Here we show only terms which can contribute to $b \to s\gamma$ process:

$$
\begin{aligned}
\mathcal{L}^{(0)}_{\text{dim.5}} \;\supset\;& vg\,\{\mathcal{C}^{(1)ji}_{\phi q} \quad \mathcal{C}^{(3)ji}_{\phi q}\}\overline{d^j_L}\gamma^\mu d^i_L(W^+_\mu\chi \quad + W_\mu\ \chi^+) \\
& + i\{\mathcal{C}^{(1)ji}_{\phi q} \quad \mathcal{C}^{(3)ji}_{\phi q}\}\overline{d^j_L}\gamma^\mu d^i_L(\chi\ \ \partial_\mu\chi^+ \quad \chi^+\partial_\mu\chi\ \ ) \\
& + \Big[\frac{v}{\sqrt{2}}\{\mathcal{C}^{jk}_{d\phi} + 2\mathcal{C}^{(3)ji}_{\phi q}y_d^{ik}\}\overline{d^j_L}\,d^k_R\,\chi^+\chi \quad + h.c.\Big],
\end{aligned}
\tag{4.49}
$$

$$
\mathcal{L}^{(0)}_{\text{dim.6}} \;\supset\; 2e\{\mathcal{C}^{(1)ji}_{\phi q} \quad \mathcal{C}^{(3)ji}_{\phi q}\}\overline{d^j_L}\gamma^\mu d^i_L\,\chi^+\chi\ \ A_\mu\,. \tag{4.50}
$$

We can see that all the terms in Eqs.(4.49) and (4.50) vanish if the relation Eqs.(4.10) and (4.11) is taken into account.

Next we consider a diagonalization of the down-type quark mass matrix in Eq.(4.48). The 3×3 mass matrix of the down-type quarks is,

$$
m_d^{jk} \;\equiv\; \frac{v}{\sqrt{2}}\Big(y_d^{jk} \quad \frac{v^2}{2}\mathcal{C}^{jk}_{d\phi}\Big). \tag{4.51}
$$

We diagonalize the mass matrix m_d^{jk} by two steps. First we diagonalize only the SM Yukawa coupling y_d^{jk} with unitary matrices K_L and K_R:

$$
\begin{cases} d^i_L = K_L^{im}d_L^{(0)m} \\ d^i_R = K_R^{im}d_R^{(0)m} \end{cases}, \qquad \to \qquad (K_L^{\dagger mk}y_d^{jk}K_R^{kn}) \;\equiv\; y_d^{(0)m}\delta^{mn}, \tag{4.52}
$$

where we define the diagonal Yukawa coupling $y_d^{(0)}$. The indices (0) indicates the basis where the SM Yukawa coupling y_d is diagonal. That basis corresponds to the mass basis of the SM. The whole mass matrix m_d^{jk} becomes,

$$\begin{aligned} K_L^{\dagger mj} m_d^{jk} K_R^{kn} &= \frac{v}{\sqrt{2}}\left(y_d^{(0)m}\delta^{mn} \quad \frac{v^2}{2} K_L^{\dagger mj} \mathcal{C}_{d\phi}^{jk} K_R^{kn} \right) \\ &\equiv \frac{v}{\sqrt{2}}\left(y_d^{(0)m}\delta^{mn} \quad \frac{v^2}{2}\tilde{\mathcal{C}}_{d\phi}^{mn} \right), \end{aligned} \tag{4.53}$$

Here we define the Wilson coefficients in the mass basis of the SM as $\tilde{\mathcal{C}}_{d\phi}^{mn}$. The definitions of the Wilson coefficients in the mass basis of the SM are,

$$\tilde{\mathcal{C}}_{\phi q}^{(1)mn} \equiv K_L^{\dagger mj} \mathcal{C}_{\phi q}^{(1)jk} K_L^{kn}\,, \tag{4.54}$$

$$\tilde{\mathcal{C}}_{\phi q}^{(3)mn} \equiv K_L^{\dagger mj} \mathcal{C}_{\phi q}^{(3)jk} K_L^{kn}\,, \tag{4.55}$$

$$\tilde{\mathcal{C}}_{d\phi}^{mn} \equiv K_L^{\dagger mj} \mathcal{C}_{d\phi}^{jk} K_R^{kn}\,. \tag{4.56}$$

Explicit forms of the $\tilde{\mathcal{C}}_{\phi q}^{(1)mn}$, $\tilde{\mathcal{C}}_{\phi q}^{(3)mn}$ and $\tilde{\mathcal{C}}_{d\phi}^{mn}$ at the scale μ_{VLQ} are:

$$\tilde{\mathcal{C}}_{\phi q}^{(1)mn}(\mu_{\text{VLQ}}) \equiv K_L^{\dagger mj} \mathcal{C}_{\phi q}^{(1)jk}(\mu_{\text{VLQ}}) K_L^{kn} = \frac{y_d^{(0)m4} y_d^{(0)n4*}}{4M_4^2}\,, \tag{4.57}$$

$$\tilde{\mathcal{C}}_{\phi q}^{(3)mn}(\mu_{\text{VLQ}}) = \tilde{\mathcal{C}}_{\phi q}^{(1)mn}(\mu_{\text{VLQ}})\,, \tag{4.58}$$

$$\tilde{\mathcal{C}}_{d\phi}^{mn}(\mu_{\text{VLQ}}) \equiv K_L^{\dagger mj} \mathcal{C}_{d\phi}^{jk}(\mu_{\text{VLQ}}) K_R^{kn} = \frac{y_d^{(0)m4} y_d^{(0)l4*}}{2M_4^2} y_d^{(0)l}\delta^{ln}\,, \tag{4.59}$$

where we used the relation Eqs.(4.10) and (4.11) and define the Yukawa couplings among the SM quarks and the VLQ in the mass basis of the SM as,

$$y_d^{(0)m4} \equiv K_L^{\dagger mj} y_d^{j4}\,. \tag{4.60}$$

The mass matrix Eq.(4.53) is still non-diagonal. We introduce unitary matrices V_L and V_R which diagonalize the whole mass matrix Eq.(4.53):

$$\begin{cases} d_L^{(0)m} = V_L^{mp} d_L'^{\,p} \\ d_R^{(0)m} = V_R^{mp} d_R'^{\,p} \end{cases}, \quad \to \quad V_L^{\dagger pm}\left(y_d^{(0)m}\delta^{mn} \quad \frac{v^2}{2}\tilde{\mathcal{C}}_{d\phi}^{mn} \right) V_R^{nq} \equiv y_d'^{\,p}\delta^{pq}, \tag{4.61}$$

where the prime indicates the complete mass basis of the SM down-type quarks with the diagonal mass matrix,

$$M_d \equiv \frac{v}{\sqrt{2}} y_d' = \text{diag}[m_d, m_s, m_b]\,. \tag{4.62}$$

The mixing angles of the unitary matrices $V_{L,R}$ are of the order of $\mathcal{O}(v^2/M_4^2)$ since the off-diagonal elements of the mass matrix Eq.(4.53) is of the order of $v^2\tilde{\mathcal{C}}_{d\phi}^{mn} \sim v^2/M_4^2$. We define the Yukawa coupling in the complete mass basis as,

$$y_d'^{\,p4} \equiv V_L^{\dagger pm} y_d^{(0)m4} \simeq \delta^{pm} y_d^{(0)m4} + \mathcal{O}\left(\frac{v^2}{M_4^2}\right), \tag{4.63}$$

then we can take,

$$V_L^{\dagger pm}\tilde{\mathcal{C}}_{\phi q}^{(1)mn}(\mu_{\rm VLQ})V_L^{nq} \;=\; \frac{y_d'^{p4}y_d'^{q4*}}{4M_4^2} \;\simeq\; \tilde{\mathcal{C}}_{\phi q}^{(1)pq}+\mathcal{O}\left(\frac{v^4}{M_4^4}\right), \tag{4.64}$$

$$V_L^{\dagger pm}\tilde{\mathcal{C}}_{\phi q}^{(3)mn}(\mu_{\rm VLQ})V_L^{nq} \;=\; \frac{y_d'^{p4}y_d'^{q4*}}{4M_4^2} \;\simeq\; \tilde{\mathcal{C}}_{\phi q}^{(3)pq}+\mathcal{O}\left(\frac{v^4}{M_4^4}\right), \tag{4.65}$$

$$V_L^{\dagger pm}\tilde{\mathcal{C}}_{d\phi}^{mn}(\mu_{\rm VLQ})V_R^{nq} \;\simeq\; \frac{y_d'^{p4}y_d'^{q4*}}{2M_4^2}y_d'^{q}+\mathcal{O}\left(\frac{v^4}{M_4^4}\right) \;\simeq\; \tilde{\mathcal{C}}_{d\phi}^{pq}(\mu_{\rm VLQ})+\mathcal{O}\left(\frac{v^4}{M_4^4}\right). \tag{4.66}$$

After the transformations Eqs.(4.52) and (4.61), we obtain the kinetic terms and interactions among the SM quarks induced by the dim.4 Lagrangian $\mathcal{L}^{(0)}_{\rm dim.4}$ in the mass basis as,

$$\mathcal{L}^{(0)}_{\rm dim.4} \;=\; \mathcal{L}_K^q+\mathcal{L}_A^q+\mathcal{L}_W^q+\mathcal{L}_Z^q+\mathcal{L}_{\chi^\pm}^q+\mathcal{L}_h^q+\mathcal{L}_{\chi_0}^q\,. \tag{4.67}$$

The each part of the Lagrangian is given as follows:

$$\mathcal{L}_K^q \;=\; \bar{u^i}(i\gamma^\mu\partial_\mu \quad M_u^i)u^i+\bar{d^p}(i\gamma^\mu\partial_\mu \quad M_d^p)d^p\,, \tag{4.68}$$

$$\mathcal{L}_A^q \;=\; \quad e[Q_u\overline{u^i}\gamma^\mu u^i+Q_d\overline{d^p}\gamma^\mu d^p]A_\mu\,, \tag{4.69}$$

$$\mathcal{L}_W^q \;=\; \quad \frac{g}{\sqrt{2}}[\overline{u_L^j}V_{\rm CKM}^{jp}\gamma^\mu d_L^p W_\mu^+ + h.c.]\,, \tag{4.70}$$

$$\mathcal{L}_Z^q \;=\; \quad \frac{g}{c_w}\left[\overline{u^j}\gamma^\mu\left(\frac{1}{2}Z_{u\rm NC}^{ji}L \quad Q_u s_w^2\delta^{ji}\right)u^i \quad \overline{d^p}\gamma^\mu\left(\frac{1}{2}Z_{d\rm NC}^{pq}L+Q_d s_w^2\delta^{pq}\right)d^q\right]Z_\mu\,, \tag{4.71}$$

$$\mathcal{L}_{\chi^\pm}^q \;=\; \frac{g}{\sqrt{2}M_W}[\overline{u^j}V_{\rm CKM}^{jq}(M_u^iL \quad M_d^qR)d^q\chi^+ + h.c.]\,, \tag{4.72}$$

$$\mathcal{L}_h^q \;=\; \quad \frac{g}{2M_W}[M_u^i\bar{u^i}u^i+\bar{d^p}H_{d\rm NC}^{pq}(M_d^qR+M_d^pL)d^q]h\,, \tag{4.73}$$

$$\mathcal{L}_{\chi_0}^q \;=\; \frac{i\,g}{2M_W}[\overline{u^j}Z_{u\rm NC}^{ji}(M_u^iR \quad M_u^jL)u^i \quad \overline{d^p}Z_{d\rm NC}^{pq}(M_d^qR \quad M_d^pL)d^q]\chi_0\,, \tag{4.74}$$

where we omit the prime on the down-type quark fields for simplicity. The symbols L and R denote the chiral projection operators. The matrix $M_u^i \equiv v y_u^i/\sqrt{2}$ is diagonal up-type quark mass matrix. The 3×3 matrix $V_{\rm CKM}$ is the CKM matrix defined as,

$$V_{\rm CKM}^{jp} \;\equiv\; K_L^{jm}\{\delta^{mn}+v^2\tilde{\mathcal{C}}_{\phi q}^{(3)mn}\}V_L^{np}\,. \tag{4.75}$$

We can see from Eqs.(4.71) and (4.74) that the FCNCs arise from the 3×3 non-diagonal matrix $Z_{d\rm NC}$ and $Z_{u\rm NC}$ in the Z and χ_0 interactions. The matrix $Z_{d\rm NC}$ and $Z_{u\rm NC}$ are given as follows:

$$Z_{d\rm NC}^{pq} \;\equiv\; \delta^{pq}+v^2V_L^{\dagger pm}\{\tilde{\mathcal{C}}_{\phi q}^{(1)mn}+\tilde{\mathcal{C}}_{\phi q}^{(3)mn}\}V_L^{nq} \;\simeq\; \delta^{pq}+v^2\{\tilde{\mathcal{C}}_{\phi q}^{(1)pq}+\tilde{\mathcal{C}}_{\phi q}^{(3)pq}\}\,, \tag{4.76}$$

$$Z_{u\rm NC}^{ji} \;\equiv\; \delta^{ji} \quad v^2\{\mathcal{C}_{\phi q}^{(1)ji} \quad \mathcal{C}_{\phi q}^{(3)ji}\} \;\simeq\; \delta^{ji} \quad v^2V_{\rm CKM}^{jp}\{\tilde{\mathcal{C}}_{\phi q}^{(1)pq} \quad \tilde{\mathcal{C}}_{\phi q}^{(3)pq}\}V_{\rm CKM}^{\dagger qi}\,. \tag{4.77}$$

The matrix $Z_{u\rm NC}$ which induces the FCNC among the up-type quarks vanishes at the matching scale $\mu_{\rm VLQ}$ because of the relation Eq.(4.10). It is clear that the FCNC interactions are suppressed by the factor v^2/M_4^2 since the Wilson coefficients are

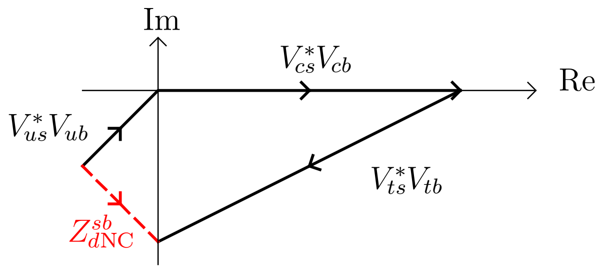

Figure 4.4. The relation Eq.(4.82) in complex plane [84].

order of $M_4{}^2$. Therefore, the FCNC processes are suppressed even though the GIM mechanism does not work. If we neglect RG effect, the matrix $Z_{d\mathrm{NC}}$ can be written as,

$$Z^{pq}_{d\mathrm{NC}}(\mu_{\mathrm{VLQ}}) \;\simeq\; \delta^{pq} + v^2\{\tilde{\mathcal{C}}^{(1)pq}_{\phi q}(\mu_{\mathrm{VLQ}}) + \tilde{\mathcal{C}}^{(3)pq}_{\phi q}(\mu_{\mathrm{VLQ}})\} \;=\; \delta^{pq} \quad v^2\frac{y_d'^{p4}y_d'^{q4*}}{2M_4^2}\,. \tag{4.78}$$

The FCNC in the h interaction Eq.(4.73) is only in the down-type quark sector and induced by the 3×3 non-diagonal matrix,

$$H^{pq}_{d\mathrm{NC}}M^q_d \;\equiv\; \frac{v}{\sqrt{2}}[\delta^{pq}y_d'^q \quad v^2\tilde{\mathcal{C}}^{pq}_{d\phi}]\,. \tag{4.79}$$

The matrix $H_{d\mathrm{NC}}$ is equal to the matrix $Z_{d\mathrm{NC}}$ at the matching scale μ_{VLQ} because of the relations Eqs.(4.10) and (4.11):

$$H^{pq}_{d\mathrm{NC}}(\mu_{\mathrm{VLQ}})M^q_d \;=\; Z^{pq}_{d\mathrm{NC}}(\mu_{\mathrm{VLQ}})M^q_d\,. \tag{4.80}$$

In the case of the SM, the CKM matrix is unitary matrix, i.e. $V^{\mathrm{SM}}_{\mathrm{CKM}}V^{\mathrm{SM}\dagger}_{\mathrm{CKM}} = V^{\mathrm{SM}\dagger}_{\mathrm{CKM}}V^{\mathrm{SM}}_{\mathrm{CKM}} = 1$. However, the unitarity of the 3×3 CKM matrix V_{CKM} does not hold in the present model since the Wilson coefficient $\tilde{\mathcal{C}}^{(3)mn}_{\phi q}$ in Eq.(4.75) is not unitary matrix. Using the expression Eq.(4.75), the product $V^\dagger_{\mathrm{CKM}}V_{\mathrm{CKM}}$ is given as,

$$\sum_{i=u,c,t} V^{ip*}_{\mathrm{CKM}}V^{iq}_{\mathrm{CKM}} \;\simeq\; \delta^{pq} + 2v^2\tilde{\mathcal{C}}^{(3)pq}_{\phi q} \;=\; Z^{pq}_{d\mathrm{NC}} \quad v^2\{\tilde{\mathcal{C}}^{(1)pq}_{\phi q} \quad \tilde{\mathcal{C}}^{(3)pq}_{\phi q}\}\,. \tag{4.81}$$

Therefore, the product $V^\dagger_{\mathrm{CKM}}V_{\mathrm{CKM}}$ is equal to the matrix $Z^{pq}_{d\mathrm{NC}}$ which induces the FCNC among the down-type quarks at the matching scale μ_{VLQ}:

$$\sum_{i=u,c,t} V^{ip*}_{\mathrm{CKM}}V^{iq}_{\mathrm{CKM}} \;\simeq\; Z^{pq}_{d\mathrm{NC}}\,. \tag{4.82}$$

This relation can be expressed as a quadrangle in complex plane shown in Fig.4.4. We note that there is the same relation as Eq.(4.81) in the case of 3×4 CKM matrix in the full theory Eq.(2.52). Therefore, the violation of the CKM unitarity $V_{\mathrm{CKM}}V^\dagger_{\mathrm{CKM}} \neq 1$ comes from the existence of the VLQ, not the effect of integrating out the VLQ. Similarly, the product $V_{\mathrm{CKM}}V^\dagger_{\mathrm{CKM}}$ is given as,

$$\sum_{p=d,s,b} V^{ip}_{\mathrm{CKM}}V^{jp*}_{\mathrm{CKM}} \;\simeq\; \delta^{ij} + 2v^2\mathcal{C}^{(3)ij}_{\phi q} \;=\; Z^{ij}_{u\mathrm{NC}} + v^2\{\mathcal{C}^{(1)ij}_{\phi q} + \mathcal{C}^{(3)ij}_{\phi q}\}\,. \tag{4.83}$$

In the case of full theory, the product of the $V_{\mathrm{CKM}}^{\dagger}V_{\mathrm{CKM}}$ is equal to one if we sum up all the flavor of SM down-type quarks in addition to the VLQ as shown in Eq.(2.53). Thus the violation of the CKM unitarity in Eq.(4.83) comes from the effect of integrating out the VLQ. Finally we present the dim.5 and 6 effective operators in Eqs.(4.49) and (4.50) after the unitary transformations Eqs.(4.52) and (4.61):

$$\begin{aligned}
\mathcal{L}^{(0)}_{\mathrm{dim.5}} \;\supset\;\; & vg\,\{\tilde{\mathcal{C}}^{(1)pq}_{\phi q} \quad \tilde{\mathcal{C}}^{(3)pq}_{\phi q}\}\overline{d^p_L}\gamma^\mu d^q_L(W^+_\mu\chi \quad + W_\mu\ \chi^+) \\
& + i\{\tilde{\mathcal{C}}^{(1)pq}_{\phi q} \quad \tilde{\mathcal{C}}^{(3)pq}_{\phi q}\}\overline{d^p_L}\gamma^\mu d^q_L(\chi \quad \partial_\mu\chi^+ \quad \chi^+\partial_\mu\chi \quad) \\
& + \left[\frac{v}{\sqrt{2}}\{\tilde{\mathcal{C}}^{pq}_{d\phi} + 2\tilde{\mathcal{C}}^{(3)pq}_{\phi q}M^q_d\}\overline{d^p_L}\, d^q_R\,\chi^+\chi \quad + h.c.\right], \qquad (4.84) \\
\mathcal{L}^{(0)}_{\mathrm{dim.6}} \;\supset\;\; & 2e\{\tilde{\mathcal{C}}^{(1)pq}_{\phi q} \quad \tilde{\mathcal{C}}^{(3)pq}_{\phi q}\}\overline{d^p_L}\gamma^\mu d^q_L\,\chi^+\chi \quad A_\mu\,. \qquad (4.85)
\end{aligned}$$

where we omit the prime on the down-type quark fields for simplicity.

4.4.2 One-loop level effective operators (dipole operators)

We substitute Eq.(4.46) for the Higgs doublet ϕ in the one-loop level effective operators in Eq.(4.27) with Eqs.(4.28)-(4.31). Here we focus on the dipole operators and set $h, \chi^{\pm}, \chi_0 \to 0$ in Eq.(4.46) since we need only the terms which are proportional to the VEV v in next chapter. After the unitary transformations Eqs.(4.52) and (4.61), the dipole operators in Eq.(4.27) with Eqs.(4.28)-(4.31) become,

$$\begin{aligned}
\mathcal{L}^{(1)}_{eff} \;\supset\;\; & +\frac{v}{\sqrt{2}}(c_w\mathcal{C}^{ji}_{uW} \quad s_w\mathcal{C}^{ji}_{uB})[\overline{u^j_L}\sigma^{\mu\nu}u^i_R Z_{\mu\nu}] + \frac{v}{\sqrt{2}}(s_w\mathcal{C}^{ji}_{uW} + c_w\mathcal{C}^{ji}_{uB})[\overline{u^j_L}\sigma^{\mu\nu}u^i_R F_{A\mu\nu}] \\
& +\frac{v}{\sqrt{2}}(\quad c_w\tilde{\mathcal{C}}^{pq}_{dW} \quad s_w\tilde{\mathcal{C}}^{pq}_{dB})\overline{d^p_L}\sigma^{\mu\nu}d^q_R Z_{\mu\nu} + \frac{v}{\sqrt{2}}(\quad s_w\tilde{\mathcal{C}}^{pq}_{dW} + c_w\tilde{\mathcal{C}}^{pq}_{dB})\overline{d^p_L}\sigma^{\mu\nu}d^q_R F_{A\mu\nu} \\
& +\frac{v}{\sqrt{2}}\mathcal{C}^{ji}_{uG}\left[\overline{u^j_L}\sigma^{\mu\nu}\frac{\lambda^a}{2}u^i_R G^a_{\mu\nu}\right] + \frac{v}{\sqrt{2}}\tilde{\mathcal{C}}^{pq}_{dG}\left[\overline{d^p_L}\sigma^{\mu\nu}\frac{\lambda^a}{2}d^q_R G^a_{\mu\nu}\right] \\
& +vV^{pj*}_{\mathrm{CKM}}\mathcal{C}^{ji}_{uW}[\overline{d^p_L}\sigma^{\mu\nu}u^i_R W_{\mu\nu}] + vV^{jp}_{\mathrm{CKM}}\tilde{\mathcal{C}}^{pq}_{dW}[\overline{u^j_L}\sigma^{\mu\nu}d^q_R W^+_{\mu\nu}] + h.c.\,, \qquad (4.86)
\end{aligned}$$

where $c_w = \cos\theta_w$ and $s_w = \sin\theta_w$ with the Weinberg angle θ_w. We define the Wilson coefficients in the down-type quark mass basis as,

$$\tilde{\mathcal{C}}^{pq}_x \;\equiv\; V^{\dagger pm}_L K^{\dagger mj}_L \mathcal{C}^{jk}_x K^{kn}_R V^{nq}_R \;\simeq\; K^{\dagger pj}_L \mathcal{C}^{jk}_x K^{kq}_R + \mathcal{O}\left(\frac{v^4}{M_4^4}\right), \qquad (4.87)$$

with the index $x = uB, uW, uG, dB, dW, dG$. The field strengths $Z^{\mu\nu}$, $F^{\mu\nu}_A$ and $W^{\pm\mu\nu}$ are defined as,

$$\begin{aligned}
Z^{\mu\nu} &\equiv \partial^\mu Z^\nu \quad \partial^\nu Z^\mu\,, \qquad (4.88) \\
F^{\mu\nu}_A &\equiv \partial^\mu A^\nu \quad \partial^\nu A^\mu\,, \qquad (4.89) \\
W^{\pm\mu\nu} &\equiv \partial^\mu W^{\pm\nu} \quad \partial^\nu W^{\pm\mu}\,. \qquad (4.90)
\end{aligned}$$

$\mathcal{C}_{uG}^{ji}(\mu_{\rm VLQ})$	$\frac{1}{24}\cdot\frac{g_s}{16\pi^2 M_4^2}\cdot\frac{\sqrt{2}}{v}V_{\rm CKM}^{jp}y_d'^{p4}y_d'^{q4*}V_{\rm CKM}^{iq*}M_u^i$
$\mathcal{C}_{uW}^{ji}(\mu_{\rm VLQ})$	$\frac{1}{24}\cdot\frac{g}{16\pi^2 M_4^2}\cdot\frac{\sqrt{2}}{v}V_{\rm CKM}^{jp}y_d'^{p4}y_d'^{q4*}V_{\rm CKM}^{iq*}M_u^i$
$\mathcal{C}_{uB}^{ji}(\mu_{\rm VLQ})$	$\frac{g'}{16\pi^2 M_4^2}\left(\frac{Y_{qL}}{2}\cdot\frac{1}{12}\quad\frac{Y_{dR}}{2}\cdot\frac{1}{8}\right)\cdot\frac{\sqrt{2}}{v}V_{\rm CKM}^{jp}y_d'^{p4}y_d'^{q4*}V_{\rm CKM}^{iq*}M_u^i$
$\tilde{\mathcal{C}}_{dG}^{pq}(\mu_{\rm VLQ})$	$\frac{1}{24}\cdot\frac{g_s}{16\pi^2 M_4^2}\cdot\frac{\sqrt{2}}{v}y_d'^{p4}y_d'^{q4*}M_d^q$
$\tilde{\mathcal{C}}_{dW}^{pq}(\mu_{\rm VLQ})$	$\frac{1}{24}\cdot\frac{g}{16\pi^2 M_4^2}\cdot\frac{\sqrt{2}}{v}y_d'^{p4}y_d'^{q4*}M_d^q$
$\tilde{\mathcal{C}}_{dB}^{pq}(\mu_{\rm VLQ})$	$\frac{g'}{16\pi^2 M_4^2}\left(\frac{Y_{qL}}{2}\cdot\frac{1}{12}\quad\frac{Y_{dR}}{2}\cdot\frac{1}{8}\right)\cdot\frac{\sqrt{2}}{v}y_d'^{p4}y_d'^{q4*}M_d^q$

Table 4.3. The Wilson coefficients of the dipole operators in the mass basis [84].

Table 4.3 shows the Wilson coefficients of dipole operators in the mass basis. We note that,

$$\begin{aligned}\frac{v}{\sqrt{2}}(&\quad s_w\tilde{\mathcal{C}}_{dW}^{pq}(\mu_{\rm VLQ})+c_w\tilde{\mathcal{C}}_{dB}^{pq}(\mu_{\rm VLQ}))\overline{d_L^p}\sigma^{\mu\nu}d_R^q F_{A\mu\nu} \\ = &\quad \frac{e}{16\pi^2}\cdot\frac{G_F}{6\sqrt{2}}Q_d\cdot v^2\,\frac{y_d'^{p4}y_d'^{q4*}}{2M_4^2}M_d^q\overline{d_L^p}\sigma^{\mu\nu}d_R^q F_{A\mu\nu}\,. \end{aligned} \tag{4.91}$$

This is consistent with Ref.[84].

4.5 Renormalization Group Effects

We investigate RG effects from the matching scale $\mu_{\rm VLQ}$ to the EW scale $\mu_{\rm EW}$. The RG equations for the Wilson coefficients in the SMEFT are defined by,

$$16\pi^2\mu\frac{d}{d\mu}\mathcal{C}_a(\mu) \;=\; \gamma_{ab}\mathcal{C}_b(\mu)\,, \tag{4.92}$$

where γ_{ab} is an anomalous dimension matrix in the SMEFT given in Refs.[75, 76, 77]. We solve the RG equations under the first leading log approximation (LLA) [77, 83]:

$$\mathcal{C}_a(\mu_{\rm EW}) \;\simeq\; \left[\delta_{ab}\quad\frac{\gamma_{ab}}{16\pi^2}\ln\frac{\mu_{\rm VLQ}}{\mu_{\rm EW}}\right]\mathcal{C}_b(\mu_{\rm VLQ})\,. \tag{4.93}$$

In the following, we focus on the RG effects for only the tree level Wilson coefficients $\tilde{\mathcal{C}}_{\phi q}^{(1)pq}$, $\tilde{\mathcal{C}}_{\phi q}^{(3)pq}$ since the coefficient $\tilde{\mathcal{C}}_{d\phi}^{pq}$ does not appear in our numerical analysis.

4.5.1 RG effects for $\tilde{\mathcal{C}}_{\phi q}^{(1)pq}$ and $\tilde{\mathcal{C}}_{\phi q}^{(3)pq}$

The solutions of the RG equations for $\tilde{\mathcal{C}}_{\phi q}^{(1)pq}$ and $\tilde{\mathcal{C}}_{\phi q}^{(3)pq}$ are obtained under the first LLA as follows:

$$\tilde{\mathcal{C}}_{\phi q}^{(1)pq}(\mu_{\rm EW}) \;\simeq\; \tilde{\mathcal{C}}_{\phi q}^{(1)pq}(\mu_{\rm VLQ})\quad\frac{K_L^{\dagger pi}\dot{\mathcal{C}}_{\phi q}^{(1)ij}K_L^{jq}}{(4\pi)^2}\ln\frac{\mu_{\rm VLQ}}{\mu_{\rm EW}}\,, \tag{4.94}$$

$$\tilde{\mathcal{C}}_{\phi q}^{(3)pq}(\mu_{\rm EW}) \;\simeq\; \tilde{\mathcal{C}}_{\phi q}^{(3)pq}(\mu_{\rm VLQ})\quad\frac{K_L^{\dagger pi}\dot{\mathcal{C}}_{\phi q}^{(3)ij}K_L^{jq}}{(4\pi)^2}\ln\frac{\mu_{\rm VLQ}}{\mu_{\rm EW}}\,. \tag{4.95}$$

The coefficients of logarithmic terms are given as [77, 83],

$$\begin{aligned}
\dot{\mathcal{C}}_{\phi q}^{(1)ij} &= 2[y_u y_u^\dagger]_{ik}\mathcal{C}_{\phi q}^{(1)kj}(\mu_{\rm VLQ}) + 2\mathcal{C}_{\phi q}^{(1)ik}(\mu_{\rm VLQ})[y_u y_u^\dagger]_{kj} + 6\,\mathrm{Tr}[y_u y_u^\dagger]\mathcal{C}_{\phi q}^{(1)ij}(\mu_{\rm VLQ}) \\
&\quad \frac{9}{2}[y_u y_u^\dagger]_{ik}\mathcal{C}_{\phi q}^{(3)kj}(\mu_{\rm VLQ}) \quad \frac{9}{2}\mathcal{C}_{\phi q}^{(3)ik}(\mu_{\rm VLQ})[y_u y_u^\dagger]_{kj}\,, \qquad (4.96) \\
\dot{\mathcal{C}}_{\phi q}^{(3)ij} &= [y_u y_u^\dagger]_{ik}\mathcal{C}_{\phi q}^{(3)kj}(\mu_{\rm VLQ}) + \mathcal{C}_{\phi q}^{(3)ik}(\mu_{\rm VLQ})[y_u y_u^\dagger]_{kj} + 6\,\mathrm{Tr}[y_u y_u^\dagger]\mathcal{C}_{\phi q}^{(3)ij}(\mu_{\rm VLQ}) \\
&\quad \frac{3}{2}[y_u y_u^\dagger]_{ik}\mathcal{C}_{\phi q}^{(1)kj}(\mu_{\rm VLQ}) \quad \frac{3}{2}\mathcal{C}_{\phi q}^{(1)ik}(\mu_{\rm VLQ})[y_u y_u^\dagger]_{kj}\,, \qquad (4.97)
\end{aligned}$$

where we take only the terms which are proportional to the up-type Yukawa coupling into account. Since the top Yukawa coupling gives leading contributions, we focus on the top Yukawa contributions:

$$\begin{aligned}
K_L^{\dagger pi}\dot{\mathcal{C}}_{\phi q}^{(1)ij}K_L^{jq} &\simeq \frac{4m_t^2}{v^2}\left[\lambda_{pp'}^t\tilde{\mathcal{C}}_{\phi q}^{(1)p'q}(\mu_{\rm VLQ}) + \tilde{\mathcal{C}}_{\phi q}^{(1)pp'}(\mu_{\rm VLQ})\lambda_{p'q}^t\right] + \frac{12m_t^2}{v^2}\tilde{\mathcal{C}}_{\phi q}^{(1)pq}(\mu_{\rm VLQ}) \\
&\quad \frac{9m_t^2}{v^2}\left[\lambda_{pp'}^t\tilde{\mathcal{C}}_{\phi q}^{(3)p'q}(\mu_{\rm VLQ}) + \tilde{\mathcal{C}}_{\phi q}^{(3)pp'}(\mu_{\rm VLQ})\lambda_{p'q}^t\right], \qquad (4.98) \\
K_L^{\dagger pi}\dot{\mathcal{C}}_{\phi q}^{(3)ij}K_L^{jq} &\simeq \frac{2m_t^2}{v^2}\left[\lambda_{pp'}^t\tilde{\mathcal{C}}_{\phi q}^{(3)p'q}(\mu_{\rm VLQ}) + \tilde{\mathcal{C}}_{\phi q}^{(3)pp'}(\mu_{\rm VLQ})\lambda_{p'q}^t\right] + \frac{12m_t^2}{v^2}\tilde{\mathcal{C}}_{\phi q}^{(3)pq}(\mu_{\rm VLQ}) \\
&\quad \frac{3m_t^2}{v^2}\left[\lambda_{pp'}^t\tilde{\mathcal{C}}_{\phi q}^{(1)p'q}(\mu_{\rm VLQ}) + \tilde{\mathcal{C}}_{\phi q}^{(1)pp'}(\mu_{\rm VLQ})\lambda_{p'q}^t\right], \qquad (4.99)
\end{aligned}$$

where $\lambda_{pq}^t \equiv V_{\rm CKM}^{tp*}V_{\rm CKM}^{tq}$. We simply replace K_L by $V_{\rm CKM}$ since we neglect $\mathcal{O}\left(\frac{v^4}{M_4^4}\right)$ terms. We consider the case of $p=s$ and $q=b$ to estimate the RG effects:

$$\begin{aligned}
K_L^{\dagger si}\dot{\mathcal{C}}_{\phi q}^{(1)ij}K_L^{jb} &\simeq \left[\frac{4m_t^2}{v^2}\lambda_{bb}^t + \frac{12m_t^2}{v^2}\right]\tilde{\mathcal{C}}_{\phi q}^{(1)sb}(\mu_{\rm VLQ}) \quad \frac{9m_t^2}{v^2}\tilde{\mathcal{C}}_{\phi q}^{(3)sb}(\mu_{\rm VLQ})\lambda_{bb}^t\,, \qquad (4.100) \\
K_L^{\dagger si}\dot{\mathcal{C}}_{\phi q}^{(3)ij}K_L^{jb} &\simeq \left[\frac{2m_t^2}{v^2}\lambda_{bb}^t + \frac{12m_t^2}{v^2}\right]\tilde{\mathcal{C}}_{\phi q}^{(3)sb}(\mu_{\rm VLQ}) \quad \frac{3m_t^2}{v^2}\tilde{\mathcal{C}}_{\phi q}^{(1)sb}(\mu_{\rm VLQ})\lambda_{bb}^t\,, \qquad (4.101)
\end{aligned}$$

where we leave leading order terms with respect to the CKM matrix elements, that is $\lambda_{bb}^t = |V_{\rm CKM}^{tb}|^2 \approx 1$. Since $\tilde{\mathcal{C}}_{\phi q}^{(1)sb}(\mu_{\rm VLQ}) = \tilde{\mathcal{C}}_{\phi q}^{(3)sb}(\mu_{\rm VLQ})$ as seen in Eq.(4.10), we obtain,

$$\begin{aligned}
\tilde{\mathcal{C}}_{\phi q}^{(1)sb}(\mu_{\rm EW}) &\simeq \left[1 \quad \frac{m_t^2}{(4\pi)^2v^2}(\quad 5\lambda_{bb}^t + 12)\ln\frac{\mu_{\rm VLQ}}{\mu_{\rm EW}}\right]\tilde{\mathcal{C}}_{\phi q}^{(1)sb}(\mu_{\rm VLQ})\,, \qquad (4.102) \\
\tilde{\mathcal{C}}_{\phi q}^{(3)sb}(\mu_{\rm EW}) &\simeq \left[1 \quad \frac{m_t^2}{(4\pi)^2v^2}(\quad \lambda_{bb}^t + 12)\ln\frac{\mu_{\rm VLQ}}{\mu_{\rm EW}}\right]\tilde{\mathcal{C}}_{\phi q}^{(3)sb}(\mu_{\rm VLQ})\,. \qquad (4.103)
\end{aligned}$$

It is clear that the combination $\tilde{\mathcal{C}}_{\phi q}^{(1)sb}(\mu_{\rm EW}) \quad \tilde{\mathcal{C}}_{\phi q}^{(3)sb}(\mu_{\rm EW}) \neq 0$ because of the RG effects. However, such a combination is suppressed by the factor $1/(4\pi)^2$ compared with $\tilde{\mathcal{C}}_{\phi q}^{(1)sb}(\mu_{\rm EW}) + \tilde{\mathcal{C}}_{\phi q}^{(3)sb}(\mu_{\rm EW})$. We estimate numerical values of the ratio $\tilde{\mathcal{C}}_{\phi q}^{(1)sb}(\mu_{\rm EW})/\tilde{\mathcal{C}}_{\phi q}^{(1)sb}(\mu_{\rm VLQ})$ and $\tilde{\mathcal{C}}_{\phi q}^{(3)sb}(\mu_{\rm EW})/\tilde{\mathcal{C}}_{\phi q}^{(3)sb}(\mu_{\rm VLQ})$. We set $\lambda_{bb}^t = 1$ for simplicity and take $m_t = 173.1$ GeV, $v = 246$ GeV with $\mu_{\rm EW} = M_Z = 91.1876$ GeV [65] and $\mu_{\rm VLQ} = 1$ TeV. The left figure in Fig.4.5 shows the dependence of the numerical values of $\tilde{\mathcal{C}}_{\phi q}^{(1)sb}(\mu_{\rm EW})/\tilde{\mathcal{C}}_{\phi q}^{(1)sb}(\mu_{\rm VLQ})$ and $\tilde{\mathcal{C}}_{\phi q}^{(3)sb}(\mu_{\rm EW})/\tilde{\mathcal{C}}_{\phi q}^{(3)sb}(\mu_{\rm VLQ})$ on the matching scale $\mu_{\rm VLQ}$. The horizontal axis is the matching scale $\mu_{\rm VLQ}$. The vertical axis is the

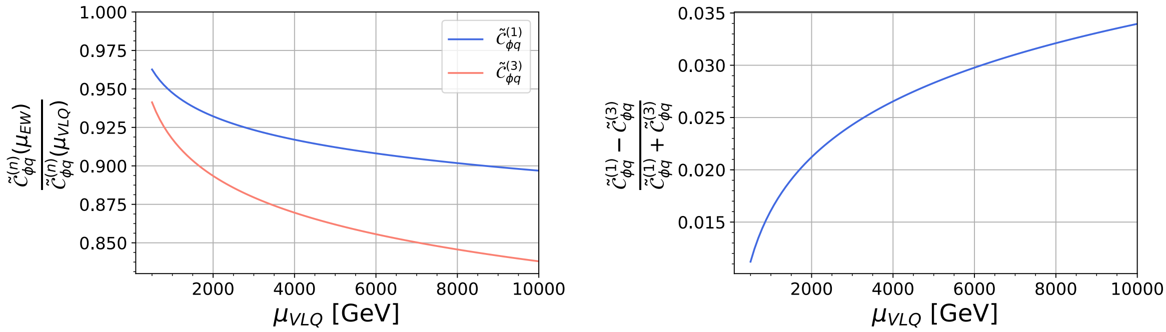

Figure 4.5. *Left*: The scale dependence of ratio $\tilde{\mathcal{C}}^{(n)sb}_{\phi q}(\mu_{\rm EW})/\tilde{\mathcal{C}}^{(n)sb}_{\phi q}(\mu_{\rm VLQ})$ with $n=1,3$. The horizontal axis is the matching scale $\mu_{\rm VLQ}$. The vertical axis is the ratio $\tilde{\mathcal{C}}^{(n)sb}_{\phi q}(\mu_{\rm EW})/\tilde{\mathcal{C}}^{(n)sb}_{\phi q}(\mu_{\rm VLQ})$. The blue line represents the dependence of the ratio for $\tilde{\mathcal{C}}^{(1)sb}_{\phi q}$ on $\mu_{\rm VLQ}$ while the red line corresponds to that of the ratio for $\tilde{\mathcal{C}}^{(3)sb}_{\phi q}$. Here the scale $\mu_{\rm VLQ}$ varies from 500 GeV to 10 TeV and $\mu_{\rm EW}=M_Z$. *Right*: The numerical value of the ratio $\{\tilde{\mathcal{C}}^{(1)sb}_{\phi q}(\mu_{\rm EW})\quad \tilde{\mathcal{C}}^{(3)sb}_{\phi q}(\mu_{\rm EW})\}/\{\tilde{\mathcal{C}}^{(1)sb}_{\phi q}(\mu_{\rm EW})+\tilde{\mathcal{C}}^{(3)sb}_{\phi q}(\mu_{\rm EW})\}$ as a function of the matching scale $\mu_{\rm VLQ}$.

ratio $\tilde{\mathcal{C}}^{(n)sb}_{\phi q}(\mu_{\rm EW})/\tilde{\mathcal{C}}^{(n)sb}_{\phi q}(\mu_{\rm VLQ})$. The blue line represents the dependence of the ratio for $\tilde{\mathcal{C}}^{(1)sb}_{\phi q}$ on $\mu_{\rm VLQ}$ while the red line corresponds to that of the ratio for $\tilde{\mathcal{C}}^{(3)sb}_{\phi q}$. We find from the left figure in Fig.4.5 that the Wilson coefficients at the EW scale $\tilde{\mathcal{C}}^{(1)sb}_{\phi q}(\mu_{\rm EW})$ and $\tilde{\mathcal{C}}^{(3)sb}_{\phi q}(\mu_{\rm EW})$ are $\mathcal{O}(10\%)$ smaller than that at the matching scale $\mu_{\rm VLQ}$ because of the RG effects. The right figure of Fig.4.5 shows numerical value of the ratio,

$$\frac{\tilde{\mathcal{C}}^{(1)sb}_{\phi q}(\mu_{\rm EW})\quad \tilde{\mathcal{C}}^{(3)sb}_{\phi q}(\mu_{\rm EW})}{\tilde{\mathcal{C}}^{(1)sb}_{\phi q}(\mu_{\rm EW})+\tilde{\mathcal{C}}^{(3)sb}_{\phi q}(\mu_{\rm EW})} = \frac{\frac{m_t^2}{(4\pi)^2v^2}4\lambda^t_{bb}\ln\frac{\mu_{\rm VLQ}}{\mu_{\rm EW}}}{2\quad \frac{m_t^2}{(4\pi)^2v^2}(\quad 6\lambda^t_{bb}+24)\ln\frac{\mu_{\rm VLQ}}{\mu_{\rm EW}}}. \tag{4.104}$$

One finds that the combination $\tilde{\mathcal{C}}^{(1)sb}_{\phi q}(\mu_{\rm EW})\quad \tilde{\mathcal{C}}^{(3)sb}_{\phi q}(\mu_{\rm EW})$ is approximately ten times smaller than $\tilde{\mathcal{C}}^{(1)sb}_{\phi q}(\mu_{\rm EW})+\tilde{\mathcal{C}}^{(3)sb}_{\phi q}(\mu_{\rm EW})$ and thus negligible.

4.6 Short Summary

We summarize the present chapter. We derive the effective operators in Eqs.(4.12) and (4.27) with Eqs.(4.28)-(4.31) by integrating out the VLQ up to one-loop level. After inserting the VEV into the Higgs doublet ϕ and diagonalizing the down-type quark mass matrix Eq.(4.51), we obtain the higer dimensional operators Eqs.(4.84), (4.85) and (4.86) in addition to the dim.4 operators in Eq.(4.67) with Eqs.(4.68)-(4.74). In next chapter, we construct the weak EFT from the effective Lagrangian shown in Eqs.(4.67) and (4.86). In the following chapters, we denote the elements of the CKM matrix $V^{ij}_{\rm CKM}$ as V_{ij} for simplicity.

Chapter 5
B Meson Systems in Model with VLQ

In this chapter, we investigate the neutral B meson systems in the model with VLQ. This can be done by calculating Wilson coefficients of the weak EFT. In this thesis, we take account of the RG effects from μ_{VLQ} to μ_{EW} in only the $B_s^0 \to \mu^+\mu$ process. This is because new physics effects for the $B_s^0 \to \mu^+\mu$ process is induced at the tree level while new physics contribute to the B_s^0-$\overline{B_s^0}$ mixing and the $\overline{B_d^0} \to X_s\gamma$ at the one-loop level or $\mathcal{O}(Z_{d\mathrm{NC}}^2)$. We give derivations of formulae for the observables of the neutral B meson systems in Appendix.A.

5.1 B_s^0-$\overline{B_s^0}$ Mixing and Δm_{B_s}

The effective Hamiltonian for the B_s^0-$\overline{B_s^0}$ mixing is,

$$\mathcal{H}_{eff}^{\Delta B=2} = \frac{G_F^2}{4\pi^2} M_W^2 (\lambda_{sb}^t)^2 C_{\mathrm{VLL}} O_{\mathrm{VLL}} + h.c. \tag{5.1}$$

with a product of the CKM matrix elements $\lambda_{sb}^t \equiv V_{ts}^* V_{tb}$ and an effective operator,

$$O_{\mathrm{VLL}} = [\overline{s_L}\gamma^\mu b_L][\overline{s_L}\gamma_\mu b_L]\,. \tag{5.2}$$

Here we use the notation of Ref.[97]. New contributions to the Wilson coefficient C_{VLL} from the effective Lagrangian shown in Eq.(4.67) are the violation of the CKM unitarity and the tree level FCNC. These contributions are computed in Refs.[98, 99, 100, 101] in terms of the full theory description. The violation of the CKM unitarity Eq.(4.82) leads to new contributions to the effective Hamiltonian:

$$\mathcal{H}_{eff}^{(1)\Delta B=2} = \frac{G_F^2}{4\pi^2} M_W^2 (\lambda_{sb}^t)^2 \left(\bar{E}_{tt} \quad 4\frac{Z_{\mathrm{NC}}^{sb}}{\lambda_{sb}^t} \overline{E_t'} \right) [\overline{s_L}\gamma^\mu b_L][\overline{s_L}\gamma_\mu b_L]\,, \tag{5.3}$$

where we leave only the top quark contributions. The first term in the parentheses corresponds to the SM contribution shown in Eq.(A.34) with $\bar{E}_{tt} = \quad S_0(x_t)$ [102]. The second term is the result of the violation of CKM unitarity. The function $\overline{E_t'}$ is given as,

$$\overline{E_t'} = \frac{3}{8}\frac{x_i}{(x_i \quad 1)^2}\ln x_i + \frac{3}{8}\frac{x_i}{x_i \quad 1} + \gamma(x_i,\xi) \quad \gamma(0,\xi)\,, \tag{5.4}$$

with [102],

$$\gamma(x_i,\xi) = \frac{\xi}{x_i \quad \xi}\left(\frac{3}{4}\frac{1}{x_i \quad 1} + \frac{1}{8}\frac{\xi}{x_i \quad \xi}\right) x_i \ln x_i \quad \frac{1}{8}\frac{\xi^2}{x_i \quad \xi}\left[\quad \left(\frac{5+\xi}{1 \quad \xi} \quad \frac{\xi}{x_i \quad \xi}\right)\ln\xi + 1\right], \tag{5.5}$$

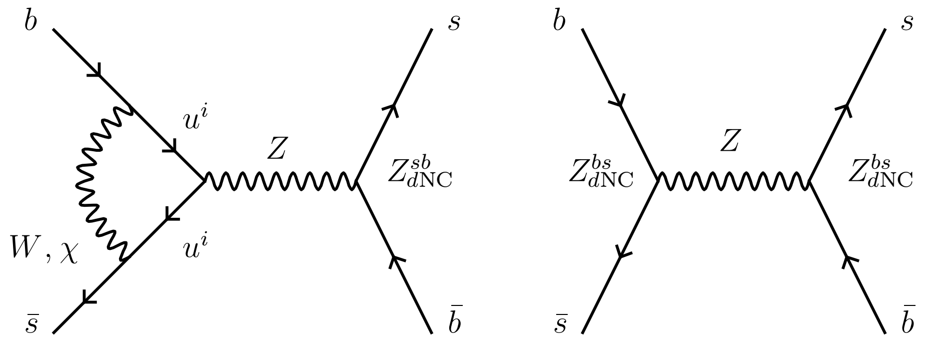

Figure 5.1. New diagrams which contribute to the Wilson coefficient C_{VLL} [84].

where ξ is the gauge fixing parameter of the R_ξ gauge.

The diagrams including the tree level FCNC contributes to the Wilson coefficient C_{VLL}. These diagrams are shown in Fig.5.1 and lead to the following effective Hamiltonian:

$$\mathcal{H}_{eff}^{(\mathrm{NC})\Delta B=2} = \frac{G_F^2}{4\pi^2} M_W^2 \lambda_{sb}^t 4 Z_{\mathrm{NC}}^{sb} \bar{\ }_t [\overline{s_L}\gamma^\mu b_L][\overline{s_L}\gamma_\mu b_L] \,, \tag{5.6}$$

$$\mathcal{H}_{eff}^{(\mathrm{tree})\Delta B=2} = \frac{G_F}{\sqrt{2}} (Z_{\mathrm{NC}}^{sb})^2 [\overline{s_L}\gamma^\mu b_L][\overline{s_L}\gamma_\mu b_L] \,, \tag{5.7}$$

where

$$\bar{\ }_t = \frac{1}{4} x_i \quad \frac{3}{8} \frac{x_i}{x_i \quad 1} + \frac{3}{8} \frac{2x_i^2 \quad x_i}{(x_i \quad 1)^2} \ln x_i + \gamma(x_i, \xi) \quad \gamma(0, \xi) \,. \tag{5.8}$$

The $\mathcal{H}_{eff}^{(\mathrm{NC})\Delta B=2}$ comes from the left-hand side diagram in Fig.5.1 while $\mathcal{H}_{eff}^{(\mathrm{tree})\Delta B=2}$ is derived by the right-hand side diagram in Fig.5.1. These results are consistent with full theory calculations [98, 99, 100, 101]. Then the new physics contributions to the Wilson coefficients are given as,

$$C_{\mathrm{LVV}}^{(\mathrm{uv+NC})}(\mu_{\mathrm{EW}}) = 4(\bar{\ }_t \quad \bar{E}'_t) \frac{Z_{\mathrm{NC}}^{sb}}{\lambda_{sb}^t} \equiv 8 Y_0(x_t) \frac{Z_{\mathrm{NC}}^{sb}}{\lambda_{sb}^t} \,, \tag{5.9}$$

$$C_{\mathrm{LVV}}^{(\mathrm{tree})}(\mu_{\mathrm{EW}}) = \frac{4\pi s_w^2}{\alpha_{em}} \left(\frac{Z_{\mathrm{NC}}^{sb}}{\lambda_{sb}^t} \right)^2 , \tag{5.10}$$

where the function $Y_0(x)$ is defined by [102, 103],

$$Y_0(x) = \frac{x}{8} \quad \frac{3}{8} \frac{x}{x \quad 1} + \frac{3}{8} \frac{x^2}{(x \quad 1)^2} \ln x \,. \tag{5.11}$$

It is clear that the function $Y_0(x)$ does not depend on the gauge parameter ξ. The total effective Hamiltonian can be written as,

$$\mathcal{H}_{eff}^{\Delta B=2} = \frac{G_F^2}{4\pi^2} M_W^2 (\lambda_{sb}^t)^2 C_{\mathrm{VLL}} O_{\mathrm{VLL}} + h.c. . \tag{5.12}$$

with

$$C_{\mathrm{VLL}} = C_{\mathrm{VLL}}^{\mathrm{SM}} + C_{\mathrm{LVV}}^{(\mathrm{uv+NC})} + C_{\mathrm{LVV}}^{(\mathrm{tree})} \,. \tag{5.13}$$

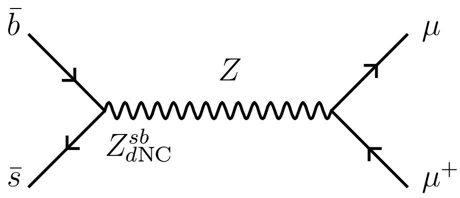

Figure 5.2. The tree level FCNC contribution to the C_{10} [84].

Finally, the mass difference of B_s^0 meson is given by (see Appendix A.1),

$$\Delta m_{B_s} \;\simeq\; 2|M_{12}^{B_s}| \;=\; \frac{G_F^2}{6\pi^2} M_W^2 m_{B_s} f_{B_s}^2 B_s \eta_{B_s} |\lambda_{sb}^t|^2 |C_{\mathrm{VLL}}(\mu_{\mathrm{EW}})| \,. \tag{5.14}$$

5.2 $B_s^0 \to \mu^+\mu$ Process

5.2.1 Branching ratio

The effective Hamiltonian for the $\overline{B_s^0} \to \mu^+\mu$ process is,

$$\mathcal{H}_{eff}^{\Delta B=1} \;=\; \frac{4G_F}{\sqrt{2}} \frac{\alpha_{\mathrm{em}}}{4\pi} \lambda_{sb}^t C_{10} O_{10} + h.c. \,, \tag{5.15}$$

with the effective operator,

$$O_{10} \;=\; [\overline{s_L}\,\gamma^\mu b_L][\overline{\mu}\,\gamma_\mu \gamma_5 \mu] \,, \tag{5.16}$$

where we follow the notation of Refs.[104, 105, 106, 107]. In order to compute the branching ratio of the $B_s^0 \to \mu^+\mu$ process in the present model, we have to determine the Wilson coefficient C_{10}. The tree level FCNC contributes to the C_{10} as shown in Fig.5.2. The new physics contribution appears as the tree level diagram while the SM contribution comes from the one-loop diagrams shown in Fig.A.2. Therefore, the violation effect of the CKM unitarity is suppressed by factor $e^2/(16\pi^2)$ compared with the tree level new physics contribution. The contribution to C_{10} from the tree level diagram in Fig.5.2 is,

$$C_{10}^{\mathrm{NP}}(\mu_{\mathrm{EW}}) \;=\; \frac{\pi}{\alpha_{\mathrm{em}}} \cdot \frac{Z^{sb}_{d\mathrm{NC}}(\mu_{\mathrm{EW}})}{\lambda_{sb}^t} \,, \tag{5.17}$$

with,

$$\begin{aligned} Z^{sb}_{d\mathrm{NC}}(\mu_{\mathrm{EW}}) \;&=\; v^2 \{ \tilde{\mathcal{C}}_{\phi q}^{(1)pq}(\mu_{\mathrm{EW}}) + \tilde{\mathcal{C}}_{\phi q}^{(3)pq}(\mu_{\mathrm{EW}}) \} \\ &\simeq\; \left[1 \quad \frac{m_t^2}{(4\pi)^2 v^2} (\quad 3\lambda_{bb}^t + 12) \ln \frac{\mu_{\mathrm{VLQ}}}{\mu_{\mathrm{EW}}} \right] Z^{sb}_{d\mathrm{NC}}(\mu_{\mathrm{VLQ}}) \,, \end{aligned} \tag{5.18}$$

where we take Eq.(4.78) into account. The branching ratio is given by Eq.(A.62):

$$\overline{\mathrm{BR}}[B_s^0 \to \mu^+\mu \;\;] \;=\; \tau_{B_s} \frac{G_F^4 M_W^4 s_w^4}{8\pi^5} \sqrt{1 \quad \frac{4m_\mu^2}{m_{B_s}^2}} f_{B_s}^2 m_{B_s} m_\mu^2 |\lambda_{sb}^t|^2 |\eta_Y C_{10}(\mu_{\mathrm{EW}})|^2 \left[\frac{1 + y_s A_\Delta^{\mu\mu}}{1 \quad y_s^2} \right] , \tag{5.19}$$

with the total Wilson coefficient,

$$C_{10} \;=\; C_{10}^{\mathrm{SM}} + C_{10}^{\mathrm{NP}} \,. \tag{5.20}$$

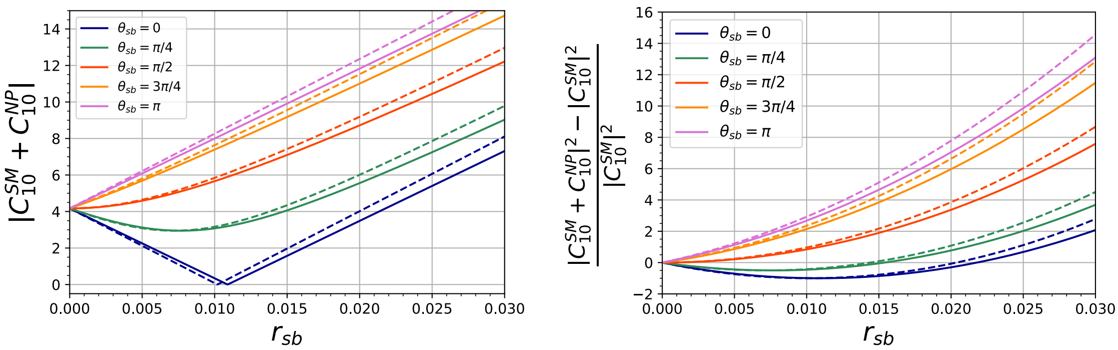

Figure 5.3. *Left*: The numerical value of $|C_{10}|$ as a function of the parameter r_{sb}. *Right*: Difference between the numerical value of $|C_{10}|^2$ in the model with VLQ and the SM. In both figures, the different colors of the line represent to different values of the phase θ_{sb}. The solid lines correspond to the numerical value of $|C_{10}|$ with RG effect, that is $|C_{10}|=|C_{10}^{\rm SM}+C_{10}^{\rm NP}(\mu_{\rm EW})|$. The dashed lines are the values without RG effect, $|C_{10}|=|C_{10}^{\rm SM}+C_{10}^{\rm NP}(\mu_{\rm VLQ})|$. Here we set $m_t=m_{t,\overline{\rm MS}}(m_t)$ with the pole mass $m_{t,{\rm pole}}=173.1$ GeV [65] and $\mu_{\rm VLQ}=1$ TeV, $\mu_{\rm EW}=M_W$.

where we define $C_{10}^{\rm SM}\equiv \frac{Y_0(x_t)}{s_w^2}$ [102].

5.2.2 Numerical evaluation of the Wilson coefficient

We evaluate the new physics contribution to the Wilson coefficient C_{10} numerically. We define parameters related to the FCNC coupling $Z_{d\rm NC}^{sb}$,

$$r_{sb} \equiv \left|\frac{Z_{d\rm NC}^{sb}(\mu_{\rm VLQ})}{\lambda_{sb}^t}\right|, \tag{5.21}$$

$$\theta_{sb} \equiv \arg\left[\frac{Z_{d\rm NC}^{sb}(\mu_{\rm VLQ})}{\lambda_{sb}^t}\right]. \tag{5.22}$$

The left figure of Fig.5.3 shows the numerical value of $|C_{10}|$ as a function of the parameter r_{sb}. The right figure of 5.3 shows the difference between the numerical value of $|C_{10}|^2$ in the model with VLQ and the SM. In both figures, the different colors of the line represent to different values of the phase θ_{sb}. The solid lines correspond to the numerical value of $|C_{10}|$ with the RG effect, that is $|C_{10}|=|C_{10}^{\rm SM}+C_{10}^{\rm NP}(\mu_{\rm EW})|$. The dashed lines are the values without the RG effect, $|C_{10}|=|C_{10}^{\rm SM}+C_{10}^{\rm NP}(\mu_{\rm VLQ})|$. Here we take the top quark mass as the $\overline{\rm MS}$ mass $m_t=m_{t,\overline{\rm MS}}(m_t)$ computed by leading order QCD correction with the pole mass $m_{t,{\rm pole}}=173.1$ GeV [65] and $\mu_{\rm VLQ}=1$ TeV, $\mu_{\rm EW}=M_W$. There is the point where the absolute value $|C_{10}|$ approaches zero in the left figure of Fig.5.3 because of the large new physics contribution. Moreover, one finds in the right figure of Fig.5.3 that the new physics contribution can become as large as the SM contribution. Also the RG effect from $\mu_{\rm VLQ}$ to $\mu_{\rm EW}$ increases as the parameter r_{sb} grows.

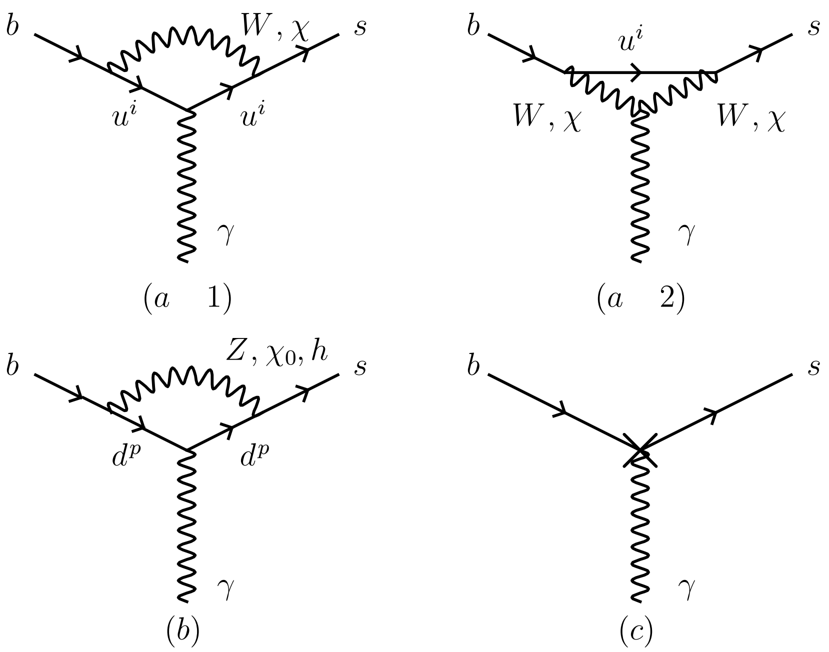

Figure 5.4. The diagrams contributing to the $b \to s\gamma^{(*)}$ process [84]. The diagrams $(a \quad 1)$ and $(a \quad 2)$ also exist in the case of the SM. The diagram (b) contains the tree level FCNC interactions. The diagram (c) corresponds to conterterms coming from the quark self-energy and diagrams shown in Fig.5.5.

5.3 Branching ratio of $\overline{B_d^0} \to X_s\gamma$

We present effective Hamiltonian for the $\overline{B_d^0} \to X_s\gamma$ process in Eq.(A.66). In the branching ratio of the $\overline{B_d^0} \to X_s\gamma$ process, we take account of new physics contributions to C_2, $C_{7\gamma}$ and C_{8g} with effective operators of the weak EFT,

$$O_2 = (\overline{s_L}\gamma_\mu c_L)(\overline{c_L}\gamma^\mu b_L)\,, \tag{5.23}$$

$$O_{7\gamma} = \frac{e}{16\pi^2} m_b (\overline{s_L}\sigma^{\mu\nu} b_R) F_{A\mu\nu}\,, \tag{5.24}$$

$$O_{8g} = \frac{g_s}{16\pi^2} m_b (\overline{s_L}\sigma^{\mu\nu} T^a b_R) G^a_{\mu\nu}\,. \tag{5.25}$$

The new physics contribution to C_2 comes from the violation of the CKM unitarity,

$$\frac{4G_F}{\sqrt{2}}\lambda^c_{sb} C_2 O_2 \simeq \frac{4G_F}{\sqrt{2}}\lambda^t_{sb}\left(1 \quad \frac{Z^{sb}_{d\mathrm{NC}}}{\lambda^t_{sb}}\right) C_2 O_2 \to C_2^{\mathrm{NP}}(\mu_{\mathrm{EW}}) = \frac{Z^{sb}_{d\mathrm{NC}}}{\lambda^t_{sb}}\,, \tag{5.26}$$

where the small product of the CKM matrix element λ^u_{sb} is neglected. We give an example of the computation for the $\overline{B_d^0} \to X_s\gamma$ process in Appendix.B.

5.3.1 Effective Lagrangian in weak EFT

In order to obtain new physics contributions to the Wilson coefficients $C_{7\gamma}$ and C_{8g}, we calculate the amplitude of the $b \to s\gamma$ and $b \to s\gamma^*$ processes where γ^* denotes off-shell photon. The diagrams shown in Fig.5.4 in addition to the effective Lagrangian Eq.(4.86) are contribute to the $b \to s\gamma^{(*)}$ process. The diagrams $(a \quad 1)$ and $(a \quad 2)$

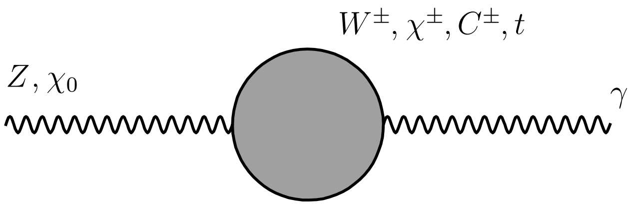

Figure 5.5. The Z-γ, χ_0-γ mixing diagram at one-loop level [84]. The symbol $C^{\pm}$ represents the Faddeev–Popov ghost field.

are the same diagrams as the SM calculation [102]. The diagram (b) contains the tree level FCNC interactions. The diagram (c) corresponds to conterterms coming from the quark self-energy and the Z-γ, χ_0-γ mixing diagrams shown in Fig.5.5. The effective Lagrangian for the radiative decay process with on-shell photon $b \to s\gamma$ has been calculated in terms of the full theory of the model with VLQ [108, 109, 110]. On the other hand, the effective Lagrangian for the $b \to s\gamma^*$ process has not been calculated yet. In order to check cancellation of the divergence in the amplitude, we compute the radiative decay process including the off-shell photon contributions.

As shown in Appendix.B, the wavefunction renormalization determined by the quark self-energy diagrams in Fig.(B.1) can remove the divergence in the diagrams (a 1) and (a 2) of Fig.5.4 in the case of the SM. This is because the terms which do not contain the up-type quark masses vanish after using the CKM unitarity in the SM. This means that the wavefunction renormalization cannot remove all the divergence in the diagrams (a 1) and (a 2) of Fig.5.4 if the CKM unitarity does not hold. We explicitly show this fact in Appendix.B. The remaining divergence is not taken the calculations of Refs.[108, 109, 110] into account since the divergence appears in the $b \to s\gamma^*$.

In order to remove all the divergence, we have to take account of the Z-γ, χ_0-γ mixing diagrams shown in Fig.5.5. This diagram leads to a wave function renormalization [111]:

$$\begin{pmatrix} Z_0^{\mu} \\ A_0^{\mu} \end{pmatrix} = \begin{pmatrix} \sqrt{Z_{\text{ZZ}}} & \sqrt{Z_{\text{ZA}}} \\ \sqrt{Z_{\text{AZ}}} & \sqrt{Z_{\text{AA}}} \end{pmatrix} \begin{pmatrix} Z^{\mu} \\ A^{\mu} \end{pmatrix}, \tag{5.27}$$

where the subscript "0" means bare quantities. The symbols $\sqrt{Z_{ij}}$ with $i, j = Z, A$ are the renormalization constants. The off-diagonal elements $\sqrt{Z_{\text{ZA}}}$ and $\sqrt{Z_{\text{AZ}}}$ are determined by the diagrams in Fig.5.5. In the $\overline{\text{MS}}$ scheme, we obtain,

$$\sqrt{Z_{\text{ZA}}} = \frac{egc_w}{8\pi^2} C_{\text{UV}}, \tag{5.28}$$

$$\sqrt{Z_{\text{AZ}}} = \frac{egc_w}{16\pi^2} C_{\text{UV}} \left(\frac{17}{3} + \frac{41}{6} \frac{M_Z^2}{M_W^2} \right), \tag{5.29}$$

as shown in Appendix B.2. The tree level FCNC through the Z boson leads to a counterterm for $b \to s\gamma^{(*)}$ vertex:

$$Z_{\rm dNC}^{sb}\bar{s}\gamma_\mu L\, b\, Z_0^\mu \;\;\to\;\; \sqrt{Z_{ZA}}Z_{\rm dNC}^{sb}\bar{s}\gamma_\mu L\, b\, A^\mu\,. \tag{5.30}$$

All the divergence in the diagrams (a 1) and (a 2) of Fig.5.4 are cancelled by the counterterm Eq.(5.30) in addition to the counterterms induced by the wavefunction renormalization of the external quark fields.

The finite part of the amplitude from the diagram in Fig.5.5 contributes to the effective Lagrangian for the $b \to s\gamma^*$ process. Finally, we obtain the effective Lagrangian $\mathcal{L}_{eff}(b \to s\gamma)$ for the on-shell photon and the effective Lagrangian $\mathcal{L}_{eff}(b \to s\gamma^*)$ for the off-shell photon. We divide these effective Lagrangian into,

$$\mathcal{L}_{eff}(b \to s\gamma) \;\equiv\; \mathcal{L}_{eff}^{\rm CC}(b \to s\gamma) + \mathcal{L}_{eff}^{uv}(b \to s\gamma) + \mathcal{L}_{eff}^{\rm NC}(b \to s\gamma)\,, \tag{5.31}$$

$$\mathcal{L}_{eff}(b \to s\gamma^*) \;\equiv\; \mathcal{L}_{eff}^{\rm CC}(b \to s\gamma^*) + \mathcal{L}_{eff}^{uv}(b \to s\gamma^*) + \mathcal{L}_{eff}^{\rm NC}(b \to s\gamma^*) + \mathcal{L}_{eff}^{\rm Mix}(b \to s\gamma^*)\,, \tag{5.32}$$

where the indices "CC" mean the contributions from the diagrams in (a 1) and (a 2) of Fig.5.4 with the CKM unitarity relation, namely the SM contributions. The subscripts "uv" and "NC" indicate the contributions from the violation of CKM unitarity in (a 1) and (a 2) of Fig.5.4 and the diagram in Fig.5.4(b), respectively. The index "Mix" represents the contributions from the finite part of the Z-γ and χ_0-γ mixing diagrams. Concrete form of these Lagrangian are given as follows [84]:

$$\mathcal{L}_{eff}^{\rm CC}(b \to s\gamma) \;=\; \frac{G_F e}{8\sqrt{2}\pi^2}\sum_{i=c,t}\lambda_{sb}^i\{Q_u F_u(x_i) + F_W(x_i)\}\bar{s}\sigma_{\mu\nu}(m_b R + m_s L)bF_A^{\mu\nu}\,, \tag{5.33}$$

$$\mathcal{L}_{eff}^{uv}(b \to s\gamma) \;=\; \frac{G_F e}{8\sqrt{2}\pi^2}Z_{\rm dNC}^{sb}\left(\frac{2}{3}Q_u + \frac{5}{6}\right)\bar{s}\sigma_{\mu\nu}(m_b R + m_s L)bF_A^{\mu\nu}\,, \tag{5.34}$$

$$\begin{aligned}\mathcal{L}_{eff}^{\rm NC}(b \to s\gamma) \;=\;& \frac{G_F e}{8\sqrt{2}\pi^2}Q_d\sum_{p=d,s,b}Z_{\rm dNC}^{sp}Z_{\rm dNC}^{pb}F_{ZZ}(r_p, w_p)\bar{s}\sigma_{\mu\nu}(m_b R + m_s L)bF_A^{\mu\nu} \\ &+ \frac{G_F e}{8\sqrt{2}\pi^2}Q_d^2 s_w^2\sum_{p=d,s,b}Z_{\rm dNC}^{sb}(\delta^{sp} + \delta^{pb})F_Z(r_p)\bar{s}\sigma_{\mu\nu}(m_b R + m_s L)bF_A^{\mu\nu} \\ &\quad \frac{G_F e}{4\sqrt{2}\pi^2}Q_d^2 s_w^2\sum_{p=s,b}Z_{\rm dNC}^{sb}F_Z'(r_p)\bar{s}\sigma_{\mu\nu}(\delta^{pb}m_b R + \delta^{sp}m_s L)bF_A^{\mu\nu}\,,\end{aligned} \tag{5.35}$$

for on-shell photon case and,

$$\mathcal{L}_{eff}^{\rm CC}(b \to s\gamma^*) \;=\; \frac{G_F e}{8\sqrt{2}\pi^2}\sum_{i=c,t}\lambda_{sb}^i\{Q_u f_u(x_i) + f_W(x_i)\}\bar{s}\gamma_\nu L b\,\partial_\mu F_A^{\mu\nu}\,, \tag{5.36}$$

$$\mathcal{L}_{eff}^{uv}(b \to s\gamma^*) \;=\; \frac{G_F e}{8\sqrt{2}\pi^2}Z_{\rm dNC}^{sb}\left\{Q_u\left(\;\;\frac{2}{9} + \frac{4}{3}\ln x_u\right)\;\;\frac{16}{9}\right\}\bar{s}\gamma_\nu L b\,\partial_\mu F_A^{\mu\nu}\,, \tag{5.37}$$

$$\begin{aligned}\mathcal{L}_{eff}^{\rm NC}(b \to s\gamma^*) \;=\;& \frac{G_F e}{8\sqrt{2}\pi^2}Q_d\sum_{p=d,s,b}Z_{\rm dNC}^{sp}Z_{\rm dNC}^{pb}f_{ZZ}(r_p, w_p)\bar{s}\gamma_\nu L b\,\partial_\mu F_A^{\mu\nu} \\ &+ \frac{G_F e}{8\sqrt{2}\pi^2}Q_d^2 s_w^2\sum_{p=d,s,b}Z_{\rm dNC}^{sb}(\delta^{sp} + \delta^{pb})f_Z(r_p)\bar{s}\gamma_\nu L b\,\partial_\mu F_A^{\mu\nu}\,,\end{aligned} \tag{5.38}$$

$$
\begin{aligned}
\mathcal{L}^{\text{Mix}}_{eff}(b\to s\gamma^*) &= \frac{G_F e}{8\sqrt{2}\pi^2} Z^{sb}_{d\text{NC}} \left\{ \left(10c_w^2 + \frac{1}{3} \right) \ln \frac{\mu^2_{\text{EW}}}{M_W^2} + \frac{4}{3} c_w^2 \right\} \bar{s}\gamma_\nu L b \partial_\mu F_A^{\mu\nu} \\
&\quad + \frac{G_F e}{8\sqrt{2}\pi^2} Z^{sb}_{d\text{NC}} \left\{ \quad 2Q_u (1 \quad 4Q_u s_w^2) \ln \frac{\mu^2_{\text{EW}}}{m_t^2} \right\} \bar{s}\gamma_\nu L b \partial_\mu F_A^{\mu\nu} . \qquad (5.39)
\end{aligned}
$$

for the off-shell photon. The loop functions corresponding to the SM contributions are defined as,

$$F_u(x_i) \equiv \frac{x_i(2 + 3x_i \quad 6x_i^2 + x_i^3 + 6x_i \ln x_i)}{4(x_i \quad 1)^4} , \qquad (5.40)$$

$$F_W(x_i) \equiv \frac{x_i(1 \quad 6x_i + 3x_i^2 + 2x_i^3 \quad 6x_i^2 \ln x_i)}{4(x_i \quad 1)^4} . \qquad (5.41)$$

$$f_u(x_i) \equiv \frac{x_i\{18 \quad 29x_i + 10x_i^2 + x_i^3 + (32 \quad 18x_i)\ln x_i\}}{6(x_i \quad 1)^4} + \frac{4}{3(x_i \quad 1)^4} \ln x_i \quad \frac{4}{3} \ln x_u , \qquad (5.42)$$

$$f_W(x_i) \equiv \frac{x_i\{12 \quad 11x_i \quad 8x_i^2 + 7x_i^3 + 2x_i(12 \quad 10x_i + x_i^2)\ln x_i\}}{6(x_i \quad 1)^4} , \qquad (5.43)$$

which agree with the SM results in Ref.[102]. The functions F_{ZZ}, F_Z, and F'_Z are given by,

$$
\begin{aligned}
F_{ZZ}(r_\alpha, w_\alpha) &\equiv F_1(r_\alpha) + F_2(r_\alpha) + F_3(w_\alpha) , && (5.44) \\
F_Z(r_\alpha) &\equiv 2F_1(r_\alpha) , && (5.45) \\
F'_Z(r_\alpha) &\equiv \frac{1 \quad r_\alpha^2 + 2r_\alpha \ln r_\alpha}{(1 \quad r_\alpha)^3} , && (5.46)
\end{aligned}
$$

where $r_\alpha \equiv (m_d^p / M_Z)^2$ and $w_\alpha \equiv (m_d^p / M_h)^2$ with $m_d^p = (m_d, m_s, m_b)$. The symbol M_h denotes the physical Higgs boson mass. The functions F_1, F_2 and F_3 are,

$$
\begin{aligned}
F_1(r_\alpha) &\equiv \frac{4 \quad 9r_\alpha + 5r_\alpha^3 + 6r_\alpha(1 \quad 2r_\alpha)\ln r_\alpha}{12(1 \quad r_\alpha)^4} , && (5.47) \\
F_2(r_\alpha) &\equiv r_\alpha \frac{20 + 39r_\alpha \quad 24r_\alpha^2 + 5r_\alpha^3 + 6(\quad 2 + r_\alpha)\ln r_\alpha}{24(\quad 1 + r_\alpha)^4} , && (5.48) \\
F_3(w_\alpha) &\equiv \quad w_\alpha \frac{16 + 45w_\alpha \quad 36w_\alpha^2 + 7w_\alpha^3 + 6(\quad 2 + 3w_\alpha)\ln w_\alpha}{24(\quad 1 + w_\alpha)^4} . && (5.49)
\end{aligned}
$$

The functions F_1 and F_2 come from the diagram in Fig.5.4(b) where the exchanged particles are Z and χ_0, respectively. The function F_3 comes from the diagram in Fig.5.4(b) where the Higgs boson h is exchanged. The functions f_{ZZ} and f_Z in Eq.(5.38) are defined as follows:

$$
\begin{aligned}
f_{\text{ZZ}}(r_\alpha, w_\alpha) &\equiv f_1(r_\alpha) + f_2(r_\alpha) + f_2(w_\alpha) , && (5.50) \\
f_Z(r_\alpha, w_\alpha) &= 2f_1(r_\alpha) , && (5.51) \\
f_1(r_\alpha) &\equiv \frac{2 + 27r_\alpha \quad 54r_\alpha^2 + 25r_\alpha^3 \quad 6(2 \quad 9r_\alpha + 6r_\alpha^2)\ln r_\alpha}{18(1 \quad r_\alpha)^4} , && (5.52) \\
f_2(r_\alpha) &\equiv r_\alpha \frac{16 + 45r_\alpha \quad 36r_\alpha^2 + 7r_\alpha^3 + 6(\quad 2 + 3r_\alpha)\ln r_\alpha}{36(1 \quad r_\alpha)^4} , && (5.53) \\
f_2(w_\alpha) &= w_\alpha \frac{16 + 45w_\alpha \quad 36w_\alpha^2 + 7w_\alpha^3 + 6(\quad 2 + 3w_\alpha)\ln w_\alpha}{36(1 \quad w_\alpha)^4} . && (5.54)
\end{aligned}
$$

We can obtain the effective Lagrangian for the $b\to sg^{(*)}$ process by replacing the external photon which attached to quarks in Fig.5.4 with the gluon. They are given as,

$$\begin{aligned}\mathcal{L}_{eff}(b\to sg) &\equiv \mathcal{L}^{\rm CC}_{eff}(b\to sg)+\mathcal{L}^{uv}_{eff}(b\to sg)+\mathcal{L}^{\rm NC}_{eff}(b\to sg)\,, &(5.55)\\ \mathcal{L}_{eff}(b\to sg^*) &\equiv \mathcal{L}^{\rm CC}_{eff}(b\to sg^*)+\mathcal{L}^{uv}_{eff}(b\to sg^*)+\mathcal{L}^{\rm NC}_{eff}(b\to sg^*)\,, &(5.56)\end{aligned}$$

with

$$\begin{aligned}\mathcal{L}^{\rm CC}_{eff}(b\to sg) &= \frac{G_F g_s}{8\sqrt{2}\pi^2}\sum_{i=c,t}\lambda^i_{sb}F_u(x_i)\bar{s}\sigma_{\mu\nu}(m_bR+m_sL)\frac{\lambda^a}{2}bG^{a\mu\nu}, &(5.57)\\ \mathcal{L}^{uv}_{eff}(b\to sg) &= \frac{G_F g_s}{8\sqrt{2}\pi^2}\cdot\frac{2}{3}Z^{sb}_{d\rm NC}\bar{s}\sigma_{\mu\nu}(m_bR+m_sL)\frac{\lambda^a}{2}bG^{a\mu\nu}, &(5.58)\\ \mathcal{L}^{\rm NC}_{eff}(b\to sg) &= \frac{G_F g_s}{8\sqrt{2}\pi^2}\sum_{p=d,s,b}Z^{sp}_{d\rm NC}Z^{pb}_{d\rm NC}F_{ZZ}(r_p,w_p)\bar{s}\sigma_{\mu\nu}(m_bR+m_sL)\frac{\lambda^a}{2}bG^{a\mu\nu}\\ &\quad+\frac{G_F g_s}{8\sqrt{2}\pi^2}Q_d s_w^2\sum_{p=d,s,b}Z^{sb}_{d\rm NC}(\delta^{sp}+\delta^{pb})F_Z(r_p)\bar{s}\sigma_{\mu\nu}(m_bR+m_sL)\frac{\lambda^a}{2}bG^{a\mu\nu}\\ &\quad\frac{G_F g_s}{4\sqrt{2}\pi^2}Q_d s_w^2\sum_{p=s,b}Z^{sb}_{d\rm NC}F'_Z(r_p)\bar{s}\sigma_{\mu\nu}(\delta^{pb}m_bR+\delta^{sp}m_sL)\frac{\lambda^a}{2}bG^{a\mu\nu}, &(5.59)\end{aligned}$$

and

$$\begin{aligned}\mathcal{L}^{\rm CC}_{eff}(b\to sg^*) &= \frac{G_F g_s}{8\sqrt{2}\pi^2}\sum_{i=c,t}\lambda^i_{sb}f_u(x_i)\bar{s}\gamma_\nu\frac{\lambda^a}{2}Lb\partial_\mu G^{a\mu\nu}\,, &(5.60)\\ \mathcal{L}^{uv}_{eff}(b\to sg^*) &= \frac{G_F g_s}{8\sqrt{2}\pi^2}Z^{sb}_{d\rm NC}\left(\frac{2}{9}+\frac{4}{3}\ln x_u\right)\bar{s}\gamma_\nu\frac{\lambda^a}{2}Lb\partial_\mu G^{a\mu\nu}\,, &(5.61)\\ \mathcal{L}^{\rm NC}_{eff}(b\to sg^*) &= \frac{G_F g_s}{8\sqrt{2}\pi^2}\sum_{p=d,s,b}Z^{sp}_{d\rm NC}Z^{pb}_{d\rm NC}f_{ZZ}(r_p,w_p)\bar{s}\gamma_\nu\frac{\lambda^a}{2}Lb\partial_\mu G^{a\mu\nu}\\ &\quad+\frac{G_F g_s}{8\sqrt{2}\pi^2}Q_d s_w^2\sum_{p=d,s,b}Z^{sb}_{d\rm NC}(\delta^{sp}+\delta^{pb})f_Z(r_p)\bar{s}\gamma_\nu\frac{\lambda^a}{2}Lb\partial_\mu G^{a\mu\nu}\,. &(5.62)\end{aligned}$$

5.3.2 Determination of the Wilson coefficients $C^{eff}_{7\gamma}$ and C^{eff}_{8g}

We show the effective Hamiltonian for $b\to s\gamma$ process in Eq.(A.66). In $b\to s\gamma$ process, it is convenient to introduce so-called "effective coefficients" $C^{(0)eff}_i$ [112, 113]. Concrete definition is given in Appendix A.3. As we see in Eq.(A.79), we can directly take the leading order Wilson coefficients $C^{(0)eff}_{7\gamma}$ and $C^{(0)eff}_{8g}$ from the amplitudes computed in the full theory at the one-loop level, that is the effective Lagrangian $\mathcal{L}_{eff}(b\to s\gamma)$ and $\mathcal{L}_{eff}(b\to sg)$. We define $C^{(0)eff}_{7\gamma}$ and $C^{(0)eff}_{8g}$ as,

$$\begin{aligned}C^{(0)eff}_{7\gamma} &= C^{{\rm SM}(0)eff}_{7\gamma}+C^{{\rm SMEFT}(0)eff}_{7\gamma}+C^{{\rm NC}(0)eff}_{7\gamma}\,, &(5.63)\\ C^{(0)eff}_{8g} &= C^{{\rm SM}(0)eff}_{8g}+C^{{\rm SMEFT}(0)eff}_{8g}+C^{{\rm NC}(0)eff}_{8g}\,. &(5.64)\end{aligned}$$

The coefficients with the index "SM" are the SM contributions:

$$C_{7\gamma}^{\mathrm{SM}(0)eff}(\mu_{\mathrm{EW}}) = \frac{1}{2}[Q_u F_u(x_t) + F_W(x_t)]\,, \tag{5.65}$$

$$C_{8g}^{\mathrm{SM}(0)eff}(\mu_{\mathrm{EW}}) = \frac{1}{2}F_u(x_t)\,. \tag{5.66}$$

The Wilson coefficients $C_{7\gamma}^{\mathrm{SMEFT}(0)eff}$ and $C_{8g}^{\mathrm{SMEFT}(0)eff}$ comes from the effective Lagrangian shown in Eq.(4.86). When we neglect the RG effects, we obtain,

$$C_{7\gamma}^{\mathrm{SMEFT}(0)eff}(\mu_{\mathrm{EW}}) = C_{7\gamma}^{\mathrm{SMEFT}(0)eff}(\mu_{\mathrm{VLQ}}) = \frac{Q_d}{24}\cdot\frac{Z_{d\mathrm{NC}}^{sb}}{\lambda_{sb}^{t}}\,, \tag{5.67}$$

$$C_{8g}^{\mathrm{SMEFT}(0)eff}(\mu_{\mathrm{EW}}) = C_{8g}^{\mathrm{SMEFT}(0)eff}(\mu_{\mathrm{VLQ}}) = \frac{1}{24}\cdot\frac{Z_{d\mathrm{NC}}^{sb}}{\lambda_{sb}^{t}}\,, \tag{5.68}$$

where we use Eqs.(4.78) and (4.91). The Wilson coefficients $C_{7\gamma}^{\mathrm{NP}(0)eff}$ and $C_{8g}^{\mathrm{NP}(0)eff}$ are defined by,

$$C_{7\gamma}^{\mathrm{NP}(0)eff} \equiv C_{7\gamma}^{uv(0)eff} + C_{7\gamma}^{\mathrm{NC}(0)eff}\,, \tag{5.69}$$

$$C_{8g}^{\mathrm{NP}(0)eff} \equiv C_{8g}^{uv(0)eff} + C_{8g}^{\mathrm{NC}(0)eff}\,, \tag{5.70}$$

where indices "uv" and "NC" corresponds to the subscripts in Eqs.(5.31) and (5.55). These Wilson coefficients can be taken from Eqs.(5.34), (5.35), (5.58) and (5.59):

$$C_{7\gamma}^{uv(0)eff}(\mu_{\mathrm{EW}}) = \frac{1}{2}\left(\frac{2}{3}Q_u + \frac{5}{6}\right)\frac{Z_{d\mathrm{NC}}^{sb}}{\lambda_{sb}^{t}}\,, \tag{5.71}$$

$$C_{7\gamma}^{\mathrm{NC}(0)eff}(\mu_{\mathrm{EW}}) = \frac{Q_d}{3}(1 \quad Q_d s_w^2)\frac{Z_{d\mathrm{NC}}^{sb}}{\lambda_{sb}^{t}}\,, \tag{5.72}$$

$$C_{8g}^{uv(0)eff}(\mu_{\mathrm{EW}}) = \frac{Z_{d\mathrm{NC}}^{sb}}{3\lambda_{sb}^{t}}\,, \tag{5.73}$$

$$C_{8g}^{\mathrm{NC}(0)eff}(\mu_{\mathrm{EW}}) = \frac{1}{3}(1 \quad Q_d s_w^2)\frac{Z_{d\mathrm{NC}}^{sb}}{\lambda_{sb}^{t}}\,. \tag{5.74}$$

Here we set $r_\alpha = w_\alpha = 0$ in the loop functions F_{ZZ}, F_Z, and F_Z' since the Z and Higgs bosons are much heavier than the down-type quarks. Then the remaining contribution for $C_{7\gamma}^{\mathrm{NC}(0)eff}$ and $C_{8g}^{\mathrm{NC}(0)eff}$ comes from the function $F_1(r_\alpha)$ and $F_Z'(r_\alpha)$, which corresponds to the contributions from the Z boson exchanged diagram. We also neglect $\mathcal{O}(Z_{d\mathrm{NC}}^2)$ terms. In our numerical analysis, we include these new physics effects in only $\mathcal{O}(\alpha_s^0)$ term, that is the first term of D in Eq.(A.87).

Chapter 6

Numerical Analysis

In the present chapter, we make the numerical analysis for the neutral B meson systems which we investigate in Chap.5 and Appendix.A. We cannot use the SM value for the product of the CKM matrix elements $\lambda_{sb}^t \equiv V_{ts}^* V_{tb}$ in the model with VLQ since the new physics contributions in $C_{\rm VLL}$ affect the determination of the CKM matrix elements. Therefore, we determine the absolute value of λ_{sb}^t as a function of the new physics parameters r_{sb} and θ_{sb} through the mass difference of B_s^0 meson Δm_{B_s} in Eq.(5.14):

$$|\lambda_{sb}^t|^2 \ \propto \ \frac{[\Delta m_{B_s}]_{\rm exp}}{|C_{\rm VLL}(r_{sb}, \theta_{sb})|}\,, \tag{6.1}$$

where $[\Delta m_{B_s}]_{\rm exp}$ is experimental value of Δm_{B_s}. In addition, we take account of a constraint from the violation of CKM unitarity shown in Eqs.(4.81) and (4.82),

$$\lambda_{sb}^u + \lambda_{sb}^c + \lambda_{sb}^t \ \simeq \ Z_{d\rm NC}^{sb}(\mu_{\rm VLQ})\,. \tag{6.2}$$

Here we omit the tiny RG effect compared with $Z_{d\rm NC}^{sb}(\mu_{\rm VLQ})$ for simplicity. The relation Eq.(6.2) can be rewritten as,

$$\left|\frac{\lambda_{sb}^c}{\lambda_{sb}^t}\right|^2 \left(1 - 2\left|\frac{\lambda_{sb}^u}{\lambda_{sb}^c}\right| \cos\gamma_s + \left|\frac{\lambda_{sb}^u}{\lambda_{sb}^c}\right|^2\right) \ = \ 1 - 2 r_{sb}\cos\theta_{sb} + r_{sb}^2\,, \tag{6.3}$$

where the angle γ_s is defined by $\gamma_s \equiv -\arg\left[-\frac{\lambda_{sb}^u}{\lambda_{sb}^c}\right]$. We consider γ_s a free parameter and thus we set $-1 \leq \cos\gamma_s \leq +1$. In the following, we derive constraints on the r_{sb} and θ_{sb} from the branching ratios $\overline{\rm Br}[B_s^0 \to \mu^+\mu^-]$ and ${\rm Br}[\overline{B_d^0} \to X_s\gamma]$. Numerical values of input parameters are shown in Table 6.1.

First we investigate the branching ratio of the $B_s^0 \to \mu^+\mu^-$ process. The concrete expression of the branching ratio is given in Eq.(5.19). As an experimental value of the branching ratio, we adopt a result measured by LHCb [56],

$$\overline{\rm Br}[B_s^0 \to \mu^+\mu^-]_{\rm Exp} \ = \ (3.0 \pm 0.6^{+0.3}_{-0.2}) \times 10^{-9}\,. \tag{6.4}$$

$\alpha_{em}^{\ 1}(m_b \sim M_W)$	130.3 ± 2.3	[114]	$\alpha_s(M_Z)$	0.1179 ± 0.0010	[65]
M_W	80.379 ± 0.012 GeV	[65]	M_Z	91.1876 ± 0.0021 GeV	[65]
G_F	$1.16638 \times 10^{\ 5}$ GeV$^{\ 1}$	[65]	$\sin^2\theta_w$	0.23122	[65]
$m_{c,\overline{\rm MS}}$	1.28 ± 0.025 GeV	[65]	m_b	$4.18^{+0.03}_{\ 0.02}$ GeV	[65]
$m_{t,{\rm pole}}$	173.1 ± 0.9 GeV	[65]	m_μ	105.6584 MeV	[65]
m_{B_d}	5279.64 ± 0.13 MeV	[65]	m_{B_s}	5366.88 ± 0.17 MeV	[65]
τ_{B_s}	$(1.510 \pm 0.004) \times 10^{\ 12}$ s	[65]	Δm_{B_s}	$(1.1688 \pm 0.0014) \times 10^{\ 11}$ GeV	[65]
${\rm Br}[\overline{B_d^0} \to X_c e \bar{\nu}_e]_{\rm Exp}$	$(10.1 \pm 0.4) \times 10^{\ 2}$	[65]	$\Delta\ _{B_s}$	$(0.090 \pm 0.005) \times 10^{12}$ s$^{\ 1}$	[65]
η_B	0.5510 ± 0.0022	[115]	η_Y	1.0113	[116]
B_s	$1.327 \pm 0.016 \pm 0.030$	[7]	f_{B_s}	$226.0 \pm 1.3 \pm 2.0$ MeV	[7]
V_{ub}	$0.00392^{+0.00015}_{\ 0.00021}$	[7]	V_{us}	$0.224791^{+0.000170}_{\ 0.000098}$	[7]
V_{cb}	$0.04241^{+0.00040}_{\ 0.00151}$	[7]	V_{cs}	$0.973534^{+0.000057}_{\ 0.000073}$	[7]

Table 6.1. Numerical values of input parameters.

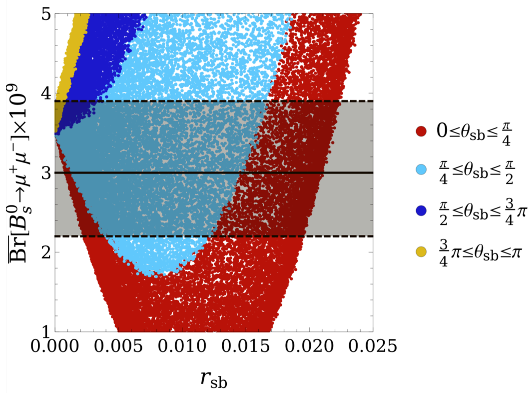

Figure 6.1. The dependence of $\overline{\rm Br}[B_s^0 \to \mu^+\mu\ \ ]$ predicted in the model with VLQ on the parameter r_{sb}. The difference between the range of θ_{sb} is expressed as the difference between colors of the dots. All the dots satisfy the constraints from Eq.(6.3) with $\ \ 1 \leq \cos\gamma_s \leq +1$. The experimentally allowed region shown in Eq.(6.4) is expressed as the gray shaded region. The figure is reproduced from Ref.[84].

Figure 6.1 shows the dependence of $\overline{\rm Br}[B_s^0 \to \mu^+\mu\ \ ]$ predicted in the model with VLQ on the parameter r_{sb}. The difference between the range of θ_{sb} is expressed as the difference between colors of the dots. All the dots satisfy the constraints from Eq.(6.3) with $\ \ 1 \leq \cos\gamma_s \leq +1$. The experimentally allowed region shown in Eq.(6.4) is expressed as the gray shaded region. We note that the predicted branching ratio is independent of the sign of θ_{sb} since the dependence of the branching ratio on the θ_{sb} comes from only ${\rm Re}[C_{10}^{\rm SM*} C_{10}^{\rm NP}] \propto \cos\theta_{sb}$. The dependence of $\overline{\rm Br}[B_s^0 \to \mu^+\mu\ \ ]$ on the r_{sb} can be understood by the left figure of Fig.5.3. We can see from the left figure of Fig.5.3 that the total Wilson coefficient $|C_{10}|$ approaches zero around $r_{sb} \simeq 0.01$ for the small θ_{sb}. In other words, the Wilson coefficient $C_{10}^{\rm NP}$ becomes $C_{10}^{\rm NP} \simeq\ \ C_{10}^{\rm SM}$ and thus $|C_{10}| = |C_{10}^{\rm SM} + C_{10}^{\rm NP}| \simeq 0$ in the region around $r_{sb} \simeq 0.01$ with $\theta_{sb} \simeq 0$. This gives rise to the small value of the branching ratio $\overline{\rm Br}[B_s^0 \to \mu^+\mu\ \ ]$ at $r_{sb} \simeq 0.01$ and $0 \leq \theta_{sb} \leq \frac{\pi}{4}$. For $r_{sb} \simeq 0.02$ with $0 \leq \theta_{sb} \leq \frac{\pi}{4}$, the value of $\overline{\rm Br}[B_s^0 \to \mu^+\mu\ \ ]$ comes close

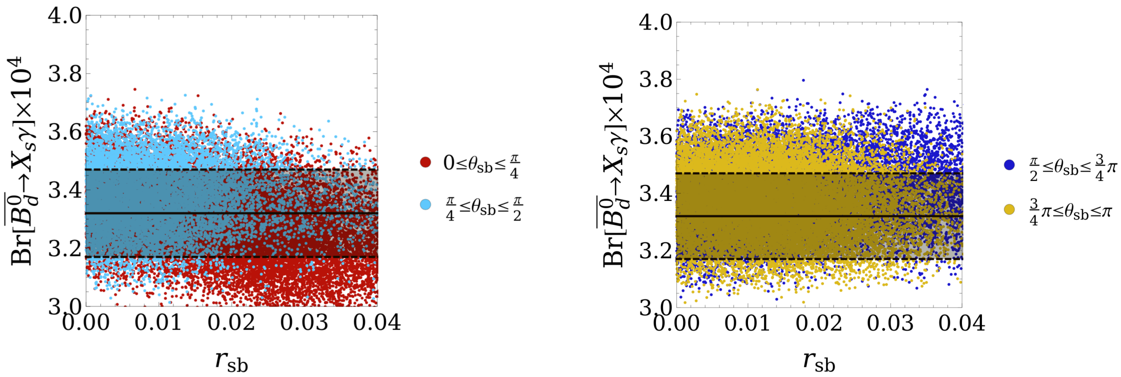

Figure 6.2. The dependence of $\mathrm{Br}[\overline{B}^0_d \to X_s\gamma]$ predicted in the model with VLQ on the parameter r_{sb}. The difference between the range of θ_{sb} is expressed as the difference between colors of the dots. All the dots satisfy the constraints from Eq.(6.3) with $\ 1 \leq \cos\gamma_s \leq +1$. The experimentally allowed region shown in Eq.(6.6) is expressed as the gray shaded region. These figures are reproduced from Ref.[84].

to the value of $\overline{\mathrm{Br}}[B^0_s \to \mu^+\mu\ \ ]$ at $r_{sb} = 0$, namely the predicted value in the SM [106, 107]:

$$\overline{\mathrm{Br}}[B^0_s \to \mu^+\mu\ \ ]_{\rm SM} \;=\; (3.57 \pm 0.16) \times 10^{\ \ 9} \,. \tag{6.5}$$

One can find in the left figure of Fig.5.3 that the total Wilson coefficient $|C_{10}|$ is also almost the same as the Wilson coefficient of the SM, $|C_{10}| \simeq |C_{10}^{\rm SM}|$ in the region around $r_{sb} \simeq 0.02$. This situation is realized by $C_{10}^{\rm NP} \simeq \ \ 2C_{10}^{\rm SM}$.

Next we analyze the branching ratio of the inclusive radiative decay $\overline{B}^0_d \to X_s\gamma$. The analytical expression of $\mathrm{Br}[\overline{B}^0_d \to X_s\gamma]$ is shown in Eq.(A.84). The new physics contributions are embedded in the Wilson coefficients $C_{7\gamma}^{(0)eff}(\mu_b)$. We set $\mu_b = m_b$ in our numerical analysis. The current average of the experimental results are [64],

$$\mathrm{Br}[\overline{B}^0_d \to X_s\gamma]_{\rm Exp} \;=\; (3.32 \pm 0.15) \times 10^{\ \ 4} \,, \tag{6.6}$$

which is given by the experimental data from BaBar [57, 58, 59], Belle [60, 61, 62] and CLEO [63] experiments. We show the dependence of $\mathrm{Br}[\overline{B}^0_d \to X_s\gamma]$ predicted in the model with VLQ on the parameter r_{sb} in Fig.6.2. The difference between the range of θ_{sb} is expressed as the difference between colors of the dots. All the dots satisfy the constraints from Eq.(6.3) with $\ \ 1 \leq \cos\gamma_s \leq +1$. The experimentally allowed region shown in Eq.(6.6) is expressed as the gray shaded region. The Fig.6.2 shows that the predicted value of $\mathrm{Br}[\overline{B}^0_d \to X_s\gamma]$ comes close to that of the SM prediction [117],

$$\mathrm{Br}[\overline{B}^0_d \to X_s\gamma]_{\rm SM} \;=\; (3.36 \pm 0.23) \times 10^{\ \ 4} \,, \tag{6.7}$$

as r_{sb} approaches zero. One finds that the filled regions by the colored dots are almost the same as each other. Therefore, the branching ratio of the $\overline{B}^0_d \to X_s\gamma$ depends on the phase θ_{sb} weakly compared with the branching ratio of the $B^0_s \to \mu^+\mu\ \ $. Moreover, the dependence of $\mathrm{Br}[\overline{B}^0_d \to X_s\gamma]$ on r_{sb} is weaker than that of $\overline{\mathrm{Br}}[B^0_s \to \mu^+\mu\ \ ]$.

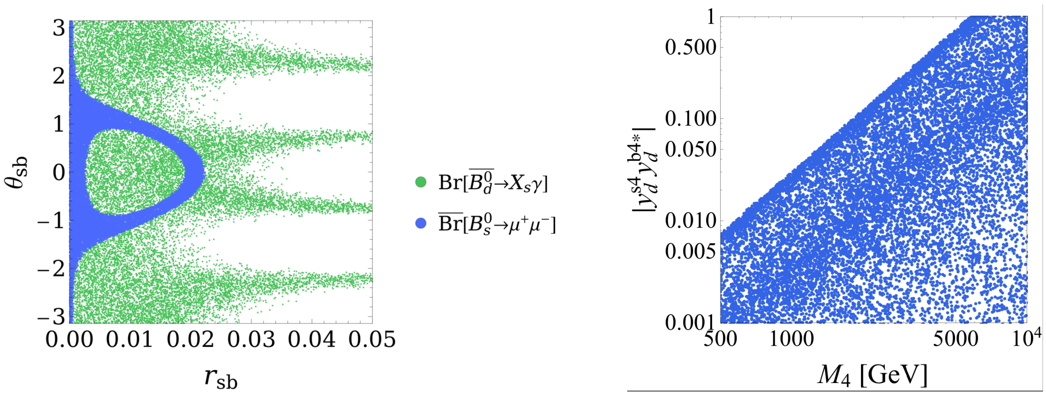

Figure 6.3. *Left* : The region of (r_{sb}, θ_{sb}) allowed by the experimental data of $\overline{\mathrm{Br}}[B_s^0 \to \mu^+\mu\ \ ]$ and $\mathrm{Br}[\overline{B_d^0} \to X_s\gamma]$ shown in Eqs.(6.4) and (6.6), respectively. The blue dots satisfy the constraints from both the $\overline{\mathrm{Br}}[B_s^0 \to \mu^+\mu\ \ ]$ and Eq.(6.3) with $\ \ 1 \leq \cos\gamma_s \leq +1$. The green dots satisfy the constraints from both the $\mathrm{Br}[\overline{B_d^0} \to X_s\gamma]$ and Eq.(6.3) with $\ \ 1 \leq \cos\gamma_s \leq +1$. *Right* : The constraints on the mass of VLQ M_4 and absolute value of product of the Yukawa couplings $|y_d'^{s4} y_d'^{b4*}|$. In the label of right figure, we omit the prime on y_d for simplicity. The blue dots satisfy the constraints from both the $\overline{\mathrm{Br}}[B_s^0 \to \mu^+\mu\ \ ]$ and Eq.(6.3) with $\ \ 1 \leq \cos\gamma_s \leq +1$. These figures are reproduced from Ref.[84].

The left figure of Fig.6.3 shows regions of (r_{sb}, θ_{sb}) allowed by the experimental data of $\overline{\mathrm{Br}}[B_s^0 \to \mu^+\mu\ \ ]$ and $\mathrm{Br}[\overline{B_d^0} \to X_s\gamma]$ shown in Eqs.(6.4) and (6.6), respectively. The blue dots satisfy the constraints from both the $\overline{\mathrm{Br}}[B_s^0 \to \mu^+\mu\ \ ]$ and Eq.(6.3) with $\ \ 1 \leq \cos\gamma_s \leq +1$. The green dots satisfy the constraints from both the $\mathrm{Br}[\overline{B_d^0} \to X_s\gamma]$ and Eq.(6.3) with $\ \ 1 \leq \cos\gamma_s \leq +1$. The values of r_{sb} and θ_{sb} in the region where the blue and green region overlap each other satisfy all the constraints from $\overline{\mathrm{Br}}[B_s^0 \to \mu^+\mu\ \ ]$, $\mathrm{Br}[\overline{B_d^0} \to X_s\gamma]$ and Eq.(6.3) with $\ \ 1 \leq \cos\gamma_s \leq +1$. In the region in the blue ring, the predicted branching ratio $\overline{\mathrm{Br}}[B_s^0 \to \mu^+\mu\ \ ]$ is smaller than the experimental allowed region. Also one can understand that the allowed region around $(r_{sb}, \theta_{sb}) \sim (0.02, 0)$ corresponds to the situation where $C_{10}^{\rm NP} \simeq\ \ 2C_{10}^{\rm SM}$. One finds that such a large new physics effect does not excluded by the measurement of $\mathrm{Br}[\overline{B_d^0} \to X_s\gamma]$ even though the branching ratio $\mathrm{Br}[\overline{B_d^0} \to X_s\gamma]$ is precisely measured at the experiments.

Finally, we show constraints on the mass of VLQ M_4 and absolute value of product of the Yukawa couplings $|y_d'^{s4} y_d'^{b4*}|$ in the right figure of Fig.6.3. One finds that the stringent constraint on (r_{sb}, θ_{sb}) is given by the branching ratio $\overline{\mathrm{Br}}[B_s^0 \to \mu^+\mu\ \ ]$ in the left figure of Fig.6.3. Hence the right figure of Fig.6.3 shows a region where the constraints from $\overline{\mathrm{Br}}[B_s^0 \to \mu^+\mu\ \ ]$ and Eq.(6.3) with $\ \ 1 \leq \cos\gamma_s \leq +1$ are satisfied, as the blue dots. One finds that the lower limit on the mass of VLQ is around 2 TeV for $|y_d'^{s4} y_d'^{b4*}| \sim 0.1$ or around 6 TeV for $|y_d'^{s4} y_d'^{b4*}| \sim 1$.

Chapter 7

Summary and Discussion

We have investigated the model with one $SU(2)_L$ singlet down-type VLQ on the basis of the SMEFT. In the model with VLQ, the GIM mechanism does not work. This fact is understood as two features of the model with VLQ. One is the existence of the tree level FCNCs induced by the Z boson, the Higgs boson and the neutral NG boson. The other is the violation of the CKM unitarity. We presented these features both in the full theory and the SMEFT descriptions in Chap.2 and Chap.4, respectively. These features lead to new contributions to the observables of the FCNC processes in the neutral B meson systems. The new physics contributions can be as large as the SM contributions. This is because the SM contributions to the FCNC processes are suppressed by the GIM mechanism while the new physics contributions are not suppressed. Hence it is expected that the FCNC processes in the neutral B meson systems give stringent constraints on the model with VLQ.

The recent lower limits for the VLQ mass from the ATLAS and CMS experiments [34, 49] are about ten times larger than the EW scale. We investigated the model with VLQ on the basis of the SMEFT. The SMEFT is the effective field theory with possible higher dimensional operators which are invariant under the SM gauge symmetry and consist of the SM fields. New physics effects are embedded in the higher dimensional operators. We constructed the SMEFT from the model with VLQ by integrating out the VLQ field. The FCNCs and the violation of the CKM unitarity were represented in terms of the Wilson coefficients of the SMEFT as shown in Eqs.(4.76) and (4.81), respectively. We took in the difference among the VLQ mass scale and the EW scale by using the RG equations with the anomalous dimension matrices in the SMEFT. One of the new points of our work [84] is matching the model with the SMEFT at the one-loop level and obtain the Wilson coefficients of the SMEFT which relates the radiative transitions of the SM quarks, such as the $b \to s\gamma$ process.

In order to clarify constraints on the parameters of the VLQ, we evaluated the FCNC processes in the neutral $B_{d,s}$ meson system; B_s^0-$\overline{B_s^0}$ mixing, $\overline{B_s^0} \to \mu^+\mu$ and $\overline{B_d^0} \to X_s\gamma$. We present the analytical expressions of the mass difference of B_s^0 meson Δm_{B_s} and the branching ratio of the $\overline{B_s^0} \to \mu^+\mu$ and the $\overline{B_d^0} \to X_s\gamma$ processes in Appendix.A. These expressions are written in terms of the Wilson coefficients of the weak EFT. We calculated the Wilson coefficients of the weak EFT by using the SMEFT derived in Chap.5. Also we computed the effective Lagrangian for the $b \to s\gamma^*$ process in addition to the $b \to s\gamma$ process to perform the renormalization of the amplitudes of $b \to s\gamma^{(*)}$ process more completely than the full theory calculations [108, 109, 110].

We performed the numerical analysis for the branching ratio of the $\overline{B_s^0} \to \mu^+\mu$ and the $\overline{B_d^0} \to X_s\gamma$ processes in Chap.7. We determined the product of the CKM matrix elements λ^t_{sb} through the mass difference of B_s^0 meson Δm_{B_s}. We found that the branching ratio $\mathrm{Br}[\overline{B_d^0} \to X_s\gamma]$ depends on the phase θ_{sb} weakly compared with the branching ratio $\overline{\mathrm{Br}}[B_s^0 \to \mu^+\mu\ ]$. The constraint on the model parameters (r_{sb}, θ_{sb}) from the branching ratio $\overline{\mathrm{Br}}[B_s^0 \to \mu^+\mu\ ]$ is more stringent than that from the branching ratio $\mathrm{Br}[\overline{B_d^0} \to X_s\gamma]$ as shown in the left figure of Fig.6.3. One can understand that the allowed region around $(r_{sb}, \theta_{sb}) \sim (0.02, 0)$ is the result of $C_{10}^{\mathrm{NP}} \simeq 2C_{10}^{\mathrm{SM}}$. We also found such a large new physics effect does not excluded by the constraint from the $\mathrm{Br}[\overline{B_d^0} \to X_s\gamma]$ even though the branching ratio $\mathrm{Br}[\overline{B_d^0} \to X_s\gamma]$ is precisely measured at the experiments.

Although we focused on the FCNC processes related to the $b \to s$ transition, the Wilson coefficients of the SMEFT and the weak EFT in this thesis can be applied to both $b \to d$ and $s \to d$ transitions. In addition, the Wilson coefficient for the radiative transition $b \to s\gamma$ also contributes to the CP asymmetry in the radiative decays [85, 86, 87], the inclusive [88, 89] and the exclusive [90, 91, 92] $b \to s l^+ l$ processes.

We comment on the additional contribution to the Wilson coefficient C_{VLL} which are used in the calculation of the mass difference Δm_{B_s}. A box diagram where the VLQ propagates in the loop contributes to the Wilson coefficient C_{VLL} [82, 83]. We denote this contribution as $C_{\mathrm{VLL}}^{(\mathrm{SMEFT})}$ here. This is given as [82, 83],

$$C_{\mathrm{VLL}}^{(\mathrm{SMEFT})} = \left[\frac{G_F^2}{4\pi^2} M_W^2 (\lambda^t_{sb})^2\right]^1 \frac{(y_d'^{s4} y_d'^{b4*})^2}{8(4\pi)^2 M_4^2}, \tag{7.1}$$

As mentioned in Ref.[82], the Wilson coefficient $C_{\mathrm{VLL}}^{(\mathrm{SMEFT})}$ becomes dominant compared with the tree level contribution $C_{\mathrm{VLL}}^{(\mathrm{tree})}$ in the large VLQ mass region. We show the absolute value of the total Wilson coefficient $C_{\mathrm{VLL}} = C_{\mathrm{VLL}}^{\mathrm{SM}} + C_{\mathrm{VLL}}^{\mathrm{NP}}$ as a

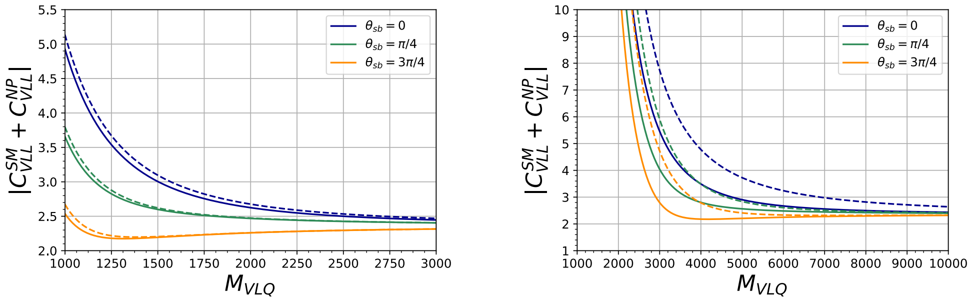

Figure 7.1. The absolute value of total Wilson coefficient $C_{\text{VLL}} = C_{\text{VLL}}^{\text{SM}} + C_{\text{VLL}}^{\text{NP}}$ as a function of the VLQ mass $M_{\text{VLQ}} = M_4$. The solid line is the result without $C_{\text{VLL}}^{(\text{SMEFT})}$ while the dashed line is the result including $C_{\text{VLL}}^{(\text{SMEFT})}$ in $C_{\text{VLL}}^{\text{NP}}$. The different colors of the line represent different values of the phase θ_{sb}. In the left figure, we take $|y_d'^{s4} y_d'^{b4*}| = 0.1$. In the right figure, we set $|y_d'^{s4} y_d'^{b4*}| = 1$. We note that the range of both vertical and horizontal axis is different between the left figure and the right figure.

function of the VLQ mass in Fig.7.1. The solid line is the result without $C_{\text{VLL}}^{(\text{SMEFT})}$ while the dashed line is the result including $C_{\text{VLL}}^{(\text{SMEFT})}$ in $C_{\text{VLL}}^{\text{NP}}$. The different colors of the line represent to different values of the phase θ_{sb}. In the left figure, we take $|y_d'^{s4} y_d'^{b4*}| = 0.1$. In the right figure, we set $|y_d'^{s4} y_d'^{b4*}| = 1$. One finds that the contribution from $C_{\text{VLL}}^{(\text{SMEFT})}$ is small in the case of $|y_d'^{s4} y_d'^{b4*}| = 0.1$. On the other hand, that is large in the case of $|y_d'^{s4} y_d'^{b4*}| = 1$. This is because $C_{\text{VLL}}^{(\text{SMEFT})}$ is proportional to $(y_d'^{s4} y_d'^{b4*})^2$. Therefore, we have to take account of the contribution from $C_{\text{VLL}}^{(\text{SMEFT})}$ to C_{VLL} in order to obtain more precise constraints for the large Yukawa coupling case $|y_d'^{s4} y_d'^{b4*}| \sim 1$.

Comment on Figs.6.1-6.3

Figures.6.1-6.3 are reproduced from the our published paper [84]. We note that we computed again to make Figs.6.1-6.3 because,

- We updated the input parameters shown in Table 6.1.
- We do not take account of the RG effects for $\tilde{\mathcal{C}}_{\phi q}^{(1)pq}$, $\tilde{\mathcal{C}}_{\phi q}^{(3)pq}$ from μ_{VLQ} to μ_{EW} and the new physics contribution to the Wilson coefficient C_2 (Eq.(5.26)) in published paper [84].

Acknowledgments.

I would like to thank my supervisor, Takuya Morozumi for valuable discussions and advices throughout this work and research activity. I am thankful to Yusuke Shimizu for many useful discussions and advices. Discussion with Takuya Morozumi and Yusuke Shimizu was very helpful for me to extend my knowledge about my study. I am grateful to Hiroyuki Umeeda for helpful discussions and advices about flavor physics. I would like to also thank Morimitsu Tanimoto for helpful discussions which extend my knowledge about the particle phenomenology. I am thankful to staff members in the Elementary Particle Theory Group at Hiroshima University: Masanori Okawa, Tomohiro Inagaki and Ken-Ichi Ishikawa provided me useful advices and comments on my study. I am also grateful to students in the Elementary Particle Theory Group at Hiroshima University for lots of advice. Finally, I would like to express my appreciation for my parents.

Appendix A
Neutral $\boldsymbol{B}$ Meson System

In the present chapter, we investigate a mixing and decay processes of the neutral B mesons, namely B_d^0 and B_s^0. The B_d^0 meson consists of the anti-bottom quark $\bar{b}$ and the down quark d while the B_s^0 meson consists of the anti-bottom quark $\bar{b}$ and the strange quark s. We focus on the decay processes $\overline{B_s^0} \to \mu^+\mu \quad$ and $\overline{B_d^0} \to X_s\gamma$ in addition to the mixing of the B_s^0 and $\overline{B_s^0}$. We note that the computation in this chapter are based on the SM, not the model with the VLQ except Subsec.A.3.3. It is useful for us to use a parametrization of the CKM matrix in the SM, so called Wolfenstein parametrization [118, 7, 65, 119]:

$$V_{\mathrm{CKM}} = \begin{pmatrix} 1 \quad \frac{\lambda^2}{2} & \lambda & A\lambda^3(\rho \quad i\eta) \\ \lambda & 1 \quad \frac{\lambda^2}{2} & A\lambda^2 \\ A\lambda^3(1 \quad \rho \quad i\eta) & A\lambda^2 & 1 \end{pmatrix} + \mathcal{O}(\lambda^4)\,, \tag{A.1}$$

where numerical values of the parameters are determined by experiments, for instance $\lambda = 0.225$ [7].

We consider a general neutral meson system before we investigate the specific processes. We follow the textbook [120]. We denote the general neutral meson as P^0 and the anti-particle of P^0 as $\overline{P^0}$. Since the neutral mesons are not stable and decay into other particles, a mass matrix of the neutral meson system can be given as,

$$\boldsymbol{R} = \boldsymbol{M} \quad \frac{i}{2} \quad , \tag{A.2}$$

$$\boldsymbol{M}^\dagger = \boldsymbol{M}\,, \tag{A.3}$$

$$^\dagger = \quad , \tag{A.4}$$

where the Hermitian matrix $\boldsymbol{M}$ is just a mass matrix while the anti-Hermitian part $\frac{i}{2}$ which is called absorptive part represents decay of the neutral meson. The matrices $\boldsymbol{M}$ and are obtained in the second-order perturbation theory,

$$M_{ij} = m_0\delta_{ij} + \langle i|\mathcal{H}_W|j\rangle + \sum_n P\frac{\langle i|\mathcal{H}_W|n\rangle\langle n|\mathcal{H}_W|j\rangle}{m_0 \quad E_n}\,, \tag{A.5}$$

$$_{ij} = 2\pi\sum_n \delta(m_0 \quad E_n)\langle i|\mathcal{H}_W|n\rangle\langle n|\mathcal{H}_W|j\rangle\,, \tag{A.6}$$

where $i,j=1,2$ with $|1\rangle=|P^0\rangle$, $|2\rangle=|\overline{P^0}\rangle$. The symbol P denotes the principal part prescription and the $\mathcal{H}_W$ represents a Hamiltonian related to the transition $|j\rangle\to|i\rangle$.

The basis of the matrix $\boldsymbol{R}$ is $|P^0\rangle$ and $|\overline{P^0}\rangle$. We can obtain eigenvalues and eigenvectors by solving an eigenvalue equation. The eigenvectors of the matrix $\boldsymbol{R}$ can be written as,

$$|P_H\rangle \;=\; p_H|P^0\rangle+q_H|\overline{P^0}\rangle\,, \tag{A.7}$$
$$|P_L\rangle \;=\; p_L|P^0\rangle\quad q_L|\overline{P^0}\rangle\,, \tag{A.8}$$

where the mixing parameters $p_{H,L}$ and $q_{H,L}$ are normalized as $\sqrt{|p_H|^2+|q_H|^2}=\sqrt{|p_L|^2+|q_L|^2}=1$. The eigenvalues are given as follows:

$$\mu_H \;=\; m_H \quad \frac{i}{2}\;{}_H\,, \tag{A.9}$$
$$\mu_L \;=\; m_L \quad \frac{i}{2}\;{}_L\,. \tag{A.10}$$

The subscripts H and L mean the heavy eigenstate and light eigenstate, respectively. We define a difference of the two eigenvalues μ_H and μ_L,

$$\Delta\mu \;\equiv\; \mu_H \quad \mu_L \;=\; \Delta m \quad \frac{i}{2}\Delta \;=\; \sqrt{4R_{12}R_{21}+(R_{22}\quad R_{11})^2}\,, \tag{A.11}$$

with $\Delta m\equiv m_H \quad m_L$ and $\Delta \;\equiv\; {}_H \quad {}_L$. The symbol R_{ij} denotes the (i,j) component of the matrix $\boldsymbol{R}$. The CPT and CP transformations for the $|P^0\rangle$ and $|\overline{P^0}\rangle$ are,

$$\mathrm{CPT}|P^0\rangle \;=\; e^{i\nu_P}|\overline{P^0}\rangle\,, \tag{A.12}$$
$$\mathrm{CPT}|\overline{P^0}\rangle \;=\; e^{i\nu_P}|P^0\rangle\,, \tag{A.13}$$
$$\mathrm{CP}|P^0\rangle \;=\; e^{i\xi_P}|\overline{P^0}\rangle\,, \tag{A.14}$$
$$\mathrm{CP}|\overline{P^0}\rangle \;=\; e^{\quad i\xi_P}|P^0\rangle\,, \tag{A.15}$$

where the phases ν_P and ξ_P are arbitrary and unphysical. We can show from Eqs.(A.5) and (A.6) that M_{22} and ${}_{22}$ are equal to M_{11} and ${}_{11}$, respectively when the Hamiltonian $\mathcal{H}_W$ is invariant under the CPT transformation, i.e. $(\mathrm{CPT})\mathcal{H}_W(\mathrm{CPT})^{\quad 1}=\mathcal{H}_W$. Also the CP invariance implies $M_{11}=M_{22}$, ${}_{11}={}_{22}$, $M_{21}=e^{2i\xi_P}M_{12}$ and ${}_{21}=e^{2i\xi_P}\;{}_{12}$. Thus, we can define a CPT and CP violating parameter θ:

$$\theta \;\equiv\; \frac{R_{22}\quad R_{11}}{\Delta\mu}\,, \tag{A.16}$$

and a CP violating real parameter δ,

$$\delta \;\equiv\; \frac{|R_{12}|\quad |R_{21}|}{|R_{12}|+|R_{21}|}\,. \tag{A.17}$$

Taking the diagonalization of the matrix $\boldsymbol{R}$ into account, we can determine the ratios of mixing parameters $p_{H,L}$ and $q_{H,L}$ in Eqs.(A.7) and (A.8) as,

$$\frac{q_H}{p_H} = \frac{\Delta\mu(1+\theta)}{2R_{12}} = \frac{2R_{21}}{\Delta\mu(1 \quad \theta)}, \tag{A.18}$$

$$\frac{q_L}{p_L} = \frac{\Delta\mu(1 \quad \theta)}{2R_{12}} = \frac{2R_{21}}{\Delta\mu(1+\theta)}. \tag{A.19}$$

It is clear that the CPT invariance leads to $\theta = 0$ and $\frac{q_H}{p_H} = \frac{q_L}{p_L}$. Therefore, the absolute value of the mixing parameter p_L is the same as p_H because of $|p_H|^2 + |q_H|^2 = |p_L|^2 + |q_L|^2 = 1$. It is convenient to set the relative phase of $|P_H\rangle$ and $|P_L\rangle$ so as to $p_H = p_L$. In this setup, the mixing parameter q_L is equals to q_H. Then, we redefine the eigenvectors as,

$$|P_H\rangle = p|P^0\rangle + q|\overline{P^0}\rangle, \tag{A.20}$$

$$|P_L\rangle = p|P^0\rangle \quad q|\overline{P^0}\rangle, \tag{A.21}$$

in the case where we assume CPT invariance. The mixing parameters p, q and the difference between the eigenvalues of $\boldsymbol{R}$ are obtained as follows:

$$\Delta\mu = \Delta m \quad \frac{i}{2}\Delta \quad = \sqrt{4R_{12}R_{21}}, \tag{A.22}$$

$$\frac{q}{p} = \frac{\Delta\mu}{2R_{12}} = \sqrt{\frac{2M_{12}^* \quad i \quad {}_{12}^*}{2M_{12} \quad i \quad {}_{12}}}, \tag{A.23}$$

Using the Eq.(A.22), we obtain,

$$(\Delta m)^2 \quad \frac{1}{4}(\Delta \quad)^2 = 4|M_{12}|^2 \quad | \quad {}_{12}|^2, \tag{A.24}$$

$$(\Delta m)(\Delta \quad) = 4\mathrm{Re}[M_{12}^* \quad {}_{12}]. \tag{A.25}$$

The above expressions are derived without any approximations. In the following sections, we consider the case of neutral B_d and B_s meson systems.

A.1 B_s^0-$\overline{B_s^0}$ Mixing and Mass difference Δm_{B_s}

We compute M_{12} at leading order in the B_s^0 meson system. The component $M_{12}^{B_s}$ is given by Eq.(A.5):

$$M_{12}^{B_s} = \langle B_s^0|\mathcal{H}_{eff}^{\Delta B=2}|\overline{B_s^0}\rangle, \tag{A.26}$$

where the Hamiltonian $\mathcal{H}_W = \mathcal{H}_{eff}^{\Delta B=2}$ is defined in terms of the weak EFT as [97],

$$\mathcal{H}_{eff}^{\Delta B=2} = \frac{G_F^2}{4\pi^2} M_W^2 (\lambda_{sb}^t)^2 C_{\mathrm{VLL}}^{\mathrm{SM}} O_{\mathrm{VLL}} + h.c. \tag{A.27}$$

with a product of the CKM matrix elements $\lambda_{sb}^t \equiv V_{ts}^* V_{tb}$ and an effective operator,

$$O_{\mathrm{VLL}} = [\overline{s_L}\gamma^\mu b_L][\overline{s_L}\gamma_\mu b_L]. \tag{A.28}$$

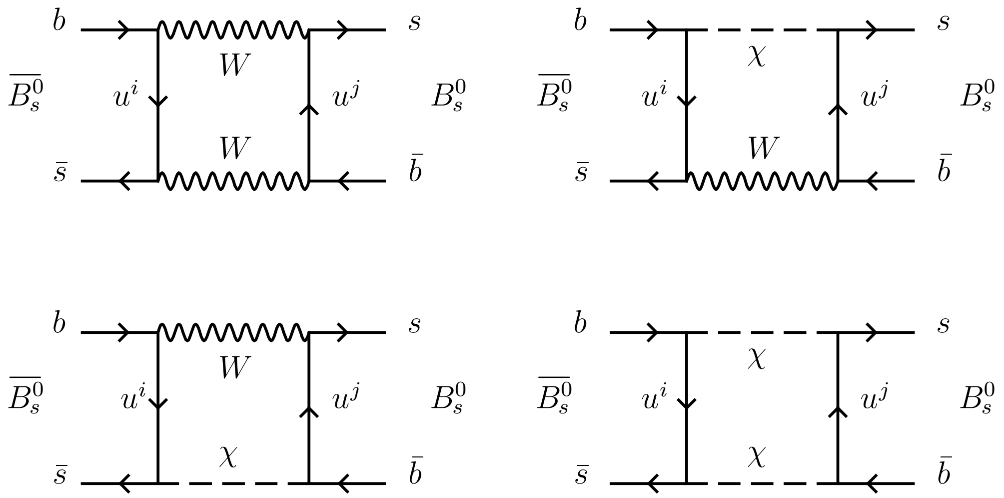

Figure A.1. Relevant diagrams to the $M_{12}^{B_s}$ in the SM. The symbol χ denotes the charged NG boson $\chi^{\pm}$. The subscripts i, j represent the generation of the up-type quark, that is $u^1 = u$, $u^2 = c$, and $u^3 = t$.

The Wilson coefficient $C_{\mathrm{VLL}}^{\mathrm{SM}}$ is determined by matching the weak EFT with the SM. Figure A.1 shows the relevant diagrams of the SM. Taking account of the CKM unitarity in the SM, we obtain the effective Hamiltonian as follows [102]:

$$\mathcal{H}_{eff}^{\Delta B=2} = \frac{G_F^2}{4\pi^2} M_W^2 \sum_{i=c,t} \sum_{j=c,t} \lambda_{sb}^i \lambda_{sb}^j \bar{E}_{ij} [\bar{s}_L \gamma^\mu b_L][\bar{s}_L \gamma_\mu b_L] \,, \tag{A.29}$$

where the function $\bar{E}_{ij}$ is given as,

$$\bar{E}_{ij} = \begin{cases} \left[\left\{ \frac{1}{4} \quad \frac{3}{2(x_j \quad 1)} \quad \frac{3}{4(x_j \quad 1)^2} \right\} \frac{x_i x_j \ln x_j}{x_j \quad x_i} + (i \leftrightarrow j) \quad \frac{3 x_i x_j}{4(x_i \quad 1)(x_j \quad 1)} \right], \text{for } i \neq j \\ \frac{3}{2} \left(\frac{x_i}{x_i \quad 1} \right)^3 \ln x_i \quad x_i \left\{ \frac{1}{4} \quad \frac{9}{4} \frac{1}{x_i \quad 1} \quad \frac{3}{2} \frac{1}{(x_i \quad 1)^2} \right\}, \text{ for } i = j \end{cases} \tag{A.30}$$

with the parameter $x_i \equiv (m_u^i / M_W)^2$. Numerical values of the functions $\bar{E}_{tt}$, $\bar{E}_{cc}$ and $\bar{E}_{ct} = \bar{E}_{tc}$ are,

$$|\bar{E}_{tt}| \simeq 2.5 \,, \tag{A.31}$$

$$|\bar{E}_{cc}| \simeq 2.5 \times 10^{\;4} \,, \tag{A.32}$$

$$|\bar{E}_{ct}| \simeq 2.2 \times 10^{\;3} \,, \tag{A.33}$$

with $m_t = 173.1$ GeV, $m_c = 1.27$ GeV and $M_W = 80.379$ GeV [65]. We can see from Eq.(A.1) that the product of the CKM matrix λ_{sb}^c is the same order of magnitude as λ_{sb}^t. Therefore, the dominant contribution in Eq.(A.29) comes from the top quark term which are proportional to $(\lambda_{sb}^t)^2 \bar{E}_{tt}$. We approximate Eq.(A.29) by,

$$\mathcal{H}_{eff}^{\Delta B=2} = \frac{G_F^2}{4\pi^2} M_W^2 (\lambda_{sb}^t)^2 S_0(x_t) [\bar{s}_L \gamma^\mu b_L][\bar{s}_L \gamma_\mu b_L] \,, \tag{A.34}$$

where we redefine [93, 115],

$$\bar{E}_{tt} \equiv S_0(x_t) \,. \tag{A.35}$$

Comparing Eq.(A.34) with Eq.(A.27), we determine the Wilson coefficient $C_{\mathrm{VLL}}^{\mathrm{SM}}$ as,

$$C_{\mathrm{VLL}}^{\mathrm{SM}} = S_0(x_t)\,. \tag{A.36}$$

We obtain an expression of the $M_{12}^{B_s}$ by inserting the effective Hamiltonian Eq.(A.27) into Eq.(A.26):

$$M_{12}^{B_s,\mathrm{SM}} \simeq \frac{G_F^2 M_W^2}{12\pi^2} f_{B_s}^2 m_{B_s} B_s \eta_{B_s} C_{\mathrm{VLL}}^{\mathrm{SM}} (\lambda_{sb}^t)^2 e^{i(\xi_b - \xi_s - \xi_{B_s})}\,, \tag{A.37}$$

where m_{B_s} is the mass of B_s^0 meson and $\eta_{B_s} = 0.5510 \pm 0.0022$ [115] is QCD correction. The symbols f_{B_s} and B_s represent the B_s^0 meson decay constant and the bag parameter of the B_s meson, respectively. The f_{B_s} and B_s are defined by [120],

$$\langle B_s^0 | (\bar{s}\gamma^\mu L b)(\bar{s}\gamma_\mu L b) | \overline{B_s^0} \rangle = \frac{1}{3} e^{i(\xi_b - \xi_s - \xi_{B_s})} f_{B_s}^2 m_{B_s} B_s\,, \tag{A.38}$$

with

$$\langle 0 | \bar{b}\gamma^\mu \gamma_5 s | B_s^0(p^\mu) \rangle = e^{i\varphi} p^\mu f_{B_s}\,, \tag{A.39}$$

$$\langle 0 | \bar{s}\gamma_\mu \gamma_5 b | B_s^0(p^\mu) \rangle = e^{i\varphi} e^{i(\xi_b - \xi_s - \xi_{B_s})} p_\mu f_{B_s}\,, \tag{A.40}$$

The phase φ is arbitrary. The phases ξ_b, ξ_s and ξ_{B_s} come from CP transformations of the b-quark, s-quark and B_s meson states, similar to the ξ_P in Eq.(A.14), and thus these phases are unphysical.

Since the absorptive part $\Gamma_{12}^{B_s}$ is related to the decay of B_s^0 meson, it is expected that the absorptive part is dominated by the mass of B_s^0 meson, that is $m_{B_s} \sim m_b$. On the other hand, the $M_{12}^{B_s}$ is proportional to $S_0(x_t) \sim x_t = m_t^2/M_W^2$. This implies $\left|\frac{\Gamma_{12}^{B_s}}{M_{12}^{B_s}}\right| \approx \mathcal{O}\left(\frac{m_b^2}{m_t^2}\right) \ll 1$. Also experimental results show $\frac{|\Delta\Gamma_{B_s}|}{\Delta m_{B_s}} \approx \frac{6\times 10^{-11}}{1\times 10^{-8}} \ll 1$ [65]. Taking account of $|\Gamma_{12}^{B_s}| \ll |M_{12}^{B_s}|$ and $|\Delta\Gamma_{B_s}| \ll \Delta m_{B_s}$ in Eq.(A.24), we can approximate Δm_{B_s} as,

$$\Delta m_{B_s} \simeq 2|M_{12}^{B_s,\mathrm{SM}}| = \frac{G_F^2}{6\pi^2} M_W^2 m_{B_s} f_{B_s}^2 B_s \eta_{B_s} |\lambda_{sb}^t|^2 |C_{\mathrm{VLL}}^{\mathrm{SM}}|\,. \tag{A.41}$$

A.2 $\overline{B_s^0} \to \mu^+\mu^-$ $(b \to s\mu^+\mu^-)$ Process

We investigate $\overline{B_s^0} \to \mu^+\mu^-$ process in this section. This process is induced by the FCNC among the b-quark and s-quark. As we have seen in the previous section, there is the mixing between B_s^0 and $\overline{B_s^0}$. The mixing effect leads to a time dependent oscillation among the B_s^0 and $\overline{B_s^0}$ and affects the decay process $\overline{B_s^0} \to \mu^+\mu^-$. First we show a time dependent decay rate and an "untagged" decay rate in $\overline{B_s^0} \to \mu^+\mu^-$ process which are given in [104, 105, 106, 107]. Here we follow the computation summarized in Refs.[106, 107].

A.2.1 Decay rate and branching ratio

The effective Hamiltonian for the $\overline{B_s^0} \to \mu^+\mu$ process is,

$$\mathcal{H}_{eff}^{\Delta B=1} = \frac{4G_F}{\sqrt{2}} \frac{\alpha_{\rm em}}{4\pi} \lambda_{sb}^t C_{10} O_{10} + h.c. \,, \tag{A.42}$$

with the effective operator,

$$O_{10} = [\overline{s_L}\,\gamma^\mu b_L][\overline{\mu}\,\gamma_\mu\gamma_5\mu] \,. \tag{A.43}$$

The Wilson coefficient of the SM will be given in the next subsection. Since the time evolution of the mass eigenstates $|P_H^0\rangle$ and $|P_L^0\rangle$ are written as [120],

$$|P_H^0(t)\rangle = e^{\ \, i\mu_H t}|P_H^0\rangle \,, \tag{A.44}$$

$$|P_L^0(t)\rangle = e^{\ \, i\mu_L t}|P_L^0\rangle \,, \tag{A.45}$$

with the time t which is measured at the rest frame of decaying particles, the B_s^0 meson states at time t are given as follows:

$$|B_s^0(t)\rangle = g_+(t)|B_s^0\rangle + \frac{q}{p} g\ \ (t)|\overline{B_s^0}\rangle \,, \tag{A.46}$$

$$|\overline{B_s^0}(t)\rangle = \frac{p}{q} g\ \ (t)|B_s^0\rangle + g_+(t)|\overline{B_s^0}\rangle \,, \tag{A.47}$$

where

$$g_\pm(t) \equiv \frac{1}{2}(e^{\ \, i\mu_H t} \pm e^{\ \, i\mu_L t}) \,. \tag{A.48}$$

It is useful to show relations,

$$|g_\pm(t)|^2 = \frac{e^{\ \ _{B_s}t}}{2}\left[\cosh\frac{\Delta\ \ _{B_s}t}{2} \pm \cos(\Delta m_{B_s} t)\right], \tag{A.49}$$

$$g_+^*(t) g\ \ (t) = \frac{e^{\ \ _{B_s}t}}{2}\left[\sinh\frac{\Delta\ \ _{B_s}t}{2} + i\sin(\Delta m_{B_s} t)\right], \tag{A.50}$$

where $\Delta\ \ _{B_s} \equiv\ \ _H\ \ \ \ _L$ and $\ \ _{B_s} \equiv (\ \ _H +\ \ _L)/2$. We parametrize $M_{12}^{B_s}$ by using $M_{12}^{B_s,\rm SM}$ in Eq.(A.37) as,

$$M_{12}^{B_s} = M_{12}^{B_s,\rm SM}(re^{\ \, i\theta})^2 \,, \tag{A.51}$$

The real parameter r and the phase θ represent effects from a new physics model. The case of $(r,\theta) = (1,0)$ corresponds to the SM. Similarly we introduce a phase φ_P which represents new physics effects for the Wilson coefficient C_{10}:

$$\frac{C_{10}}{C_{10}^{\rm SM}} = \left|\frac{C_{10}}{C_{10}^{\rm SM}}\right| e^{i\varphi_P} \,, \tag{A.52}$$

where $C_{10}^{\rm SM}$ is the SM contribution in the total Wilson coefficient C_{10}. The ratio of the mixing parameter $\frac{q}{p}$ in Eq.(A.23) can be written by using the parametrization Eq.(A.51):

$$\frac{q}{p} \simeq \sqrt{\frac{M_{12}^{B_s *}}{M_{12}^{B_s}}} = e^{\quad i(\xi_b \quad \xi_s \quad \xi_{B_s} \quad 2\theta)} e^{\quad 2i\arg[\lambda_{sb}^t]}, \tag{A.53}$$

where we take $|M_{12}^{B_s}| \gg | \ {}_{12}^{B_s}|$ into account. We then obtain the time dependent decay rates of $\overline{B_s^0}(t) \to \mu^+\mu$ and $B_s^0(t) \to \mu^+\mu$ after computing the matrix elements $|\langle \mu^+\mu \ |\mathcal{H}_{eff}^{\Delta B=1}|\overline{B_s^0}(t)\rangle|$ and $|\langle \mu^+\mu \ |\mathcal{H}_{eff}^{\Delta B=1}|B_s^0(t)\rangle|$:

$$\begin{aligned} [\overline{B_s^0}(t) \to \mu^+\mu \ ] &= \frac{G_F^4 M_W^4 s_w^4}{8\pi^5}\sqrt{1 \quad \frac{4m_\mu^2}{m_{B_s}^2}} f_{B_s}^2 m_{B_s} m_\mu^2 e^{\quad {}_{B_s} t}|C_{10}\lambda_{sb}^t|^2 \\ &\times\left[\cosh\frac{\Delta \ {}_{B_s}t}{2} \quad \mathcal{A}_\Delta^{\mu\mu}\sinh\frac{\Delta \ {}_{B_s}t}{2} \quad S_{\mu\mu}\sin(\Delta m_{B_s}t)\right], \end{aligned} \tag{A.54}$$

$$\begin{aligned} [B_s^0(t) \to \mu^+\mu \ ] &= \frac{G_F^4 M_W^4 s_w^4}{8\pi^5}\sqrt{1 \quad \frac{4m_\mu^2}{m_{B_s}^2}} f_{B_s}^2 m_{B_s} m_\mu^2 e^{\quad {}_{B_s} t}|C_{10}\lambda_{sb}^t|^2 \\ &\times\left[\cosh\frac{\Delta \ {}_{B_s}t}{2} \quad \mathcal{A}_\Delta^{\mu\mu}\sinh\frac{\Delta \ {}_{B_s}t}{2} + S_{\mu\mu}\sin(\Delta m_{B_s}t)\right], \end{aligned} \tag{A.55}$$

Here we define [104, 105, 106, 107],

$$A_\Delta^{\mu\mu} \equiv \cos 2(\theta + \varphi_P)\,, \tag{A.56}$$

$$S_{\mu\mu} \equiv \sin 2(\theta + \varphi_P)\,. \tag{A.57}$$

It is clear that $A_\Delta^{\mu\mu} = 1$ and $S_{\mu\mu} = 0$ in the case of the SM. From Eqs.(A.54) and (A.55), we can define the untagged decay rate [104, 105, 106, 107]:

$$\begin{aligned} \langle \ [B_s^0(t) \to \mu^+\mu \ ]\rangle &\equiv [\overline{B_s^0}(t) \to \mu^+\mu \ ] + [B_s^0(t) \to \mu^+\mu \ ] \\ &= \frac{G_F^4 M_W^4 s_w^4}{4\pi^5}\sqrt{1 \quad \frac{4m_\mu^2}{m_{B_s}^2}} f_{B_s}^2 m_{B_s} m_\mu^2 e^{\quad \frac{t}{\tau_{B_s}}}|C_{10}\lambda_{sb}^t|^2 \\ &\times\left[\cosh\left(\frac{y_s t}{\tau_{B_s}}\right) + A_\Delta^{\mu\mu}\sinh\left(\frac{y_s t}{\tau_{B_s}}\right)\right], \end{aligned} \tag{A.58}$$

where we use the parameters,

$$y_s \equiv \frac{{}_L \quad {}_H}{{}_L + {}_H} = \quad \frac{\Delta \ {}_{B_s}}{2 \ {}_{B_s}}, \tag{A.59}$$

$$\tau_{B_s} = \frac{1}{{}_{B_s}}. \tag{A.60}$$

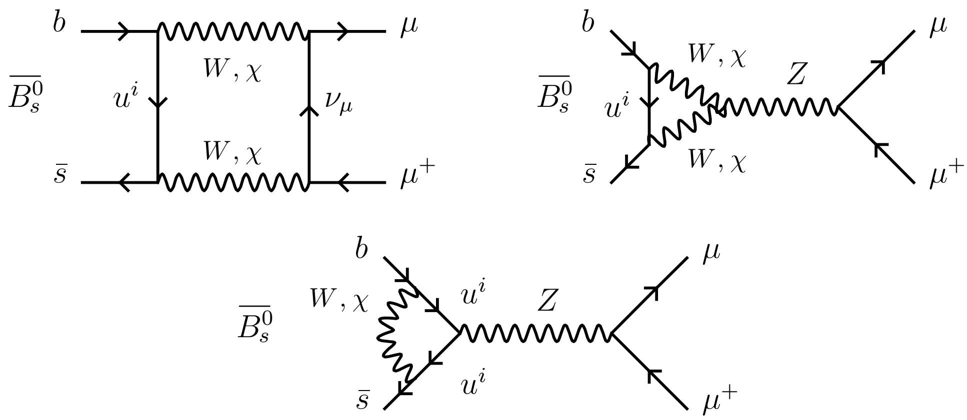

Figure A.2. Diagrams which leads leading order contribution to C_{10} in the SM.

The parameter τ_{B_s} is the life time of B_s meson. We finally define branching ratio of this process by integrating the untagged decay rate Eq.(A.58) in terms of t:

$$\overline{\mathrm{BR}}[B_s^0 \to \mu^+\mu \;\;] \;\equiv\; \frac{1}{2}\int_0^\infty dt \,\langle \;\; [B_s^0(t) \to \mu^+\mu \;\;]\rangle\,. \tag{A.61}$$

The concrete form of the branching ratio is given as,

$$\overline{\mathrm{BR}}[B_s^0 \to \mu^+\mu \;\;] \;=\; \tau_{B_s}\frac{G_F^4 M_W^4 s_w^4}{8\pi^5}\sqrt{1 \quad \frac{4m_\mu^2}{m_{B_s}^2}}\, f_{B_s}^2 m_{B_s} m_\mu^2 |\lambda_{sb}^t|^2 |C_{10}|^2 \left[\frac{1+y_s A_\Delta^{\mu\mu}}{1 \quad y_s^2}\right], \tag{A.62}$$

This expression can be rewritten by using the branching ratio of $\overline{B_s^0} \to \mu^+\mu$ without the B_s^0-$\overline{B_s^0}$ mixing effect, which is denoted as $\mathrm{Br}[\overline{B_s^0} \to \mu^+\mu \;\;]$:

$$\overline{\mathrm{BR}}[B_s^0 \to \mu^+\mu \;\;] \;=\; \left[\frac{1+y_s A_\Delta^{\mu\mu}}{1 \quad y_s^2}\right]\mathrm{Br}[\overline{B_s^0} \to \mu^+\mu \;\;]\,. \tag{A.63}$$

A.2.2 Wilson coefficient C_{10} in the SM

Here we show the leading order contribution of the SM to the Wilson coefficient C_{10}. Since there is no FCNC in the SM, the leading order contribution to C_{10} comes from one-loop diagrams. The typical diagrams are shown in Fig.A.2. The result is [102],

$$C_{10}^{\mathrm{SM}} \;=\; \frac{\eta_Y Y_0(x_t)}{s_w^2}\,, \tag{A.64}$$

where $\eta_Y = 1.0113$ [116] is NLO correction. We used the CKM unitarity relation and take only the top quark contribution into account. The function $Y_0(x)$ is given as,

$$Y_0(x) \;=\; \frac{x}{8} \quad \frac{3}{8}\frac{x}{x \quad 1} + \frac{3}{8}\frac{x^2 \ln x}{(x \quad 1)^2}\,. \tag{A.65}$$

A.3 $\overline{B_d^0}\to X_s\gamma$ $(b\to s\gamma)$ Process

The inclusive radiative decay process $\overline{B_d^0}\to X_s\gamma$ is the FCNC process induced by the photon while the FCNC process $\overline{B_s^0}\to\mu^+\mu$ in the previous section is induced by the Z boson. The radiative decay process $\overline{B_d^0}\to X_s\gamma$ is described by the effective Hamiltonian of the weak EFT [114, 115, 121]:

$$\mathcal{H}_{eff}^{b\to s\gamma} = \frac{4G_F}{\sqrt{2}}\lambda_{sb}^c\sum_{i=1}^{2} C_iO_i \quad \frac{4G_F}{\sqrt{2}}\lambda_{sb}^t\left[\sum_{i=3}^{6} C_iO_i+\sum_{i=7\gamma,8g} C_iO_i\right], \tag{A.66}$$

where the effective operators are 4-Fermi operators,

$$O_1 = (\overline{s_L}\gamma_\mu T^a c_L)(\overline{c_L}\gamma^\mu T^a b_L)\,, \tag{A.67}$$
$$O_2 = (\overline{s_L}\gamma_\mu c_L)(\overline{c_L}\gamma^\mu b_L)\,, \tag{A.68}$$

the QCD penguin operators,

$$O_3 = (\overline{s_L}\gamma_\mu b_L)\sum_{q=u,d,s,c,b}(\bar{q}\gamma^\mu q)\,, \tag{A.69}$$
$$O_4 = (\overline{s_L}\gamma_\mu T^a b_L)\sum_{q=u,d,s,c,b}(\bar{q}\gamma^\mu T^a q)\,, \tag{A.70}$$
$$O_5 = (\overline{s_L}\gamma_\mu\gamma_\nu\gamma_\rho b_L)\sum_{q=u,d,s,c,b}(\bar{q}\gamma^\mu\gamma^\nu\gamma^\rho q)\,, \tag{A.71}$$
$$O_6 = (\overline{s_L}\gamma_\mu\gamma_\nu\gamma_\rho T^a b_L)\sum_{q=u,d,s,c,b}(\bar{q}\gamma^\mu\gamma^\nu\gamma^\rho T^a q)\,, \tag{A.72}$$

and the dipole operators,

$$O_{7\gamma} = \frac{e}{16\pi^2}m_b(\overline{s_L}\sigma^{\mu\nu}b_R)F_{A\mu\nu}\,, \tag{A.73}$$
$$O_{8g} = \frac{g_s}{16\pi^2}m_b(\overline{s_L}\sigma^{\mu\nu}T^a b_R)G^a_{\mu\nu}\,. \tag{A.74}$$

The symbols $F_{A\mu\nu}$ and $G^a_{\mu\nu}$ denote the field strength of the photon and gluons, respectively. The dipole operator $O_{7\gamma}$ mainly contributes to the $\overline{B_d^0}\to X_s\gamma$ process and the other effective operators contribute through RG effects. We neglect $\lambda_{sb}^u = V_{us}^*V_{ub}\ll\lambda_{sb}^t$ and thus $\lambda_{sb}^c\simeq\quad\lambda_{sb}^t$ in the SM.

A.3.1 Wilson coefficients and effective coefficients

It is convenient to introduce so-called "effective coefficients" C_i^{eff} [112, 113] in the computation of the branching ratio of the $\overline{B_d^0}\to X_s\gamma$ process. In the present operator basis, the effective coefficients are defined as follows [114]:

$$C_i^{eff}(\mu) = \begin{cases} C_i(\mu)\,, & \text{for } i\neq 7\gamma, 8g,\\ C_{7\gamma}(\mu)+\sum_{i=1}^6 y_i C_i(\mu)\,, & \text{for } i=7\gamma,\\ C_{8g}(\mu)+\sum_{i=1}^6 z_i C_i(\mu)\,, & \text{for } i=8g,\end{cases} \tag{A.75}$$

where $y_i = \left(0, 0, \frac{1}{3}, \frac{4}{9}, \frac{20}{3}, \frac{80}{8}\right)$ and $z_i = \left(0, 0, 1, \frac{1}{6}, 20, \frac{10}{3}\right)$ in the dimensional regularization with $\{\gamma^\mu, \gamma_5\} = 0$ scheme, so-called naive dimensional regularization (NDR) scheme. We briefly show why the effective coefficients are introduced on the basis of Ref.[112]. We consider the computation of the $b \to s\gamma$ amplitude by using the weak EFT Hamiltonian Eq.(A.66). We write the amplitudes as,

$$\mathcal{A}_{\rm EFT} \sim C_{7\gamma}\langle s\gamma|O_{7\gamma}|b\rangle_{\rm tree} + \sum_j C_j \langle s\gamma|O_j|b\rangle_{\text{one-loop}}\,, \tag{A.76}$$

where the subscript "tree" means a tree level matrix element while "one-loop" denotes one-loop level matrix elements. If the matrix element of the effective operator O_j is nonzero and contributes to the $b \to s\gamma$ process, we can rewrite the matrix element $\langle s\gamma|O_j|b\rangle_{\text{one-loop}}$ by using the tree level matrix element $\langle s\gamma|O_{7\gamma}|b\rangle_{\rm tree}$:

$$\begin{aligned} \mathcal{A}_{\rm EFT} &= C_{7\gamma}\langle s\gamma|O_{7\gamma}|b\rangle_{\rm tree} + \sum_j C_j \langle s\gamma|O_j|b\rangle_{\text{one-loop}} \\ &= C_{7\gamma}\langle s\gamma|O_{7\gamma}|b\rangle_{\rm tree} + \sum_j y_j C_j \langle s\gamma|O_{7\gamma}|b\rangle_{\rm tree} \\ &= [C_{7\gamma} + \textstyle\sum_j y_j C_j]\langle s\gamma|O_{7\gamma}|b\rangle_{\rm tree}\,, \end{aligned} \tag{A.77}$$

where y_j is a number given by computing the one-loop level matrix element $\langle s\gamma|O_j|b\rangle_{\text{one-loop}}$ and corresponds to the parameter y_i in Eq.(A.75). We can see that the amplitude of the $b \to s\gamma$ process is proportional to the combination $C_{7\gamma} + \sum_j y_j C_j$ at the one-loop level. Therefore, it is convenient to define new coefficient $C_{7\gamma}^{eff} \equiv C_{7\gamma} + \sum_j y_j C_j$ and consider a RG equation with respect to the coefficient $C_{7\gamma}^{eff}$. We note that we can express the amplitude of $b \to s\gamma$ process in the SM as,

$$\mathcal{A}_{\rm SM} = A_{7\gamma}\langle s\gamma|O_{7\gamma}|b\rangle_{\rm tree}\,. \tag{A.78}$$

Since the matiching condition is $\mathcal{A}_{\rm SM} = \mathcal{A}_{\rm EFT}$ at the scale $\mu_{\rm EW}$, the condition leads to,

$$A_{7\gamma} = C_{7\gamma} + \textstyle\sum_j y_j C_j = C_{7\gamma}^{eff}\,, \tag{A.79}$$

at the one-loop level. We consider the scale dependence of the effective coefficients. The RG equations for the effective coefficients $C_i^{eff}(\mu)$ are written as [114],

$$\mu\frac{\partial}{\partial\mu}C_i^{eff}(\mu) = C_j^{eff}(\mu)\gamma_{ji}^{eff}(\mu)\,. \tag{A.80}$$

We expand the effective coefficients and the anomalous dimension matrix $\gamma_{ji}^{eff}(\mu)$ with respect to the QCD coupling $\alpha_s(\mu)$:

$$C_i^{eff} = C_i^{(0)eff} + \frac{\alpha_s(\mu)}{4\pi}C_i^{(1)eff} + \cdots\,, \tag{A.81}$$

$$\gamma^{eff} = \frac{\alpha_s(\mu)}{4\pi}\gamma^{(0)eff} + \frac{\alpha_s^2(\mu)}{(4\pi)^2}\gamma^{(0)eff} + \cdots\,. \tag{A.82}$$

The leading order anomalous dimension matrix $\gamma^{(0)eff}$ in NDR is [114],

$$\gamma^{(0)eff} = \begin{pmatrix} 4 & \frac{8}{3} & 0 & \frac{2}{9} & 0 & 0 & \frac{208}{243} & \frac{173}{162} \\ 12 & 0 & 0 & \frac{4}{3} & 0 & 0 & \frac{416}{81} & \frac{70}{27} \\ 0 & 0 & 0 & \frac{52}{3} & 0 & 2 & \frac{176}{81} & \frac{14}{27} \\ 0 & 0 & \frac{40}{9} & \frac{100}{9} & \frac{4}{9} & \frac{5}{6} & \frac{152}{243} & \frac{587}{162} \\ 0 & 0 & 0 & \frac{256}{3} & 0 & 20 & \frac{6272}{81} & \frac{6596}{27} \\ 0 & 0 & \frac{256}{9} & \frac{56}{9} & \frac{40}{9} & \frac{2}{3} & \frac{4624}{243} & \frac{4772}{81} \\ 0 & 0 & 0 & 0 & 0 & 0 & \frac{32}{3} & 0 \\ 0 & 0 & 0 & 0 & 0 & 0 & \frac{32}{9} & \frac{28}{3} \end{pmatrix}, \tag{A.83}$$

and $\gamma^{(1)eff}$ is also given in [114]. The Wilson coefficients in Eq.(A.75) at the matching scale $\mu_{\rm EW} \simeq M_W$ are evolved to the B_d meson mass scale $\mu_b \simeq m_b$. This can be done by solving the RG equation Eq.(A.80) with the anomalous dimension matrices $\gamma^{(0)eff}$ and $\gamma^{(1)eff}$.

A.3.2 Branching ratio of $\overline{B_d^0} \to X_s\gamma$

In this thesis, we use a next-to-leading order (NLO) expression for the branching ratio of the $\overline{B_d^0} \to X_s\gamma$ process [114]:

$$\mathrm{Br}[\overline{B_d^0} \to X_s\gamma] = \mathrm{Br}[\overline{B_d^0} \to X_c e \bar{\nu}_e] \cdot R_{\rm quark}(\delta) \left(1 \quad \frac{\delta_{sl}^{\rm NP}}{m_b^2} + \frac{\delta_{rad}^{\rm NP}}{m_b^2} \right), \tag{A.84}$$

where $\delta_{sl}^{\rm NP}$ and $\delta_{rad}^{\rm NP}$ are non-perturbative corrections for the semi-leptonic and the radiative decay rates which are computed by Heavy-Quark Effective Theory (HQET), respectively [122, 114]. The symbol $R_{\rm quark}(\delta)$ at NLO is defined as,

$$R_{\rm quark}(\delta) = \frac{[b \to X_s\gamma]^{E_\gamma > (1 \quad \delta) E_\gamma^{\rm max}}}{[b \to X_c e \bar{\nu}_e]} \cdot \frac{|\lambda_{sb}^t|^2}{|V_{cb}|^2} \cdot \frac{6\alpha_{em}}{\pi g(z)} F(z) \{ |D|^2 + A(\delta) \} \,. \tag{A.85}$$

The function $g(z)$ with $z = m_{c,\rm pole}^2 / m_{b,\rm pole}^2$ is the phase space factor of the semi-leptonic decay. The function $F(z)$ includes the difference between the pole mass and the $\overline{\rm MS}$ mass of the b-quark and the NLO correction for the semi-leptonic decay. The symbol δ represents the lower cut on the photon energy in bremsstrahlung corrections, $E_\gamma > (1 \quad \delta) E_\gamma \equiv (1 \quad \delta) \frac{m_b}{2}$. In our numerical analysis, we take $E_\gamma > 1.6$ GeV. The function $A(\delta)$ originates from the bremsstrahlung and virtual corrections [114, 123, 124, 125]:

$$A(\delta) = \left\{ e^{\quad \frac{\alpha_s(\mu_b)}{3\pi}(7 + 2\ln\delta)\ln\delta} \quad 1 \right\} |C_{7\gamma}^{(0)eff}(\mu_b)|^2 + \frac{\alpha_s(\mu_b)}{\pi} \sum_{\substack{i,j=1 \\ i \le j}} f_{ij}(\delta) C_i^{(0)eff}(\mu_b) C_j^{(0)eff}(\mu_b) \,, \tag{A.86}$$

where the functions $f_{ij}(\delta)$ are summarized in Ref.[114].

The term $|D|^2$ consists of the LO and NLO effective coefficient $C_{7\gamma}^{(0)eff}, C_{7\gamma}^{(1)eff}$ and the virtual corrections for $b \to s\gamma$ process [114, 123, 124],

$$D \;=\; C_{7\gamma}^{(0)eff}(\mu_b) + \frac{\alpha_s(\mu_b)}{4\pi}\left[C_{7\gamma}^{(1)eff}(\mu_b) + \sum_{i=1}^{8} C_i^{(0)eff}(\mu_b)\left\{r_i + \gamma_{i7}^{(0)eff}\ln\frac{m_b}{\mu_b}\right\}\right], \tag{A.87}$$

where r_i can be found in Ref.[114].

A.3.3 EW penguin contribution to Wilson coefficients

It is pointed out in Refs.[109, 110] that the tree level FCNC contributes to the Wilson coefficients of the electroweak penguin operators,

$$O_3^Q \;=\; (\overline{s}_L\gamma_\mu b_L)\sum_{q=u,d,s,c,b} Q_q(\bar{q}\gamma^\mu q)\,, \tag{A.88}$$

$$O_4^Q \;=\; (\overline{s}_L\gamma_\mu T^a b_L)\sum_{q=u,d,s,c,b} Q_q(\bar{q}\gamma^\mu T^a q)\,, \tag{A.89}$$

$$O_5^Q \;=\; (\overline{s}_L\gamma_\mu\gamma_\nu\gamma_\rho b_L)\sum_{q=u,d,s,c,b} Q_q(\bar{q}\gamma^\mu\gamma^\nu\gamma^\rho q)\,, \tag{A.90}$$

$$O_6^Q \;=\; (\overline{s}_L\gamma_\mu\gamma_\nu\gamma_\rho T^a b_L)\sum_{q=u,d,s,c,b} Q_q(\bar{q}\gamma^\mu\gamma^\nu\gamma^\rho T^a q)\,. \tag{A.91}$$

Including these opeartors, the effective coefficients are defined as [126, 127],

$$C_i^{eff}(\mu) \;=\; \begin{cases} C_i(\mu)\,, & \text{for } i \neq 7\gamma, 8g, \\ C_{7\gamma}(\mu) + \sum_{i=1}^{6} y_i\left[C_i(\mu) \quad \frac{1}{3}C_i^Q(\mu)\right], & \text{for } i = 7\gamma, \\ C_{8g}(\mu) + \sum_{i=1}^{6} z_i\left[C_i(\mu) \quad \frac{1}{3}C_i^Q(\mu)\right], & \text{for } i = 8g, \end{cases} \tag{A.92}$$

where $C_1^Q = C_2^Q = 0$ and $y_i = \;\; 0, 0, \;\; \frac{1}{3}, \;\; \frac{4}{9}, \;\; \frac{20}{3}, \;\; \frac{80}{8})$ and $z_i = \;\; 0, 0, 1, \;\; \frac{1}{6}, 20, \;\; \frac{10}{3})$ in the NDR scheme. One can find the leading order anomalous dimension matrix in Refs.[126, 127].

The tree level FCNC contribution comes from the diagram shown in Fig.A.3. The Wilson coefficients from this diagram are obtained as follows:

$$C_3^{\mathrm{NP}}(\mu_{\mathrm{EW}}) \;=\; \frac{1}{18}\cdot\frac{Z_{d\mathrm{NC}}^{sb}}{\lambda_{sb}^t}\,, \tag{A.93}$$

$$C_5^{\mathrm{NP}}(\mu_{\mathrm{EW}}) \;=\; \quad\frac{1}{72}\cdot\frac{Z_{d\mathrm{NC}}^{sb}}{\lambda_{sb}^t}\,, \tag{A.94}$$

$$C_3^{Q,\mathrm{NP}}(\mu_{\mathrm{EW}}) \;=\; \left(\frac{4}{3} \quad s_w^2\right)\cdot\frac{Z_{d\mathrm{NC}}^{sb}}{\lambda_{sb}^t}\,, \tag{A.95}$$

$$C_5^{Q,\mathrm{NP}}(\mu_{\mathrm{EW}}) \;=\; \quad\frac{1}{12}\cdot\frac{Z_{d\mathrm{NC}}^{sb}}{\lambda_{sb}^t}\,, \tag{A.96}$$

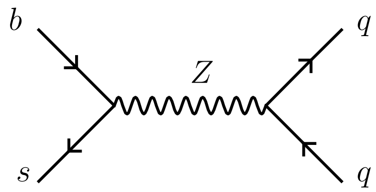

Figure A.3. The tree level FCNC contribution to the penguin operators.

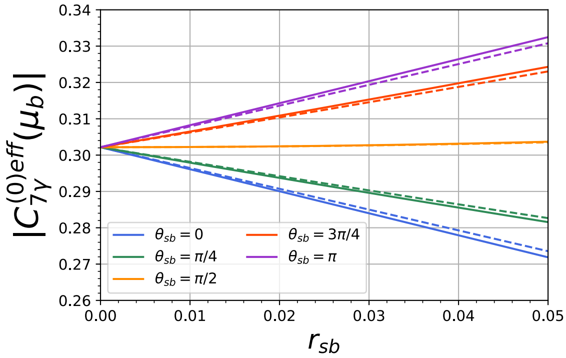

Figure A.4. The dependence of $\left|C_{7\gamma}^{(0)eff}(\mu_b = 5\text{ GeV})\right|$ on the parameter r_{sb} and θ_{sb}. The solid line is the value of $\left|C_{7\gamma}^{(0)eff}(\mu_b)\right|$ with taking the Wilson coefficients of the penguin operators shown in Eqs.(A.93)-(A.96). The dashed line is the value of $\left|C_{7\gamma}^{(0)eff}(\mu_b)\right|$ without the Wilson coefficients of the penguin operators shown in Eqs.(A.93)-(A.96). The different colors of the line represent to different values of the phase θ_{sb}. Here we set $\mu_b = 5$ GeV.

and the other Wilson coefficients of the penguin operators are zero at the tree level. We estimate effects of these new physics contributions. Since there is no SM contribution to the leading order Wilson coefficients of the penguin operators $C_i^{(0)}$ and $C_i^{Q(0)}$, we only take account of the new physics contributions $C_{3,5}^{\rm NP}$ and $C_{3,5}^{Q,\rm NP}$. After solving the RG equation, we obtain the effective Wilson coefficient $C_{7\gamma}^{(0)eff}(\mu_b)$:

$$\begin{aligned} C_{7\gamma}^{(0)eff}(5\text{ GeV}) &= 0.695\,C_{7\gamma}^{(0)eff}(M_W) + 0.086\,C_{8g}^{(0)eff}(M_W) \quad 0.158\,C_2^{(0)}(M_W) \\ &\quad +0.094\,C_3^{\rm NP}(M_W) + 2.099\,C_5^{\rm NP}(M_W) \\ &\quad +0.044\,C_3^{Q,\rm NP}(M_W) \quad 0.110\,C_5^{Q,\rm NP}(M_W)\,, \end{aligned} \tag{A.97}$$

where we set $\mu_b = 5$ GeV and $\alpha_s(M_Z) = 0.1179$ [65]. Figure A.4 shows the dependence of the absolute value of $C_{7\gamma}^{(0)eff}(\mu_b = 5\text{ GeV})$ on the parameter r_{sb} and θ_{sb}. The solid line is the value of $|C_{7\gamma}^{(0)eff}(\mu_b)|$ with taking the Wilson coefficients of the penguin operators shown in Eqs(A.93)-(A.96), that is Eq.(A.97). The dashed line is the value of $|C_{7\gamma}^{(0)eff}(\mu_b)|$ without the Wilson coefficients of the penguin operators shown in Eqs(A.93)-(A.96). The different colors of the line represent to different values of the phase θ_{sb}. One finds that the Wilson coefficients Eqs.(A.93)-(A.96) give rise to the $\mathcal{O}(10^{\;3})$ correction to the dependence of $|C_{7\gamma}^{(0)eff}(\mu_b)|$ on r_{sb}. In Chap.6, we neglect that modification since it is about ten times smaller than the leading order new physics contributions to the $C_{7\gamma}^{(0)eff}$.

Appendix B

CKM Unitarity Violation in $b \to s\gamma$

B.1 Amplitude of $b \to s\gamma$ without unitarity

In this section, we briefly show the computation of the amplitude of the $b \to s\gamma$ process. We focus on the diagrams which also exist in the SM. We do not use the CKM unitarity in contrast to the SM calculations [102]. The relevant diagrams are shown in Figs.B.1 and B.2. The Fig.B.1 shows the self-energy diagrams which contribute to counterterms for the $b \to s\gamma$ vertex. The diagrams for the $b \to s\gamma$ vertex are shown in Fig.B.2. Here we denote the up-type quark masses as m_i with $i = u, c, t$.

B.1.1 Master Formulae

$$
\begin{aligned}
I_1^{\mu}(p, p', q; m_i, M_W) &\equiv \int \frac{d^d k}{(2\pi)^d i} \frac{\not{p}' + \not{k} + m_i)\gamma^{\mu}(\not{p} + \not{k} + m_i)}{[(p+k)^2 \quad m^2][(p+k)^2 \quad m^2][k^2 \quad M_W^2]} \\
&= \frac{1}{16\pi^2}\left[\frac{1}{2}(1 \quad C_{\mathrm{UV}})\,\gamma^{\mu} + I_{ly}\gamma^{\mu} \quad \frac{\gamma^{\mu}}{M_W^2}\left\{\frac{q^2}{6} I_{3y} + \frac{p^2 + p'^2}{2}(I_{2y} \quad I_{3y})\right\}\right] \\
&\quad \frac{1}{16\pi^2}\left[x_i\, I_{1y}\gamma^{\mu} + \frac{m_i}{M_W^2}\{ \quad \gamma^{\mu}\not{p} + \not{p}'\gamma^{\mu})I_{1y} \quad (p+p')^{\mu} I_{2y}\right\} \\
&\quad + \frac{1}{M_W^2}\left\{\not{p}'\gamma^{\mu}\not{p}\,(I_{1y} \quad 2I_{2y} + I_{3y}) + \quad \not{p}'\gamma^{\mu}\not{q} \quad \not{q}\gamma^{\mu}\not{p})\frac{I_{2y} \quad I_{3y}}{2} \quad \frac{\not{q}\gamma^{\mu}\not{q}}{6} I_{3y}\right\}\Bigg] \\
&\quad \frac{1}{16\pi^2}\gamma^{\mu}\left\{ \quad \frac{q^2}{6 M_W^2} x_i \frac{\partial}{\partial x_i} I_{2y} \quad \frac{p'^2 + p^2}{2 M_W^2} x_i \frac{\partial}{\partial x_i}(I_{1y} \quad I_{2y})\right\}, \qquad \text{(B.1)}
\end{aligned}
$$

$$
\begin{aligned}
I_2^{\mu\nu}(p, p', q; m_i, M_W) &\equiv \int \frac{d^d k}{(2\pi)^d i} \frac{k^{\mu} k^{\nu}}{[k^2 \quad m_i^2][(p+k)^2 \quad M_W^2][(p'+k)^2 \quad M_W^2]} \\
&= \frac{g^{\mu\nu}}{64\pi^2}\left(C_{\mathrm{UV}} \quad \ln\frac{M_W^2}{\mu^2}\right) \quad \frac{g^{\mu\nu}}{32\pi^2} I_{yl}
\end{aligned}
$$

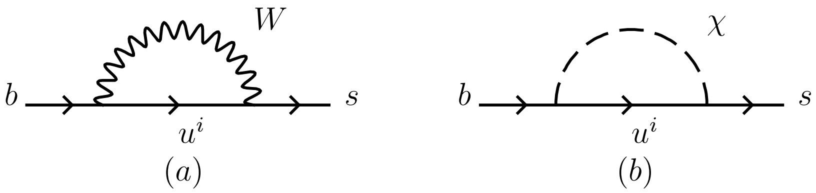

Figure B.1. Self-energy diagrams which contribute to counterterms for the $b \to s\gamma$ vertex. The symbol u^i with $i = 1, 2, 3$ represents the SM up-type quarks.

$$
\begin{aligned}
&+\frac{g^{\mu\nu}}{64\pi^2 M_W^2}\left\{\frac{q^2}{3}I_{y3} + (p^2 + p'^2)(I_{y2} \quad I_{y3})\right\} \\
&\quad \frac{1}{16\pi^2 M_W^2}\left\{\frac{1}{3}(p^\mu p^\nu + p'^\mu p'^\nu) + \frac{1}{6}(p^\mu p'^\nu + p^\nu p'^\mu)\right\} I_{y3}\,,
\end{aligned} \tag{B.2}
$$

$$
\begin{aligned}
I_3^\mu(p, p', q; m_i, M_W) &\equiv \int \frac{d^dk}{(2\pi)^d i}\frac{k^\mu}{[k^2 \quad m_i^2][(p+k)^2 \quad M_W^2][(p'+k)^2 \quad M_W^2]} \\
&= \frac{(p+p')^\mu}{32\pi^2 M_W^2} I_{y2}\,,
\end{aligned} \tag{B.3}
$$

$$
\begin{aligned}
I_4(p, p', q; m_i, M_W) &= \int \frac{d^dk}{(2\pi)^d i}\frac{1}{[k^2 \quad m_i^2][(p+k)^2 \quad M_W^2][(p'+k)^2 \quad M_W^2]} \\
&= \quad \frac{1}{16\pi^2 M_W^2} I_{y1} \quad \frac{1}{32\pi^2 M_W^2}\left\{\frac{q^2}{3M_W^2}I'_{y3} + \frac{p^2 + p'^2}{M_W^2}(I'_{y2} \quad I'_{y3})\right\},
\end{aligned} \tag{B.4}
$$

where $x_i \equiv m_i^2 / M_W^2$, $C_{\mathrm{UV}} = \frac{2}{\eta} \quad \gamma + \ln 4\pi$ with $d = 4 \quad \eta$ and

$$
I_{ny} = \int_0^1 dy\, \frac{y^n}{x_i y + 1 \quad y}\,, \tag{B.5}
$$

$$
I_{ly} = \int_0^1 dy\, y \ln[m^2 y + M^2(1 \quad y)]\,, \tag{B.6}
$$

$$
I_{yl} \equiv \int_0^1 dy\, y \ln[y + x_i(1 \quad y)]\,, \tag{B.7}
$$

$$
I_{yn} \equiv \int_0^1 dy\, \frac{y^n}{y + x_i(1 \quad y)}\,, \tag{B.8}
$$

$$
I'_{yn} \equiv \int_0^1 dy\, \frac{y^n}{[y + x_i(1 \quad y)]^2}\,. \tag{B.9}
$$

B.1.2 Wavefunction renormalization for quark fields

The QED Lagrangian with the bare down-type quark fields is,

$$
\mathcal{L}_d^Q = \overline{d_L^{0i}}(i\partial\!\!\!/ \quad eQ_d A\!\!\!/)d_L^{0i} + \overline{d_R^{0i}}(i\partial\!\!\!/ \quad eQ_d A\!\!\!/)d_R^{0i} \quad \overline{d_L^{0i}}\, m_d^{0i} d_R^{0i} \quad \overline{d_R^{0i}}\, m_d^{0i} d_L^{0i}\,. \tag{B.10}
$$

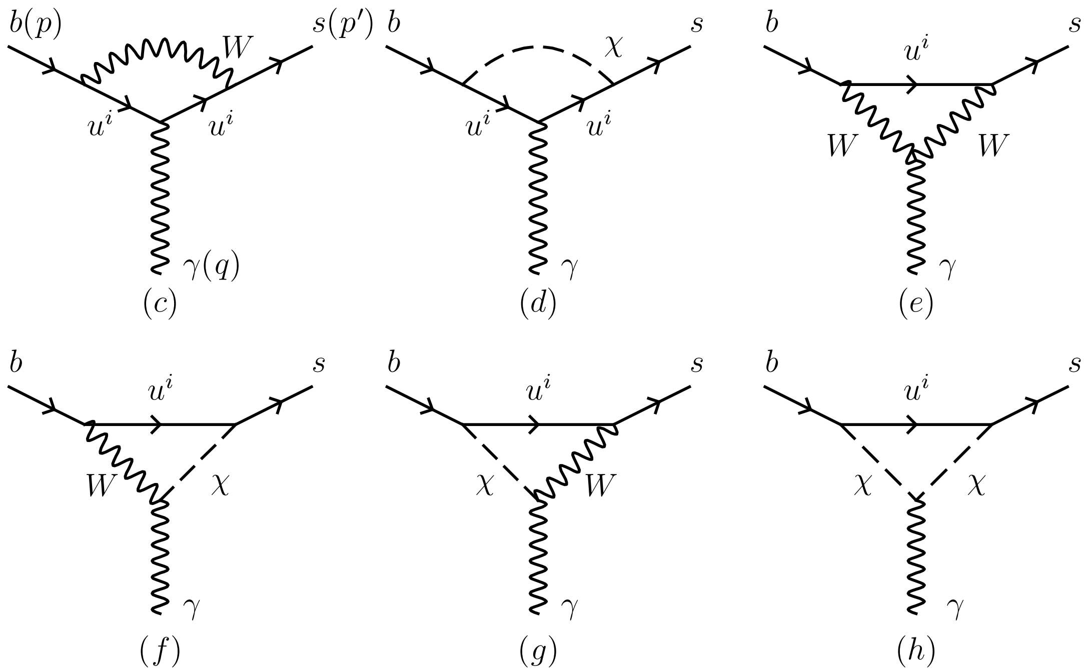

Figure B.2. The diagrams for the $b \to s\gamma$ vertex in the SM. The symbols p, p' and q denote the momentum of the b-quark, s-quark and photon, respectively. The symbol u^i with $i = 1, 2, 3$ represents the SM up-type quarks.

where index $i = 1, 2$ and 3 corresponds to the d-, s- and b-quark, respectively. The subscript "0" means bare quantities. We define the wave function renormalization constant for the down-type quark fields:

$$d_L^{0i} = \sqrt{Z_L}^{ij} d_L^j \,, \tag{B.11}$$

$$d_R^{0i} = \sqrt{Z_R}^{ij} d_R^j \,. \tag{B.12}$$

The quantities without the subscript "0" are renormalized quantities. The other renormalization constants, such as the wave function renormalization of the photon field, do not lead to the flavor changing counterterms. Therefore, it is sufficient to take account of only the renormalization of the down-type quark fields in our calculations. We obtain counterterms by inserting Eqs.(B.11) and (B.12) into Eq.(B.10):

$$\begin{aligned} \mathcal{L}_d^Q \;=\; & \bar{d}_L^j \,(i\not\partial \quad eQ_d \not{A}) d_L^j + \bar{d}_R^j \,(i\not\partial \quad eQ_d \not{A})\, d_R^j \quad \bar{d}_L^j \, m_d^j \, d_R^j \quad \bar{d}_R^j \, m_d^j \, d_L^j \\ & + \bar{d}_L^j \,(\sqrt{Z_L}^{\dagger ji} \sqrt{Z_L}^{ik} \quad \delta^{jk})\, i\not\partial \, d_L^k + \bar{d}_R^j (\sqrt{Z_R}^{\dagger ji} \sqrt{Z_R}^{ik} \quad \delta^{jk}) i\not\partial \, d_R^k \\ & \quad \bar{d}_L^j \,(\sqrt{Z_L}^{\dagger ji} \, m_d^{0i} \sqrt{Z_R}^{ik} \quad m_d^j \, \delta^{jk}) d_R^k \quad \bar{d}_R^j \,(\sqrt{Z_R}^{\dagger ji} \, m_d^{0i} \sqrt{Z_L}^{ik} \quad m_d^j \, \delta^{jk}) d_L^k \\ & \quad eQ_d \, \bar{d}_L^j \,(\sqrt{Z_L}^{\dagger ji} \sqrt{Z_L}^{ik} \quad \delta^{jk}) \not{A} d_L^k \quad eQ_d \, \bar{d}_R^j (\sqrt{Z_R}^{\dagger ji} \sqrt{Z_R}^{ik} \quad \delta^{jk}) \not{A} \, d_R^k \,. \end{aligned} \tag{B.13}$$

The off-diagonal part of the counterterms is given as,

$$\begin{aligned} \Sigma_{\text{count.}}^{ij}(p) \;=\; & (\sqrt{Z_L}^{\dagger} \sqrt{Z_L})^{ij} \not{p} L + (\sqrt{Z_R}^{\dagger} \sqrt{Z_R})^{ij} \not{p} R \\ & (\sqrt{Z_L}^{\dagger} \, m_d^0 \sqrt{Z_R})^{ij} R \quad (\sqrt{Z_R}^{\dagger} \, m_d^0 \sqrt{Z_L})^{ij} L \,, \end{aligned} \tag{B.14}$$

$${}^{\mu,ij}_{\text{count.}} \;=\; \quad eQ_d \,(\sqrt{Z_L}^{\dagger} \sqrt{Z_L})^{ij} \gamma^\mu L \quad eQ_d \,(\sqrt{Z_R}^{\dagger} \sqrt{Z_R})^{ij} \gamma^\mu R \,, \tag{B.15}$$

with $i \neq j$. The renormalization constants $\sqrt{Z_L}$ and $\sqrt{Z_R}$ are determined so as to remove the divergence in the amplitudes of the self-energy diagrams. We parametrize the amplitudes of the self-energy diagrams as,

$$\Sigma^{sb}(p) \;=\; A^{sb}_{\mathrm{LL}}(p^2)\not{p}L + A^{sb}_{\mathrm{RR}}(p^2)\not{p}R + A^{sb}_{\mathrm{LR}}(p^2)R + A^{sb}_{\mathrm{RL}}(p^2)L\,, \tag{B.16}$$

where the functions A^{sb}_{LL}, A^{sb}_{RR}, A^{sb}_{LR} and A^{sb}_{RL} can be obtained by computing the amplitudes of the self-energy diagrams shown in Fig.B.1. Adding the counterterm $\Sigma^{sb}_{\mathrm{count.}}$ to Σ^{sb}, we obtain the renormalized amplitude of the self-energy diagrams:

$$\begin{aligned}\Sigma^{sb}_{\mathrm{ren.}}(p) \;&=\; \Sigma^{sb}(p) + \Sigma^{sb}_{\mathrm{count.}}(p)\\ &=\; \{A^{sb}_{\mathrm{LL}}(p^2) + (\sqrt{Z_L}^{\dagger}\sqrt{Z_L})^{sb}\}\not{p}L + \{A^{sb}_{\mathrm{RR}}(p^2) + (\sqrt{Z_R}^{\dagger}\sqrt{Z_R})^{sb}\}\not{p}R\\ &\quad +\{A^{sb}_{\mathrm{LR}}(p^2) - (\sqrt{Z_L}^{\dagger}\, m^0_d\sqrt{Z_R})^{sb}\}R + \{A^{sb}_{\mathrm{RL}}(p^2) - (\sqrt{Z_R}^{\dagger}\, m^0_d\sqrt{Z_L})^{sb}\}L\,.\end{aligned} \tag{B.17}$$

The functions A^{sb}_{LL}, A^{sb}_{RR}, A^{sb}_{LR} and A^{sb}_{RL} contain divergence. There are some freedom of how to subtract the divergence in these functions. Here we impose the on-shell renormalization conditions [111]:

$$\{\not{p} - m_b + \Sigma^{sb}_{\mathrm{ren.}}(p)\}u_b(p) \;=\; 0\,, \quad \text{with: } \not{p}u_b(p) = m_b u_b(p),\ \text{and } p^2 = m_b^2\,, \tag{B.18}$$

$$\bar{u_s}(p)\{\not{p} - m_s + \Sigma^{sb}_{\mathrm{ren.}}(p)\} \;=\; 0\,, \quad \text{with: } \bar{u_s}(p)\not{p} = m_s\bar{u_s}(p),\ \text{and } p^2 = m_s^2\,, \tag{B.19}$$

where $u_b(p)$ and $\bar{u_s}(p)$ denote the spinor of the b- and s-quark, respectively. Inserting Eq.(B.17) into these conditions, we obtain expressions of the renormalization constants in terms of the functions A^{sb}_{LL}, A^{sb}_{RR}, A^{sb}_{LR} and A^{sb}_{RL}:

$$\begin{aligned}\sqrt{Z_L}^{\dagger}\sqrt{Z_L} \;&=\; \frac{1}{m_b^2 - m_s^2}[A_{\mathrm{LL}}(m_b^2)m_b^2 - A_{\mathrm{LL}}(m_s^2)m_s^2 + \{A_{\mathrm{RR}}(m_b^2) - A_{\mathrm{RR}}(m_s^2)\}m_b m_s\\ &\quad +\{A_{\mathrm{LR}}(m_b^2) - A_{\mathrm{LR}}(m_s^2)\}m_b + \{A_{\mathrm{RL}}(m_b^2) - A_{\mathrm{RL}}(m_s^2)\}m_s]\,,\end{aligned} \tag{B.20}$$

$$\begin{aligned}\sqrt{Z_R}^{\dagger}\sqrt{Z_R} \;&=\; \frac{1}{m_b^2 - m_s^2}[A_{\mathrm{RR}}(m_b^2)m_b^2 - A_{\mathrm{RR}}(m_s^2)m_s^2 + \{A_{\mathrm{LL}}(m_b^2) - A_{\mathrm{LL}}(m_s^2)\}m_b m_s\\ &\quad +\{A_{\mathrm{RL}}(m_b^2) - A_{\mathrm{RL}}(m_s^2)\}m_b + \{A_{\mathrm{LR}}(m_b^2) - A_{\mathrm{LR}}(m_s^2)\}m_s]\,.\end{aligned} \tag{B.21}$$

We calculate the amplitudes of the sefl-energy diagrams in Fig.B.1 to determine the functions A^{sb}_{LL}, A^{sb}_{RR}, A^{sb}_{LR} and A^{sb}_{RL}.

B.1.3 Self-energy diagrams and counterterms

We define the loop integral,

$$\begin{aligned}I_{\mathrm{self}}(p; m_i, M_W) \;&\equiv\; \int \frac{d^dk}{(2\pi)^d i}\cdot\frac{1}{[\not{p} + \not{k} - m_i][k^2 - M_W^2]}\\ &=\; \frac{1}{16\pi^2}\left(\frac{\not{p}}{2} + m_i\right)C_{\mathrm{UV}} - \frac{1}{16\pi^2}\int_0^1 dz\,\{\not{p}(1 - z) + m_i\}\ln s^2\,,\end{aligned} \tag{B.22}$$

with

$$s^2(p^2) \equiv -p^2 z(1-z) + M_W^2(1-z) + m_i^2 z\,. \tag{B.23}$$

The amplitude of the diagram (a) in Fig.B.1 is given as,

$$\begin{aligned}\Sigma_W^{sb}(p) &= \left(-i\frac{g}{\sqrt{2}}\gamma^\mu L V_{is}^*\right) i\cdot(-i g_{\mu\nu})\, I_{\rm self}(p;m_i,M_W)\left(-i\frac{g}{\sqrt{2}}\gamma^\nu L V_{ib}\right)\\ &= \frac{g^2}{32\pi^2}\lambda_{sb}^i\left\{C_{\rm UV}-1-2\int_0^1 dz(1-z)\ln s^2(p^2)\right\}\not{p}L\,,\end{aligned} \tag{B.24}$$

where $\lambda_{sb}^i \equiv V_{is}^* V_{ib}$. The amplitude of the diagram (b) in Fig.B.1 is,

$$\begin{aligned}\Sigma_\chi^{sb}(p) &= \left\{i\frac{g}{\sqrt{2}M_W}(m_i R - m_s L)V_{is}^*\right\} i\cdot i\, I_{\rm self}\left\{i\frac{g}{\sqrt{2}M_W}(m_i L - m_b R)V_{ib}\right\}\\ &= \frac{g^2}{32\pi^2 M_W^2}\lambda_{sb}^i\left\{\frac{1}{2}C_{\rm UV}-\int_0^1 dz\,(1-z)\ln s^2(p^2)\right\}\not{p}(m_i^2 L + m_s m_b R)\\ &\quad +\frac{g^2}{32\pi^2 M_W^2}\lambda_{sb}^i\left\{-C_{\rm UV}+\int_0^1 dz\ln s^2(p^2)\right\}(m_b R + m_s L)m_i^2\,.\end{aligned} \tag{B.25}$$

The total amplitude of the self-energy is obtained as follows:

$$\begin{aligned}\Sigma^{sb}(p) &\equiv \Sigma_W^{sb}(p)+\Sigma_\chi^{sb}(p)\\ &= \frac{g^2}{32\pi^2}\lambda_{sb}^i\left\{C_{\rm UV}\left(1+\frac{m_i^2}{2M_W^2}\right)-1-2\left(1+\frac{m_i^2}{2M_W^2}\right)\int_0^1 dz(1-z)\ln s^2(p^2)\right\}\not{p}L\\ &\quad +\frac{g^2}{32\pi^2}\lambda_{sb}^i\left\{\frac{m_s m_b}{M_W^2}\left(\frac{1}{2}C_{\rm UV}-\int_0^1 dz\,(1-z)\ln s^2(p^2)\right)\right\}\not{p}R\\ &\quad +\frac{g^2}{32\pi^2}\lambda_{sb}^i\left\{-C_{\rm UV}+\int_0^1 dz\ln s^2(p^2)\right\}\frac{m_i^2}{M_W^2}m_b R\\ &\quad +\frac{g^2}{32\pi^2}\lambda_{sb}^i\left\{-C_{\rm UV}+\int_0^1 dz\ln s^2(p^2)\right\}\frac{m_i^2}{M_W^2}m_s L\,.\end{aligned} \tag{B.26}$$

The functions $A_{\rm LL}^{sb}$, $A_{\rm RR}^{sb}$, $A_{\rm LR}^{sb}$ and $A_{\rm RL}^{sb}$ are determined as,

$$A_{\rm LL}^{sb}(p^2) = \frac{g^2}{32\pi^2}\lambda_{sb}^i\left\{C_{\rm UV}\left(1+\frac{x_i}{2}\right)-1-2\left(1+\frac{x_i}{2}\right)\int_0^1 dz(1-z)\ln s^2(p^2)\right\}, \tag{B.27}$$

$$A_{\rm RR}^{sb}(p^2) = \frac{g^2}{32\pi^2}\lambda_{sb}^i\left\{\frac{m_s m_b}{M_W^2}\left(\frac{1}{2}C_{\rm UV}-\int_0^1 dz\,(1-z)\ln s^2(p^2)\right)\right\}, \tag{B.28}$$

$$A_{\rm LR}^{sb}(p^2) = \frac{g^2}{32\pi^2}\lambda_{sb}^i\left\{-C_{\rm UV}+\int_0^1 dz\ln s^2(p^2)\right\}x_i m_b\,, \tag{B.29}$$

$$A_{\rm RL}^{sb}(p^2) = \frac{g^2}{32\pi^2}\lambda_{sb}^i\left\{-C_{\rm UV}+\int_0^1 dz\ln s^2(p^2)\right\}x_i m_s\,. \tag{B.30}$$

We then abtain the renormalization constants by using Eqs.(B.20) and (B.21):

$$\sqrt{Z_L}^\dagger\sqrt{Z_L} = \frac{g^2}{32\pi^2}\lambda_{sb}^i\Big[\left\{C_{\rm UV}\left(1+\frac{x_i}{2}\right)-1\right\}-\left(1+\frac{x_i}{2}\right)\ln\left[\frac{M_W^2}{\mu^2}\right]$$

$$
\begin{aligned}
& 2\Big(1+\frac{x_i}{2}\Big)\int_0^1 dy\,(1 \quad y)\ln[(1 \quad y)+x_i y] \\
& +\frac{m_b^2+m_s^2}{M_W^2}\{2(I_{1y} \quad 2I_{2y}+I_{3y}) \quad x_i(I_{2y} \quad I_{3y})\}\Bigg], \qquad \text{(B.31)}
\end{aligned}
$$

$$
\begin{aligned}
\sqrt{Z_R}^{\dagger}\sqrt{Z_R} \;=\; & \frac{g^2}{32\pi^2}\lambda_{sb}^i\Bigg[\frac{m_s m_b}{M_W^2}\Bigg\{\frac{1}{2}C_{\rm UV} \quad \frac{1}{2}\ln\Bigg[\frac{M_W^2}{\mu^2}\Bigg] \quad \int_0^1 dy\,(1 \quad y)\ln[(1 \quad y)+x_i y]\Bigg\} \\
& +\frac{m_b m_s}{M_W^2}\{2(I_{1y} \quad 2I_{2y}+I_{3y}) \quad x_i(I_{1y} \quad I_{3y})\}\Bigg]. \qquad \text{(B.32)}
\end{aligned}
$$

Finally the counterterm for the $b \to s\gamma$ vertex $^{\mu,sb}_{\rm count.}$ in Eq.(B.15) is given as follows:

$$
\begin{aligned}
{}^{\mu,sb}_{\rm count.} \;=\; & eQ_d\,(\sqrt{Z_L}^{\dagger}\sqrt{Z_L})^{sb}\gamma^\mu L \quad eQ_d\,(\sqrt{Z_R}^{\dagger}\sqrt{Z_R})^{sb}\gamma^\mu R \\
=\; & \frac{g^2 eQ_d}{32\pi^2}\lambda_{sb}^i\Bigg[\Bigg(C_{\rm UV} \quad \ln\frac{M_W^2}{\mu^2}\Bigg)\Bigg\{\Big(1+\frac{x_i}{2}\Big)\gamma^\mu L+\frac{m_s m_b}{2M_W^2}\gamma^\mu R\Bigg\} \\
& +\Bigg\{ \quad 1 \quad 2\Big(1+\frac{x_i}{2}\Big)\int_0^1 dy\,(1 \quad y)\ln[(1 \quad y)+x_i y]\Bigg\}\gamma^\mu L \\
& +\frac{m_s m_b}{M_W^2}\,\gamma^\mu R\Bigg\{2(I_{1y} \quad 2I_{2y}+I_{3y}) \quad x_i(I_{1y} \quad I_{3y}) \quad \int_0^1 dz\,(1 \quad y)\ln[(1 \quad y)+x_i y]\Bigg\} \\
& +\frac{m_b^2+m_s^2}{M_W^2}\gamma^\mu L\{2(I_{1y} \quad 2I_{2y}+I_{3y}) \quad x_i(I_{2y} \quad I_{3y})\}\Bigg]. \qquad \text{(B.33)}
\end{aligned}
$$

Since $Q_d = \quad \frac{1}{3} = Q_u + Q_W$ with $Q_W = \quad 1$, we separate the counterterm $^{\mu,sb}_{\rm count.}$ into the terms which are proportional to Q_u and the terms which are proportional to Q_W:

$$
{}^{\mu,sb}_{\rm count.} \;=\; {}^{\mu,sb}_{c,Q_u} + {}^{\mu,sb}_{c,Q_W}\,. \qquad \text{(B.34)}
$$

B.1.4 $b \to s\gamma$ amplitudes at one-loop level

We show the result of the amplitude for the diagrams in Fig.B.2. We define $q = p \quad p'$.

$$
\begin{aligned}
{}^{(c)}_{\rho} \;=\; & \frac{g^2}{2}eQ_u\lambda_{sb}^i\,\gamma^\mu L\,I_{1\rho}(p,p',q;m_i,M_W)\gamma_\mu L \\
=\; & \frac{g^2 eQ_u\lambda_{sb}^i}{32\pi^2}\Bigg[\{ \quad (C_{\rm UV} \quad 2)+2(I_{ly} \quad x_i\,I_{1y})\}\gamma_\rho L \\
& +\Bigg\{\frac{q^2}{M_W^2}\Bigg(\frac{x_i}{3}\frac{\partial}{\partial x_i}I_{2y} \quad \frac{2}{3}I_{3y} \quad 2(I_{1y} \quad I_{2y})\Bigg)+\frac{m_b^2+m_s^2}{M_W^2}\Bigg(x_i\frac{\partial}{\partial x_i}(I_{1y} \quad I_{2y}) \quad I_{2y}+I_{3y}\Bigg)\Bigg\}\gamma_\rho L \\
& 2(I_{1y} \quad 2I_{2y}+I_{3y})\frac{m_s m_b\gamma_\rho R}{M_W^2} \quad (2I_{1y} \quad 3I_{2y}+I_{3y})\frac{1}{2M_W^2}[\not{q},\gamma_\rho](m_b R+m_s L) \\
& +\Bigg(2I_{1y} \quad I_{2y} \quad \frac{1}{3}I_{3y}\Bigg)\frac{q_\rho\not{q}}{M_W^2}L\Bigg], \qquad \text{(B.35)}
\end{aligned}
$$

$$
{}^{(d)}_{\rho} \;=\; eQ_u\frac{g^2}{2M_W^2}V_{is}^*V_{ib}(m_i R \quad m_s L)\,I_{1\rho}(p,p',q;m_i,M_W)(m_i L \quad m_b R)
$$

$$
\begin{aligned}
= \; & \frac{eQ_u g^2 \lambda^i_{sb}}{32\pi^2}\Bigg[x_i\Bigg\{\frac{1}{2}(1 \quad C_{\mathrm{UV}}) + (I_{ly} \quad x_i I_{1y})\Bigg\}\gamma_\rho L \quad \frac{m_s m_b}{2M_W^2}C_{\mathrm{UV}}\gamma_\rho R \\
& + \frac{m_b^2 + m_s^2}{M_W^2}\gamma_\rho L\Bigg\{\frac{x_i}{2}(2I_{1y} \quad 3I_{2y} + I_{3y}) + \frac{x_i^2}{2}\frac{\partial}{\partial x_i}(I_{1y} \quad I_{2y})\Bigg\} \\
& + \frac{m_s m_b}{M_W^2}\gamma_\rho R\Bigg\{\frac{1}{2} \quad x_i I_{3y} + I_{ly}\Bigg\} \quad \frac{x_i}{4M_W^2}[\not{q}, \gamma_\rho](m_b R + m_s L)(I_{2y} + I_{3y}) \\
& + \frac{q^2}{M_W^2}\gamma_\rho L\Bigg\{ \quad \frac{x_i}{3}I_{3y} + \frac{x_i^2}{6}\frac{\partial}{\partial x_i}I_{2y}\Bigg\} + \frac{q_\rho \not{q}}{M_W^2}L\Bigg\{\frac{x_i}{2}I_{2y} \quad \frac{x_i}{6}I_{3y}\Bigg\}\Bigg],
\end{aligned}
\tag{B.36}
$$

$$
\begin{aligned}
{}^{(e)}_{\rho} = \; & \int \frac{d^D k}{(2\pi)^D i}\Bigg(\quad i\frac{g}{\sqrt{2}}\gamma_\mu L V_{is}^*\Bigg)\frac{i}{\not{k} \quad m_i}\Bigg(\quad i\frac{g}{\sqrt{2}}\gamma_\nu L V_{ib}\Bigg)\frac{i g^{\mu\alpha}}{(p'+k)^2 \quad M_W^2}\frac{i g^{\nu\beta}}{(p+k)^2 \quad M_W^2} \\
& \times i e[g_{\alpha\rho}(p' \quad p + p' + k)_\beta + g_{\alpha\beta}\{ \quad p' \quad k \quad (p+k)\}_\rho + g_{\beta\rho}\{p + k \quad (p' \quad p)\}_\alpha] \\
= \; & \frac{g^2}{32\pi^2}e\lambda^i_{sb}\Bigg[(3C_{\mathrm{UV}} \quad 2 \quad 3\ln M_W^2)\gamma_\rho L \quad 6I_{yl}\gamma_\rho L + \frac{m_b^2 + m_s^2}{M_W^2}(5I_{y2} \quad 5I_{y3})\gamma_\rho L \\
& + \frac{q^2}{M_W^2}\Bigg(\frac{4}{3}I_{y3} \quad 2I_{y2}\Bigg)\gamma_\rho L + \frac{\not{q} q_\rho}{M_W^2}\Bigg(\frac{2}{3}I_{y3} + 2I_{y2}\Bigg)L + \frac{2m_s m_b}{M_W^2}(I_{y2} \quad I_{y3})\gamma_\rho R \\
& \quad \frac{\not{q}\gamma_\rho m_b R \quad m_s \gamma_\rho \not{q} L}{M_W^2}\Bigg(\frac{1}{2}I_{y2} + I_{y3}\Bigg)\Bigg],
\end{aligned}
\tag{B.37}
$$

$$
\begin{aligned}
{}^{(f)}_{\rho} = \; & \int \frac{d^d k}{(2\pi)^d i}\Bigg(\quad i\frac{g}{\sqrt{2}}\gamma_\mu L V_{is}^*\Bigg)\frac{i}{\not{k} \quad m_i}\Bigg\{i\frac{g}{\sqrt{2}M_W}(m_i L \quad m_b R)V_{ib}\Bigg\} \\
& \times \frac{i g^{\mu\alpha}}{(p'+k)^2 \quad M_W^2} i e M_W g_{\alpha\rho}\frac{i}{(p+k)^2 \quad M_W^2} \\
= \; & \frac{g^2}{32\pi^2}e\lambda^i_{sb}\Bigg[x_i I_{y1}\gamma_\rho L + \frac{x_i}{2}\Bigg\{\frac{q^2}{3M_W^2}I'_{y3} + \frac{m_b^2 + m_s^2}{M_W^2}(I'_{y2} \quad I'_{y3})\Bigg\}\gamma_\rho L \\
& \quad \frac{1}{2M_W^2}I_{y2}(2m_b^2\gamma_\rho L \quad 2q_\rho \not{p} L + m_b \not{q}\gamma_\rho R)\Bigg],
\end{aligned}
\tag{B.38}
$$

$$
\begin{aligned}
{}^{(g)}_{\rho} = \; & \int \frac{d^d k}{(2\pi)^d i}\Bigg\{i\frac{g}{\sqrt{2}M_W}(m_i R \quad m_s L)V_{is}^*\Bigg\}\frac{i}{\not{k} \quad m_i}\Bigg(\quad i\frac{g}{\sqrt{2}}\gamma_\mu L V_{ib}\Bigg) \\
& \times \frac{i}{(p'+k)^2 \quad M_W^2} i e M_W g_{\alpha\rho}\frac{i g^{\mu\alpha}}{(p+k)^2 \quad M_W^2} \\
= \; & \frac{g^2}{32\pi^2}e\lambda^i_{sb}\Bigg[x_i I_{y1}\gamma_\rho L + \frac{x_i}{2}\Bigg\{\frac{q^2}{3M_W^2}I'_{y3} + \frac{m_b^2 + m_s^2}{M_W^2}(I'_{y2} \quad I'_{y3})\Bigg\}\gamma_\rho L \\
& \quad \frac{1}{2M_W^2}I_{y2}(2m_s^2\gamma_\rho L + 2q_\rho \not{p}' L \quad m_s\gamma_\rho \not{q} L)\Bigg],
\end{aligned}
\tag{B.39}
$$

$$
\begin{aligned}
{}^{(h)}_{\rho} = \; & \int \frac{d^d k}{(2\pi)^d i}\Bigg\{i\frac{g}{\sqrt{2}M_W}(m_i R \quad m_s L)V_{is}^*\Bigg\}\frac{i}{\not{k} \quad m_i}\Bigg\{i\frac{g}{\sqrt{2}M_W}(m_i L \quad m_b R)V_{ib}\Bigg\} \\
& \times i e\{(p+k) + (p'+k)\}_\rho \frac{i}{(p'+k)^2 \quad M_W^2}\frac{i}{(p+k)^2 \quad M_W^2} \\
= \; & \frac{g^2}{32\pi^2}e\lambda^i_{sb}\Bigg[\frac{1}{2}(C_{\mathrm{UV}} \quad \ln M_W^2)\gamma_\rho\Bigg(x_i L + \frac{m_b m_s}{M_W^2}R\Bigg) \quad I_{yl}\gamma_\rho\Bigg(x_i L + \frac{m_b m_s}{M_W^2}R\Bigg) \\
& + \frac{x_i}{6M_W^2}q^2 I_{y3}\gamma_\rho L + \frac{x_i}{2M_W^2}(m_b^2 + m_s^2)(\quad 2I_{y1} + 4I_{y2} \quad 2I_{y3})\gamma_\rho L
\end{aligned}
$$

$$
\begin{aligned}
&+x_i(\;\;2I_{y1}+3I_{y2}\quad I_{y3})\left\{\frac{m_s m_b}{M_W^2}\gamma_\rho R+\frac{1}{2M_W^2}[m_b \not{q}\gamma_\rho R\quad m_s\gamma_\rho\not{q}L]\right\}\\
&+x_i\left(\frac{1}{3}I_{y3}\quad\frac{3}{2}I_{y2}+I_{y1}\right)\frac{\not{q}q_\rho}{M_W^2}L\Bigg],
\end{aligned}
\tag{B.40}
$$

where we used the on-shell relations,

$$
\not{p}u_b(p)=m_b u_b(p),\qquad p^2=m_b^2\,,
\tag{B.41}
$$

$$
\bar{u_s}(p')\not{p}'=m_s\bar{u_s}(p'),\qquad p'^2=m_s^2\,.
\tag{B.42}
$$

We sum up these amplitudes in addition to the counterterms in Eq.(B.34). Here we separate sum into two parts, $\sum_{x=c,d}\,{}^{(x)}_{\rho}+\,{}^{\mu,sb}_{c,Q_u}$ and $\sum_{x=e\sim h}\,{}^{(x)}_{\rho}+\,{}^{\mu,sb}_{c,Q_W}$. Taking account of the sum with respect to the up-typq quarks, we obtain,

$$
\begin{aligned}
&\sum_{i=u,c,t}\left[\sum_{x=c,d}\,{}^{(x)}_{\rho}+\,{}^{\mu,sb}_{c,Q_u}\right]\\
=\;&\frac{g^2eQ_u}{32\pi^2M_W^2}\sum_{i=u,c,t}\lambda_{sb}^i\left[(q^2g_{\rho\nu}\quad q_\rho q_\nu)\gamma^\nu L\frac{f_u'(x_i)}{2}+[\not{q},\gamma_\rho](m_bR+m_sL)\frac{F_u'(x_i)}{2}\right],
\end{aligned}
\tag{B.43}
$$

$$
\begin{aligned}
&\sum_{i=u,c,t}\left[\sum_{x=e\sim h}\,{}^{(x)}_{\rho}+\,{}^{\mu,sb}_{c,Q_W}\right]\\
=\;&\frac{g^2e}{32\pi^2}\sum_{i=u,c,t}\lambda_{sb}^i\Bigg[2\left(C_{\rm UV}\quad\ln\frac{M_W^2}{\mu^2}\right)\gamma_\rho L\\
&+\frac{1}{2M_W^2}\{q^2\gamma_\rho f_W^{(1)\prime}(x_i)+\not{q}q_\rho f_W^{(2)\prime}(x_i)\}L+\frac{1}{M_W^2}[\not{q},\gamma_\rho](m_bR+m_sL)\frac{F_W'(x_i)}{2}\Bigg],
\end{aligned}
\tag{B.44}
$$

where the functions $f_u'(x_i)$, $F_u'(x_i)$, $f_W^{(1)\prime}(x_i)$, $f_W^{(2)\prime}(x_i)$ and $F_W'(x_i)$ are defined as,

$$
f_u'(x_i)\;\equiv\;\frac{4+38x_i\quad 63x_i^2+14x_i^3+7x_i^4\quad 6(4\quad 16x_i+9x_i^2)\ln x_i}{18(x_i\quad 1)^4},
\tag{B.45}
$$

$$
F_u'(x_i)\;\equiv\;\frac{8+38x_i\quad 39x_i^2+14x_i^3\quad 5x_i^4+18x_i^2\ln x_i}{12(x_i\quad 1)^4},
\tag{B.46}
$$

$$
f_W^{(1)\prime}(x_i)\;\equiv\;\frac{20+116x_i\quad 153x_i^2+56x_i^3+x_i^4+6x_i^2(12\quad 10x_i+x_i^2)\ln x_i}{18(x_i\quad 1)^4},
\tag{B.47}
$$

$$
f_W^{(2)\prime}(x_i)\;\equiv\;\frac{32\quad 164x_i+225x_i^2\quad 104x_i^3+11x_i^4\quad 6x_i^2(12\quad 10x_i+x_i^2)\ln x_i}{18(x_i\quad 1)^4},
\tag{B.48}
$$

$$
F_W'(x_i)\;\equiv\;\frac{10\quad 43x_i+78x_i^2\quad 49x_i^3+4x_i^4+18x_i^3\ln x_i}{12(x_i\quad 1)^4}.
\tag{B.49}
$$

It is clear that there remain the divergence in Eq.(B.44) even though we add the counterterms obtained from the wavefunction renormalization of the quark fields. In the case of the SM where the CKM unitarity holds, the remaining divergence in Eq.(B.44) vanishes by using the CKM unitarity relation $\sum_{i=u,c,t}\lambda_{sb}^i=0$.

B.1.4.1 With CKM unitarity → SM case

When we use the CKM unitarity relation $\sum_{i=u,c,t} \lambda_{sb}^i = 0$, we obtain the amplitudes in the case of the SM:

$$
\begin{aligned}
&\sum_{i=u,c,t}\left[\sum_{x=c,d} \quad {}_{\rho}^{(x)} + \quad {}_{c,Q_u}^{\mu,sb}\right]_{\text{SM}} \\
&= \frac{g^2}{32\pi^2} e Q_u \sum_{i=c,t} \lambda_{sb}^i \left[\frac{\gamma^\nu L}{M_W^2}(q^2 g_{\rho\nu} \quad q_\rho q_\nu)\frac{f_u(x_i)}{2} + \frac{1}{M_W^2}[\not{q}, \gamma_\rho](m_b R + m_s L)\frac{F_u(x_i)}{2}\right],
\end{aligned}
\tag{B.50}
$$

$$
\begin{aligned}
&\sum_{i=u,c,t}\left[\sum_{x=e\sim h} \quad {}_{\rho}^{(x)} + \quad {}_{c,Q_W}^{\mu,sb}\right]_{\text{SM}} \\
&= \frac{g^2}{32\pi^2} e \sum_{i=c,t} \lambda_{sb}^i \left[\frac{1}{M_W^2}(q^2 g_{\rho\nu} \quad q_\rho q_\nu)\gamma^\nu L \frac{f_W(x_i)}{2} + \frac{1}{M_W^2}[\not{q}, \gamma_\rho](m_b R + m_s L)\frac{F_W(x_i)}{2}\right],
\end{aligned}
\tag{B.51}
$$

where we set $x_u \to 0$ and,

$$
f_u(x_i) \equiv \frac{x_i\{18 \quad 29x_i + 10x_i^2 + x_i^3 + (32 \quad 18x_i)\ln x_i\}}{6(x_i \quad 1)^4} + \frac{4}{3(x_i \quad 1)^4}\ln x_i \quad \frac{4}{3}\ln x_u\,, \tag{B.52}
$$

$$
F_u(x_i) \equiv \frac{x_i(2 + 3x_i \quad 6x_i^2 + x_i^3 + 6x_i \ln x_i)}{4(x_i \quad 1)^4}, \tag{B.53}
$$

$$
f_W(x_i) \equiv \frac{x_i\{12 \quad 11x_i \quad 8x_i^2 + 7x_i^3 + 2x_i(12 \quad 10x_i + x_i^2)\ln x_i\}}{6(x_i \quad 1)^4}, \tag{B.54}
$$

$$
F_W(x_i) \equiv \frac{x_i(1 \quad 6x_i + 3x_i^2 + 2x_i^3 \quad 6x_i^2 \ln x_i)}{4(x_i \quad 1)^4}. \tag{B.55}
$$

The leading order Wilson coefficient in the case of SM, denoted as $C_{7\gamma}^{(0)\text{SM}}$, can be determined by the terms which are proportional to $[\not{q}, \gamma_\rho](m_b R + m_s L)$ in Eqs.(B.50) and (B.51). We note that the functions with respect to the parameter x_i in Eqs.(B.52)-(B.55) are derived by using the functions in Eqs.(B.45)-(B.49). For example,

$$
\sum_{i=u,c,t} \lambda_{sb}^i F_u'(x_i) = \sum_{i=c,t} \lambda_{sb}^i \{F_u'(x_i) \quad F_u'(x_u)\} \overset{x_u \to 0}{\to} \sum_{i=c,t} \lambda_{sb}^i F_u(x_i)\,. \tag{B.56}
$$

The terms which do not proportional to the up-type quark masses x_i in $F_u'(x_i)$ are cancelled out because of the subtraction $F_u'(x_i) \quad F_u'(x_u)$. If the W boson is much heavier than the top quark, that is $x_t \ll 1$, the leading order terms in $\sum_{i=c,t} \lambda_{sb}^i \{F_u'(x_i) \quad F_u'(x_u)\}$ are written as,

$$
\sum_{i=c,t} \lambda_{sb}^i \{F_u'(x_i) \quad F_u'(x_u)\} \sim \lambda_{sb}^c \frac{m_c^2 \quad m_u^2}{M_W^2} + \lambda_{sb}^t \frac{m_t^2 \quad m_u^2}{M_W^2}\,. \tag{B.57}
$$

Therefore, the function $F_u(x_i)$ is suppressed by the factor $\frac{m_i^2 \quad m_u^2}{M_W^2}$ in addition to the CKM factor λ_{sb}^i. We note that $\frac{m_c^2 \quad m_u^2}{M_W^2} \sim 2.5 \times 10^{\quad 4}$ with the values in [65]. This suppression factor is the result of the GIM mechanism [6]. In realistic case where the top quark is heavier than the W boson, the parameter x_t is larger than 1 ($x_t \sim 4.6$) and thus the top quark contribution becomes $F_u(x_t) \sim \frac{1}{4} \gg \frac{m_c^2 \quad m_u^2}{M_W^2}$. It is clear that the function $F_u(x_i)$ vanishes if all the up-type quark masses are the same, that is $m_u = m_c = m_t$.

B.1.4.2 Violation of CKM unitarity

When we use the violation of the CKM unitarity in the model with VLQ Eq.(4.81),

$$\sum_{i=u,c,t} \lambda_{sb}^i \simeq Z_{d\mathrm{NC}}^{sb}\,, \tag{B.58}$$

the Eqs.(B.43) and (B.44) become,

$$\begin{aligned}
&\sum_{i=u,c,t}\left[\sum_{x=c,d} {}^{(x)}_{\rho} + {}^{\mu,sb}_{c,Q_u}\right] \\
&= \frac{g^2}{32\pi^2} e Q_u \sum_{i=c,t} \lambda_{sb}^i \left[\frac{\gamma^\nu L}{M_W^2}(q^2 g_{\rho\nu} \quad q_\rho q_\nu)\frac{f_u(x_i)}{2} + \frac{1}{M_W^2}[\not{q}, \gamma_\rho](m_b R + m_q L)\frac{F_u(x_i)}{2}\right] \\
&\quad + \frac{g^2}{32\pi^2} e Q_u Z_{\mathrm{NC}}^{sb}\left[\frac{\gamma^\nu L}{M_W^2}(q^2 g_{\rho\nu} \quad q_\rho q_\nu)\left(\ \frac{1}{9} + \frac{2}{3}\ln x_u\right) \quad \frac{1}{3M_W^2}[\not{q}, \gamma_\rho](m_b R + m_q L)\right],
\end{aligned} \tag{B.59}$$

$$\begin{aligned}
&\sum_{i=u,c,t}\left[\sum_{x=e\sim h} {}^{(x)}_{\rho} + {}^{\mu,sb}_{c,Q_W}\right] \\
&= \frac{g^2}{32\pi^2} e \sum_{i=c,t} \lambda_{sb}^i \left[\frac{1}{M_W^2}(q^2 g_{\rho\nu} \quad q_\rho q_\nu)\gamma^\nu L \frac{f_W(x_i)}{2} + \frac{1}{M_W^2}[\not{q}, \gamma_\rho](m_b R + m_s L)\frac{F_W(x_i)}{2}\right] \\
&\quad + \frac{g^2 e}{32\pi^2} Z_{d\mathrm{NC}}^{sb}\left[2\left(C_{\mathrm{UV}} \quad \ln\frac{M_W^2}{\mu^2}\right)\gamma_\rho L\right] \\
&\quad + \frac{g^2 e}{32\pi^2 M_W^2} Z_{d\mathrm{NC}}^{sb}\left[\frac{1}{2}\left(\ \frac{10}{9} q^2 \gamma_\rho + \frac{16}{9}\not{q} q_\rho\right) L + [\not{q}, \gamma_\rho](m_b R + m_s L)\frac{F'_W(x_u)}{2}\right],
\end{aligned} \tag{B.60}$$

As we see above, there remain the divergence even though we add the counterterms which come from the wave function renormalization of the external quark fields. Therefore, we need additional counterterms which do not exist in the case of the SM.

B.2 Z-γ and χ_0-γ mixing diagrams

We need additional counterterms to remove the divergence in Eq.(B.60). It is important to consider mixing the Z boson and the neutral NG boson χ_0 with the photon at the one-loop level. Relevant diagrams are shown in Figs.B.3 and B.4.

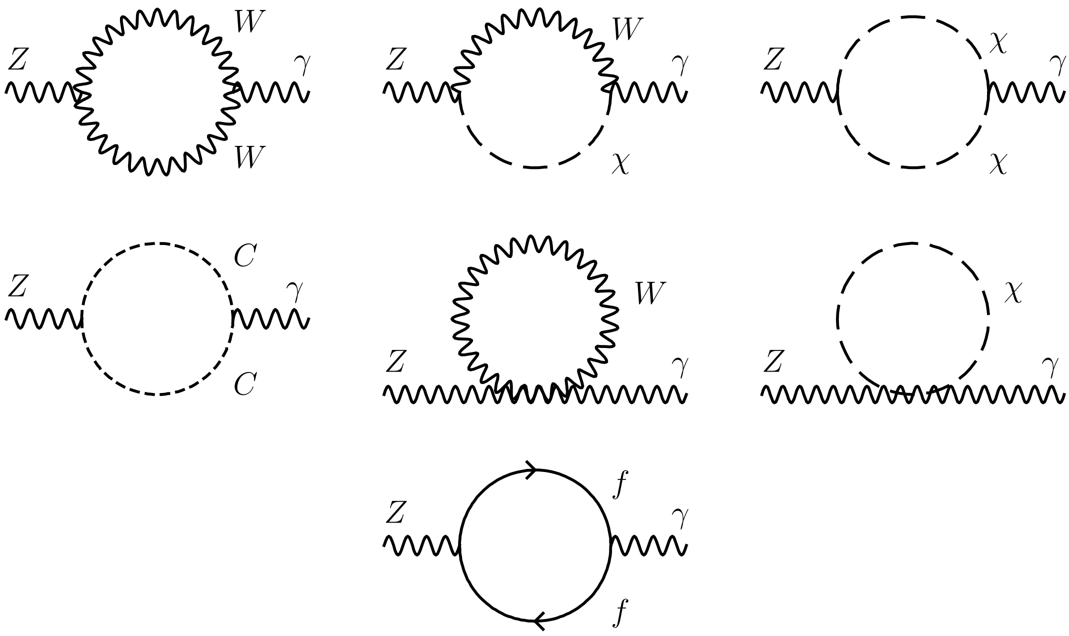

Figure B.3. Mixing Z with the photon at one-loop level. The symbol C is Faddeev–Popov ghost. The symbol f denotes fermions in the SM, that is $f = e, \mu, \tau, u^a, c^a, t^a, d^a, s^a, b^a$ where a is the color index, $a = r, g, b$.

Figure B.4. Mixing χ_0 with the photon at one-loop level. The symbol C is Faddeev–Popov ghost.

Such mixing effects lead to the following wave function renormalization [111]:

$$\begin{pmatrix} Z_0^\mu \\ A_0^\mu \end{pmatrix} = \begin{pmatrix} \sqrt{Z_{\mathrm{ZZ}}} & \sqrt{Z_{\mathrm{ZA}}} \\ \sqrt{Z_{\mathrm{AZ}}} & \sqrt{Z_{\mathrm{AA}}} \end{pmatrix} \begin{pmatrix} Z^\mu \\ A^\mu \end{pmatrix}, \tag{B.61}$$

$$\chi_{0,0} = \sqrt{Z_{\chi_0}}\chi_0 \, , \tag{B.62}$$

where the subscript "0" in the left-hand side means bare quantities while quantities in the right-hand side are renormalized. The symbols $\sqrt{Z_{ij}}$ with $i, j = Z, A$ and $\sqrt{Z_{\chi_0}}$ are the renormalization constants. In the case of the SM, there are no FCNC in both the Z and photon interactions, the wave function renormalization Eq.(B.61) does not contribute to the computation of the $b \to s\gamma$ process. On the other hand, there is FCNC in the Z boson interaction,

$$\mathcal{L}_Z \supset \frac{g}{2c_w} Z_{d\mathrm{NC}}^{sb} \, \bar{s_L} \gamma^\mu b_L Z_{0\mu} \, , \tag{B.63}$$

in the model with VLQ, as seen in Eq.(4.71). This FCNC leads to a counterterm,

$$\mathcal{L}_c \;=\; \sqrt{Z_{\rm ZA}}\frac{g}{2c_w}Z^{sb}_{d{\rm NC}}\,\bar{s_L}\gamma^\mu b_L A_\mu\,, \tag{B.64}$$

through the wave function renormalization shown in Eq.(B.61).

The renormalization constants in Eqs.(B.61) and (B.62) can be determined so as to remove the divergence in the amplitudes of the diagrams shown in Figs.B.3 and B.4. Here we use the $\overline{\rm MS}$ scheme. Counterterms for the amplitudes are given as [111],

$$\mathcal{L}_c \;=\; Z_\mu[(\sqrt{Z_{\rm ZA}}+\sqrt{Z_{\rm AZ}})(g^{\mu\nu}\Box \quad \partial^\mu\partial^\nu)+\sqrt{Z_{\rm ZA}}\,g^{\mu\nu}M_Z^2]A_\nu \quad \sqrt{Z_{\rm ZA}}M_Z A^\mu\partial_\mu\chi_0\,, \tag{B.65}$$

which lead to,

$$\Pi^{\mu\nu}_{ZA,c}(q^2) \;=\; (\sqrt{Z_{\rm ZA}}+\sqrt{Z_{\rm AZ}})(g^{\mu\nu}q^2 \quad q^\mu q^\nu)+\sqrt{Z_{\rm ZA}}\,g^{\mu\nu}M_Z^2\,, \tag{B.66}$$

$$\Pi^{\mu}_{\chi_0 A,c}(q^2) \;=\; i\sqrt{Z_{\rm ZA}}\,M_Z\,q^\mu\,. \tag{B.67}$$

We express the total amplitudes of the diagrams shown in Figs.B.3 and B.4 as,

$$\Pi^{\mu\nu}_{ZA}(q^2) \;=\; \Pi^{\mu\nu}_{ZA,{\rm div.}}(q^2)+\Pi^{\mu\nu}_{ZA,{\rm finite}}(q^2)\,, \tag{B.68}$$

$$\Pi^{\mu\nu}_{\chi_0 A}(q^2) \;=\; \Pi^{\mu\nu}_{\chi_0 A,{\rm div.}}(q^2)+\Pi^{\mu\nu}_{\chi_0 A,{\rm finite}}(q^2)\,, \tag{B.69}$$

where the terms with index "div." are proportional to the divenrgent part $C_{\rm UV}$ while the terms with index "finite" consist of finite terms. Here we focus on the divergent part which are given as,

$$\Pi^{\mu\nu}_{ZA,{\rm div.}}(q^2) \;=\; \frac{egc_w}{16\pi^2}[2g^{\mu\nu}M_Z^2+(g^{\mu\nu}q^2 \quad q^\mu q^\nu)A]C_{\rm UV}\,, \tag{B.70}$$

$$\Pi^{\mu}_{\chi_0 A,{\rm div.}}(q^2) \;=\; i\frac{egc_w}{8\pi^2}\,M_Z\,q^\mu C_{\rm UV}\,, \tag{B.71}$$

with,

$$A \;=\; 3+\frac{M_Z^2}{6M_W^2} \quad \frac{M_Z^2}{M_W^2}\left[\sum_{f=e,\mu,\tau}\frac{2}{3}Q_f(I_f \quad 2Q_f s_w^2)+3\sum_{f=u,c,t,d,s,b}\frac{2}{3}Q_f(I_f \quad 2Q_f s_w^2)\right]. \tag{B.72}$$

The factor 3 comes from the degree of freedom with respect to the SU(3)$_c$ color. We then determine the $\sqrt{Z_{\rm ZA}}$ so as to remove the divergence in $\chi_0 \quad A$ mixing,

$$\Pi^{\mu}_{\chi_0 A,{\rm div.}}(q^2)+\Pi^{\mu}_{\chi_0 A,c}(q^2) \;=\; 0\,, \;\to\; \sqrt{Z_{\rm ZA}} \;=\; \quad \frac{egc_w}{8\pi^2}C_{\rm UV}\,. \tag{B.73}$$

Then we can determine $\sqrt{Z_{\rm AZ}}$ by,

$$\Pi^{\mu}_{ZA,{\rm div.}}(q^2)+\Pi^{\mu}_{ZA,c}(q^2) \;=\; 0\,, \;\to\; \sqrt{Z_{\rm AZ}} \;=\; \frac{egc_w}{16\pi^2}C_{\rm UV}(2+A)\,. \tag{B.74}$$

These results agree with Ref.[111]. We then obtain the counterterm for the $b\to s\gamma$ vertex from Eqs.(B.64) and (B.73):

$${}^{\mu,sb}_{c,Z_{\rm NC}} \;=\; \quad \frac{eg^2}{16\pi^2}Z^{sb}_{d{\rm NC}}\,C_{\rm UV}\,\gamma^\mu L\,. \tag{B.75}$$

Also the finite part $\Pi^{\mu\nu}_{ZA,\text{finite}}$ and $\Pi^{\mu\nu}_{\chi_0 A,\text{finite}}$ in Eqs.(B.68) and (B.69) contribute to the $b \to s\gamma$ vertex as follows:

$$
\begin{aligned}
{}_{\rho}^{(ZA)} \quad &= \quad \frac{eg^2}{32\pi^2} Z^{sb}_{d\text{NC}} \left\{ \quad 2g_{\rho\nu} \ln\frac{M_W^2}{\mu^2} + \frac{1}{3M_W^2} g_{\rho\nu} q^2 \right\} \gamma^\nu L \quad \frac{eg^2}{32\pi^2} Z^{sb}_{d\text{NC}} \cdot \frac{g_{\rho\nu} q^2}{M_Z^2} \cdot 2 \left(\quad \ln\frac{M_W^2}{\mu^2} \right) \gamma^\nu L \\
& \quad \frac{eg^2}{32\pi^2} Z^{sb}_{d\text{NC}} (g_{\rho\nu} q^2 \quad q_\rho q_\nu) \left\{ \quad \left(\frac{3c_w^2}{M_W^2} + \frac{1}{6M_W^2} \right) \ln M_W^2 + \frac{2c_w^2}{3M_W^2} \right\} \gamma^\nu L \\
& \quad + \frac{eg^2 Q_u}{16\pi^2 M_W^2} Z^{sb}_{d\text{NC}} \left(\frac{1}{2} \quad 2Q_u s_w^2 \right) \ln\frac{\mu_W^2}{m_t^2} \cdot (g_{\rho\nu} q^2 \quad q_\rho q_\nu) \gamma^\nu L \,, \qquad \text{(B.76)} \\
{}_{\rho}^{(\chi_0 A)} \quad &= \quad \frac{eg^2}{32\pi^2} Z^{sb}_{d\text{NC}} \frac{q_\rho q_\nu}{M_Z^2} \left[2 \left(\quad \ln\frac{M_W^2}{\mu^2} \right) \right] \gamma^\nu L \,. \qquad \text{(B.77)}
\end{aligned}
$$

where ${}_{\rho}^{(ZA)}$ and ${}_{\rho}^{(\chi_0 A)}$ correspond to the contributions from $\Pi^{\mu\nu}_{ZA,\text{finite}}$ and $\Pi^{\mu\nu}_{\chi_0 A,\text{finite}}$, respectively. In Eq.(B.76), we do not include the contribution from the light SM particles since we do not integrate out these light particles. It is clear that the counterterm shown in Eq.(B.75) removes the divergence in the amplitude Eq.(B.60).

B.3 Unitarity Violation in the model with VLQ

Adding the amplitudes Eqs.(B.75)-(B.77) to Eqs.(B.59) and (B.60), we obtain the contributions to the $b \to s\gamma$ vertex from the same diagrams as the SM without the CKM unitarity:

$$
\begin{aligned}
& \sum_{i=u,c,t} \left[\sum_{x=c,d} {}_{\rho}^{(x)} + {}_{c,Q_u}^{\mu,sb} \right] \\
= \; & \frac{eg^2 Q_u}{64\pi^2 M_W^2} \Bigg[[\not{q}, \gamma_\rho](m_b R + m_q L) \left\{ \sum_{i=c,t} \lambda^i_{qb} F_u(x_i) \quad \frac{2}{3} Z^{sb}_{d\text{NC}} \right\} \\
& + (q^2 g_{\rho\nu} \quad q_\rho q_\nu) \gamma^\nu L \left\{ \sum_{i=c,t} \lambda^i_{qb} f_u(x_i) + Z^{sb}_{d\text{NC}} \left(\quad \frac{2}{9} + \frac{4}{3} \ln x_u \right) \right\} \Bigg] , \qquad \text{(B.78)}
\end{aligned}
$$

$$
\begin{aligned}
& \sum_{i=u,c,t} \left[\sum_{x=e\sim h} {}_{\rho}^{(x)} + {}_{c,Q_W}^{\mu,sb} + {}_{c,Z_{\text{NC}}}^{\mu,sb} + {}_{\rho}^{(ZA)} + {}_{\rho}^{(\chi_0 A)} \right] \\
= \; & \frac{eg^2}{64\pi^2 M_W^2} \Bigg[(q^2 g_{\rho\nu} \quad q_\rho q_\nu) \gamma^\nu L \left\{ \sum_{i=c,t} \lambda^i_{qb} f_W(x_i) \quad \frac{16}{9} Z^{sb}_{d\text{NC}} \right\} \\
& + [\not{q}, \gamma_\rho](m_b R + m_q L) \left(\sum_{i=c,t} \lambda^i_{qb} F_W(x_i) \quad \frac{5}{6} Z^{sb}_{d\text{NC}} \right) \\
& \quad Z^{sb}_{d\text{NC}} (g_{\rho\nu} q^2 \quad q_\rho q_\nu) \left\{ \left(10c_w^2 + \frac{1}{3} \right) \ln\frac{\mu^2}{M_W^2} + \frac{4}{3} c_w^2 \right\} \gamma^\nu L \Bigg] \\
& + \frac{eg^2 Q_u}{16\pi^2 M_W^2} Z^{sb}_{d\text{NC}} \left(\frac{1}{2} \quad 2Q_u s_w^2 \right) \ln\frac{\mu_W^2}{m_t^2} \cdot (g_{\rho\nu} q^2 \quad q_\rho q_\nu) \gamma^\nu L \,. \qquad \text{(B.79)}
\end{aligned}
$$

References

[1] M. Kobayashi and T. Maskawa, Prog. Theor. Phys. **49** (1973) 652–657.

[2] N. Cabibbo, Phys. Rev. Lett. **10** (1963) 531–533. [,648(1963)].

[3] M. Gell-Mann and M. Levy, Nuovo Cim. **16** (1960) 705.

[4] Z. Maki, M. Nakagawa and S. Sakata, Prog. Theor. Phys. **28** (1962) 870–880. [,34(1962)].

[5] B. Pontecorvo, Sov. Phys. JETP **26** (1968) 984–988. [Zh. Eksp. Teor. Fiz.53,1717(1967)].

[6] S. L. Glashow, J. Iliopoulos and L. Maiani, Phys. Rev. **D2** (1970) 1285–1292.

[7] J. Charles, A. Hocker, H. Lacker, S. Laplace, F. R. Le Diberder, J. Malcles, J. Ocariz, M. Pivk and L. Roos [CKMfitter Group], Eur. Phys. J. **C41**, 1 (2005) 1–131 [arXiv:hep-ph/0406184].

[8] M. Bona et al. [UTfit Collaboration], JHEP **03** (2008) 049 [arXiv:0707.0636[hep-ph]].

[9] I. Esteban, M. C. Gonzalez-Garcia, A. Hernandez-Cabezudo, M. Maltoni and T. Schwetz [NuFIT 4.1 (2019), www.nu-fit.org], JHEP **01** (2019) 106 [arXiv:1811.05487[hep-ph]].

[10] Y. Shimizu, K. Takagi, S. Takahashi and M. Tanimoto, JHEP **04** (2019) 074 [arXiv:1901.06146[hep-ph]].

[11] S. K. Kang, Y. Shimizu, K. Takagi, S. Takahashi and M. Tanimoto, PTEP **2018**, 8 (2018) 083B01 [arXiv:1804.10468[hep-ph]].

[12] Z. G. Berezhiani, Phys. Lett. **129B** (1983) 99–102.

[13] Z. G. Berezhiani, Phys. Lett. **150B** (1985) 177–181.

[14] S. Rajpoot, Phys. Lett. **B191** (1987) 122–126.

[15] S. Rajpoot, Phys. Rev. **D36** (1987) 1479–1483.

[16] A. Davidson and K. C. Wali, Phys. Rev. Lett. **59** (1987) 393.

[17] Z. G. Berezhiani and R. Rattazzi, Phys. Lett. **B279** (1992) 124–130.

[18] K. S. Babu and R. N. Mohapatra, Phys. Rev. **D41** (1990) 1286.

[19] G. Aad et al. [ATLAS Collaboration], Phys. Lett. **B712** (2012) 22–39 [arXiv:1112.5755[hep-ex]].

[20] G. Aad et al. [ATLAS Collaboration], Phys. Rev. Lett. **109** (2012) 071801 [arXiv:1204.1265[hep-ex]].

[21] G. Aad et al. [ATLAS Collaboration], JHEP **11** (2014) 104 [arXiv:1409.5500[hep-ex]].

[22] G. Aad et al. [ATLAS Collaboration], Phys. Rev. **D91**, 11 (2015) 112011 [arXiv:1503.05425[hep-ex]].

[23] G. Aad et al. [ATLAS Collaboration], JHEP **08** (2015) 105 [arXiv:1505.04306[hep-ex]].

[24] G. Aad et al. [ATLAS Collaboration], Phys. Rev. **D92**, 11 (2015) 112007 [arXiv:1509.04261[hep-ex]].

[25] G. Aad et al. [ATLAS Collaboration], JHEP **02** (2016) 110 [arXiv:1510.02664[hep-ex]].

[26] G. Aad et al. [ATLAS Collaboration], Eur. Phys. J. **C76**, 8 (2016) 442 [arXiv:1602.05606[hep-ex]].

[27] G. Aad et al. [ATLAS Collaboration], Phys. Lett. **B758** (2016) 249–268 [arXiv:1602.06034[hep-ex]].

[28] M. Aaboud et al. [ATLAS Collaboration], JHEP **08** (2017) 052 [arXiv:1705.10751[hep-ex]].

[29] M. Aaboud et al. [ATLAS Collaboration], JHEP **10** (2017) 141 [arXiv:1707.03347[hep-ex]].

[30] M. Aaboud et al. [ATLAS Collaboration], JHEP **07** (2018) 089 [arXiv:1803.09678[hep-ex]].

[31] M. Aaboud et al. [ATLAS Collaboration], JHEP **08** (2018) 048 [arXiv:1806.01762[hep-ex]].

[32] M. Aaboud et al. [ATLAS Collaboration], Phys. Rev. **D98**, 11 (2018) 112010 [arXiv:1806.10555[hep-ex]].

[33] M. Aaboud et al. [ATLAS Collaboration], Phys. Rev. **D98**, 9 (2018) 092005 [arXiv:1808.01771[hep-ex]].

[34] M. Aaboud et al. [ATLAS Collaboration], Phys. Rev. Lett. **121**, 21 (2018) 211801 [arXiv:1808.02343[hep-ex]].

[35] S. Chatrchyan et al. [CMS Collaboration], JHEP **01** (2013) 154 [arXiv:1210.7471[hep-ex]].

[36] S. Chatrchyan et al. [CMS Collaboration], Phys. Lett. **B729** (2014) 149–171 [arXiv:1311.7667[hep-ex]].

[37] V. Khachatryan et al. [CMS Collaboration], JHEP **06** (2015) 080 [arXiv:1503.01952[hep-ex]].

[38] V. Khachatryan et al. [CMS Collaboration], Phys. Rev. **D93**, 11 (2016) 112009 [arXiv:1507.07129[hep-ex]].

[39] V. Khachatryan et al. [CMS Collaboration], Phys. Rev. **D93**, 1 (2016) 012003 [arXiv:1509.04177[hep-ex]].

[40] V. Khachatryan et al. [CMS Collaboration], Phys. Lett. **B771** (2017) 80–105 [arXiv:1612.00999[hep-ex]].

[41] A. M. Sirunyan et al. [CMS Collaboration], JHEP **04** (2017) 136 [arXiv:1612.05336[hep-ex]].

[42] A. M. Sirunyan et al. [CMS Collaboration], JHEP **05** (2017) 029 [arXiv:1701.07409[hep-ex]].

[43] A. M. Sirunyan et al. [CMS Collaboration], Phys. Lett. **B772** (2017) 634–656 [arXiv:1701.08328[hep-ex]].

[44] A. M. Sirunyan et al. [CMS Collaboration], JHEP **11** (2017) 085 [arXiv:1706.03408[hep-ex]].

[45] A. M. Sirunyan et al. [CMS Collaboration], Phys. Lett. **B781** (2018) 574–600 [arXiv:1708.01062[hep-ex]].

[46] A. M. Sirunyan et al. [CMS Collaboration], Phys. Rev. **D97** (2018) 072008 [arXiv:1708.02510[hep-ex]].

[47] A. M. Sirunyan et al. [CMS Collaboration], Phys. Lett. **B779** (2018) 82–106 [arXiv:1710.01539[hep-ex]].

[48] A. M. Sirunyan et al. [CMS Collaboration], JHEP **06** (2018) 031 [arXiv:1802.01486[hep-ex]].

[49] A. M. Sirunyan et al. [CMS Collaboration], JHEP **08** (2018) 177 [arXiv:1805.04758[hep-ex]].

[50] A. M. Sirunyan et al. [CMS Collaboration], Eur. Phys. J. **C79** (2019) 90 [arXiv:1809.08597[hep-ex]].

[51] A. M. Sirunyan et al. [CMS Collaboration], Eur. Phys. J. **C79**, 4 (2019) 364 [arXiv:1812.09768[hep-ex]].

[52] A. M. Sirunyan et al. [CMS Collaboration], Phys. Rev. **D100**, 7 (2019) 072001 [arXiv:1906.11903[hep-ex]].

[53] R. Aaij et al. [LHCb Collaboration], Phys. Rev. Lett. **111** (2013) 101805 [arXiv:1307.5024[hep-ex]].

[54] S. Chatrchyan et al. [CMS Collaboration], Phys. Rev. Lett. **111** (2013) 101804 [arXiv:1307.5025[hep-ex]].

[55] V. Khachatryan et al. [CMS and LHCb Collaboration], Nature **522** (2015) 68–72 [arXiv:1411.4413[hep-ex]].

[56] R. Aaij et al. [LHCb Collaboration], Phys. Rev. Lett. **118**, 19 (2017) 191801 [arXiv:1703.05747[hep-ex]].

[57] B. Aubert et al. [BaBar Collaboration], Phys. Rev. **D77** (2008) 051103 [arXiv:0711.4889[hep-ex]].

[58] J. P. Lees et al. [BaBar Collaboration], Phys. Rev. Lett. **109** (2012) 191801 [arXiv:1207.2690[hep-ex]].

[59] J. P. Lees et al. [BaBar Collaboration], Phys. Rev. **D86** (2012) 052012 [arXiv:1207.2520[hep-ex]].

[60] A. Limosani et al. [Belle Collaboration], Phys. Rev. Lett. **103** (2009) 241801 [arXiv:0907.1384[hep-ex]].

[61] T. Saito et al. [Belle Collaboration], Phys. Rev. **D91**, 5 (2015) 052004 [arXiv:1411.7198[hep-ex]].

[62] A. Abdesselam et al. [Belle Collaboration], arXiv:1608.02344[hep-ex].

[63] S. Chen et al. [CLEO Collaboration], Phys. Rev. Lett. **87** (2001) 251807 [arXiv:hep-ex/0108032].

[64] Y. Amhis et al. [HFLAV Collaboration], Eur. Phys. J. **C77**, 12 (2017) 895 [arXiv:1612.07233[hep-ex]].

[65] M. Tanabashi et al. [Particle Data Group], Phys. Rev. **D98**, 3 (2018) 030001.

[66] W. Buchmuller and D. Wyler, Nucl. Phys. **B268** (1986) 621–653.

[67] B. Grzadkowski, M. Iskrzynski, M. Misiak and J. Rosiek, JHEP **10** (2010) 085 [arXiv:1008.4884[hep-ph]].

[68] J. Ellis, V. Sanz and T. You, JHEP **07** (2014) 036 [arXiv:1404.3667[hep-ph]].

[69] J. Ellis, V. Sanz and T. You, JHEP **03** (2015) 157 [arXiv:1410.7703[hep-ph]].

[70] C. W. Murphy, Phys. Rev. **D97**, 1 (2018) 015007 [arXiv:1710.02008[hep-ph]].

[71] J. Ellis, C. W. Murphy, V. Sanz and T. You, JHEP **06** (2018) 146 [arXiv:1803.03252[hep-ph]].

[72] M. Ciuchini, E. Franco, S. Mishima and L. Silvestrini, JHEP **08** (2013) 106 [arXiv:1306.4644[hep-ph]].

[73] J. d. Blas, M. Ciuchini, E. Franco, S. Mishima, M. Pierini, L. Reina and L. Silvestrini, PoS **ICHEP2016** (2017) 690 [arXiv:1611.05354[hep-ph]].

[74] J. d. Blas, M. Ciuchini, E. Franco, S. Mishima, M. Pierini, L. Reina and L. Silvestrini, PoS **EPS-HEP2017** (2017) 467 [arXiv:1710.05402[hep-ph]].

[75] E. E. Jenkins, A. V. Manohar and M. Trott, JHEP **10** (2013) 087 [arXiv:1308.2627[hep-ph]].

[76] E. E. Jenkins, A. V. Manohar and M. Trott, JHEP **01** (2014) 035 [arXiv:1310.4838[hep-ph]].

[77] R. Alonso, E. E. Jenkins, A. V. Manohar and M. Trott, JHEP **04** (2014) 159 [arXiv:1312.2014[hep-ph]].

[78] G. Barenboim, F. J. Botella and O. Vives, Nucl. Phys. **B613** (2001) 285–305 [arXiv:hep-ph/0105306].

[79] F. J. Botella, G. C. Branco and M. Nebot, JHEP **12** (2012) 040 [arXiv:1207.4440[hep-ph]].

[80] A. K. Alok, S. Banerjee, D. Kumar and S. Uma Sankar, Nucl. Phys. **B906** (2016) 321–341 [arXiv:1402.1023[hep-ph]].

[81] A. K. Alok, S. Banerjee, D. Kumar, S. U. Sankar and D. London, Phys. Rev. **D92** (2015) 013002 [arXiv:1504.00517[hep-ph]].

[82] K. Ishiwata, Z. Ligeti and M. B. Wise, JHEP **10** (2015) 027 [arXiv:1506.03484[hep-ph]].

[83] C. Bobeth, A. J. Buras, A. Celis and M. Jung, JHEP **04** (2017) 079 [arXiv:1609.04783[hep-ph]].

[84] T. Morozumi, Y. Shimizu, S. Takahashi and H. Umeeda, PTEP **2018**, 4 (2018) 043B10 [arXiv:1801.05268[hep-ph]].

[85] A. L. Kagan and M. Neubert, Phys. Rev. **D58** (1998) 094012 [arXiv:hep-ph/9803368].

[86] T. Hurth, E. Lunghi and W. Porod, Nucl. Phys. **B704** (2005) 56–74 [arXiv:hep-ph/0312260].

[87] M. Benzke, S. J. Lee, M. Neubert and G. Paz, Phys. Rev. Lett. **106** (2011) 141801 [arXiv:1012.3167[hep-ph]].

[88] S. Fukae, C. S. Kim, T. Morozumi and T. Yoshikawa, Phys. Rev. **D59** (1999) 074013 [arXiv:hep-ph/9807254].

[89] T. Huber, T. Hurth and E. Lunghi, JHEP **06** (2015) 176 [arXiv:1503.04849[hep-ph]].

[90] F. Kruger, L. M. Sehgal, N. Sinha and R. Sinha, Phys. Rev. **D61** (2000) 114028 [arXiv:hep-ph/9907386]. [Erratum: Phys. Rev.D63,019901(2001)].

[91] C. S. Kim, Y. G. Kim, C.-D. Lu and T. Morozumi, Phys. Rev. **D62** (2000) 034013 [arXiv:hep-ph/0001151].

[92] W. Altmannshofer, P. Ball, A. Bharucha, A. J. Buras, D. M. Straub and M. Wick, JHEP **01** (2009) 019 [arXiv:0811.1214[hep-ph]].

[93] A. J. Buras, arXiv:hep-ph/9806471.

[94] F. d. Aguila, M. Perez-Victoria and J. Santiago, Phys. Lett. **B492** (2000) 98–106 [arXiv:hep-ph/0007160].

[95] F. d. Aguila, M. Perez-Victoria and J. Santiago, JHEP **09** (2000) 011 [arXiv:hep-ph/0007316].

[96] C.-Y. Chen, S. Dawson and E. Furlan, Phys. Rev. **D96**, 1 (2017) 015006 [arXiv:1703.06134[hep-ph]].

[97] A. J. Buras, M. Misiak and J. Urban, Nucl. Phys. **B586** (2000) 397–426 [arXiv:hep-ph/0005183].

[98] G. C. Branco, T. Morozumi, P. A. Parada and M. N. Rebelo, Phys. Rev. **D48** (1993) 1167–1175.

[99] G. C. Branco, P. A. Parada, T. Morozumi and M. N. Rebelo, Phys. Lett. **B306** (1993) 398–402.

[100] G. C. Branco, P. A. Parada, T. Morozumi and M. N. Rebelo, Nucl. Phys. Proc. Suppl. **37A**, 1 (1994) 29–33.

[101] G. Barenboim and F. J. Botella, Phys. Lett. **B433** (1998) 385–395 [arXiv:hep-ph/9708209].

[102] T. Inami and C. S. Lim, Prog. Theor. Phys. **65** (1981) 297. [Erratum: Prog. Theor. Phys.65,1772(1981)].

[103] G. Buchalla, A. J. Buras and M. K. Harlander, Nucl. Phys. **B349** (1991) 1–47.

[104] K. De Bruyn, R. Fleischer, R. Knegjens, P. Koppenburg, M. Merk, A. Pellegrino and N. Tuning, Phys. Rev. Lett. **109** (2012) 041801 [arXiv:1204.1737[hep-ph]].

[105] A. J. Buras, R. Fleischer, J. Girrbach and R. Knegjens, JHEP **07** (2013) 077 [arXiv:1303.3820[hep-ph]].

[106] R. Fleischer, R. Jaarsma and G. Tetlalmatzi-Xolocotzi, JHEP **05** (2017) 156 [arXiv:1703.10160[hep-ph]].

[107] G. Tetlalmatzi-Xolocotzi, PoS **BEAUTY2018** (2018) 043 [arXiv:1809.00637[hep-ph]].

[108] L. T. Handoko and T. Morozumi, Mod. Phys. Lett. **A10** (1995) 309–322 [arXiv:hep-ph/9409240]. [Erratum: Mod. Phys. Lett.A10,1733(1995)].

[109] C.-H. V. Chang, D. Chang and W.-Y. Keung, arXiv:hep-ph/9811354.

[110] C.-H. V. Chang, D. Chang and W.-Y. Keung, Phys. Rev. **D61** (2000) 053007.

[111] K. I. Aoki, Z. Hioki, M. Konuma, R. Kawabe and T. Muta, Prog. Theor. Phys. Suppl. **73** (1982) 1–225.

[112] M. Ciuchini, E. Franco, G. Martinelli, L. Reina and L. Silvestrini, Phys. Lett. **B316** (1993) 127–136 [arXiv:hep-ph/9307364].

[113] A. J. Buras, M. Misiak, M. Munz and S. Pokorski, Nucl. Phys. **B424** (1994) 374–398 [arXiv:hep-ph/9311345].

[114] K. G. Chetyrkin, M. Misiak and M. Munz, Phys. Lett. **B400** (1997) 206–219 [arXiv:hep-ph/9612313]. [Erratum: Phys. Lett.B425,414(1998)].

[115] G. Buchalla, A. J. Buras and M. E. Lautenbacher, Rev. Mod. Phys. **68** (1996) 1125–1144 [arXiv:hep-ph/9512380].

[116] A. J. Buras, J. Girrbach, D. Guadagnoli and G. Isidori, Eur. Phys. J. **C72** (2012) 2172 [arXiv:1208.0934[hep-ph]].

[117] M. Misiak et al., Phys. Rev. Lett. **114**, 22 (2015) 221801 [arXiv:1503.01789[hep-ph]].

[118] L. Wolfenstein, Phys. Rev. Lett. **51** (1983) 1945.

[119] A. J. Buras, M. E. Lautenbacher and G. Ostermaier, Phys. Rev. **D50** (1994) 3433–3446 [arXiv:hep-ph/9403384].

[120] G. C. Branco, L. Lavoura and J. P. Silva, Int. Ser. Monogr. Phys. **103** (1999) 1–536.

[121] B. Grinstein, R. P. Springer and M. B. Wise, Nucl. Phys. **B339** (1990) 269–309.

[122] A. F. Falk, M. E. Luke and M. J. Savage, Phys. Rev. **D49** (1994) 3367–3378 [arXiv:hep-ph/9308288].

[123] A. Ali and C. Greub, Phys. Lett. **B361** (1995) 146–154 [arXiv:hep-ph/9506374].

[124] C. Greub, T. Hurth and D. Wyler, Phys. Rev. **D54** (1996) 3350–3364 [arXiv:hep-ph/9603404].

[125] N. Pott, Phys. Rev. **D54** (1996) 938–948 [arXiv:hep-ph/9512252].

[126] K. Baranowski and M. Misiak, Phys. Lett. **B483** (2000) 410–416 [arXiv:hep-ph/9907427].

[127] P. Gambino and U. Haisch, JHEP **10** (2001) 020 [arXiv:hep-ph/0109058].